

Contents lists available at ScienceDirect

Transportation Research Part B

journal homepage: www.elsevier.com/locate/trb



Check for updates

Hybrid MPC System for Platoon based Cooperative Lane change Control Using Machine Learning Aided Distributed Optimization

Hanyu Zhang ^a, Lili Du, Associate professor ^{b,*}, Jinglai Shen, Professor ^c

- ^a Department of Civil and Coastal Engineering, University of Florida, Gainesville, Florida, 32608
- ^b Department of Civil and Coastal Engineering, University of Florida, Gainesville, Florida, 32608
- ^c Department of Mathematics and Statistics, University of Maryland, Baltimore County, Maryland, 21250

ARTICLE INFO

Keywords: connected and autonomous vehicles cooperative lane-change vehicle platooning model predictive control hybrid system controller mixed integer nonlinear programming supervised machine learning distributed branch and bound

ABSTRACT

This study is devoted to developing a platoon-based cooperative lane-change control (PB-CLC). It coordinates the trajectories of a CAV platoon under a platoon-centered platooning control to accommodate the CAV lane-change requests from its adjacent lane, aiming to reduce the negative traffic impacts on the platoon resulting from lane-change maneuvers, on the premise of ensuring CAVs' safety and mobility. Mathematically, the PB-CLC control is established using a hybrid model predictive control (MPC) system. The hybrid MPC system involves an MPC-based mixed integer nonlinear programming optimizer (MINLP-MPC) for optimal lane-change decisions, which considers multiple objectives such as traffic smoothness, driving comfort and lane-change response promptness subject to vehicle dynamics and safety constraints. To ensure the feasible lane-change, this study investigates and provides a lower bound of the lane-change time window by analyzing the MINLP-MPC model feasibility. Apart from the optimal lane-change decision consideration, the hybrid MPC system is well designed to ensure the control continuity and smoothness. In particular, the hybrid MPC system control feasibility and stability are proved to enable the platoon's back-and-forth state switchings between car-following and lane-change accommodation states. Next, we developed a machine learning aided distributed branch and bound algorithm (ML-DBB) to solve the MINLP-MPC model within a control sampling time interval (< 1 second). Specifically, built upon computer simulation and the c-LHS sampling technique, supervised machine learning models are developed offline to predict a reduced solution space of the integer variables, which is further integrated into the distributed branch and bound method to solve the MINLP-MPC model efficiently online. Extensive numerical experiments validate the effectiveness and applicability of the ML-DBB algorithm and the PB-CLC control.

1. Introduction

The car-following and lane-change maneuvers often interweave with each other and play important roles to affect traffic safety, efficiency and sustainability. Thus, they have attracted tremendous research interests in traffic operation and control. Especially in recent years, advanced communication, information, and computation technologies have granted Connected and Autonomous (Automated) Vehicles (CAVs) superior capabilities to exchange information, accept trajectory instructions, and even conduct in-

E-mail addresses: hanyu.zhang@ufl.edu (H. Zhang), lilidu@ufl.edu (L. Du), shenj@umbc.edu (J. Shen).

^{*} Corresponding author. Lili Du, Associate professor, Department of Civil and Coastal Engineering, University of Florida, Gainesville, Florida, 32608

vehicle driving decisions at different levels. These advanced capabilities stimulated extensive research interests in developing vehicle platooning control, which instructs CAVs' longitudinal car-following maneuvers to maintain a group of CAVs traveling closely and safely at high speed. We classify the existing platooning control in literature into two categories, including (i) vehicle-centered reactive control, which equips each vehicle with a car-following control reactive to its neighborhood vehicles' movement (e.g., adaptive cruise control (ACC) (Rudin-Brown and Parker, 2004; Lu and Aakre, 2018) and cooperative adaptive cruise control (CACC) (Dey et al., 2015; Shladover et al., 2015) and (ii) platoon-centered platooning control, which implements a car-following control for the entire platoon so that it systematically reacts to traffic disturbances. (e.g., MPC based control developed in Wang et al., 2014b; Gong et al., 2016; Gong and Du, 2018; Wang et al., 2019). Both simulation and theoretical studies have shown that vehicle platooning control can improve traffic safety, efficiency, and smoothness.

Furthermore, CAV technologies inspired significant interests in developing more complicated cooperative lane-change algorithms, which coordinate CAVs' car-following and lane-change movements on adjacent lanes, intending to ensure safe and efficient lane-change maneuvers while mitigating negative traffic impacts (Hidas, 2002; Ammoun et al., 2007). Various models, control and algorithms have been developed in the existing literature. For example, Wang et al. (2015) and Talebpour et al. (2015) proposed game models for optimal lane-change decisions. Liu and Özgüner, (2015) and Liu et al. (2018) used model predictive control (MPC) approaches to control the vehicle convoy's leading CAV movements for lane-change preparation, whereas Wang et al., (2016) employed a MPC control framework to instruct smooth lane-change transitions while reducing the travel time delay. Balal et al., (2016) used fuzzy logic approach to model driver's decision to or not to execute a lane-change maneuver and Choi and Yeo, (2017) developed a cell transmission model (CTM) to predict the future traffic condition around lane-change location. Gong and Du (2016) and Cao et al. (2017) formulated optimization models to optimally determine where a lane-change instruction should be given to vehicles. Pueboobpaphan et al. (2010); Scarinci and Heydecker (2014); Xie et al. (2017) and Scarinci et al. (2017) used various model and control schemes to study optimal on-ramp merging control, which is a special case of the lane-change maneuvers. Various hierarchical cooperative lane-change frameworks, which typically include several control stages are developed in Nie et al. (2016); Li et al. (2020) and Ni et al. (2020). Even though these existing studies showed good performance in different aspects, we noticed the following research gaps, which thus motivate this study.

First, the existing cooperative lane-change control (e.g., Talebpour et al., 2015; Balal et al., 2016; Nie et al., 2016; Wang et al., 2016; Choi and Yeo, 2017; Ni et al., 2020) mainly involve a few subject vehicles and their neighborhood vehicles (often less than 5 vehicles in total) in the lane-change model. Consequently, the impact of the lane-change maneuvers on the target traffic stream is locally considered in a relatively short stretch. This study intends to scale up and involves a rather long stretch of a platoon in the target lane so that the proposed cooperative lane-change control is applicable to a traffic stream in a broader range.

Second, the existing studies often assume the platoon in the target lane are under vehicle-centered reactive platooning control such as ACC (Xie et al., 2017; Ni et al., 2020) or CACC (Pueboobpaphan et al., 2010; Liu and Özgüner, 2015; Liu et al., 2018), or even free-control (Balal et al. 2016; Choi and Yeo, 2017) rather than a platoon-centered platooning control, even though the merit of the platoon-centered platooning control compared with the vehicle-centered reactive platooning control has been well confirmed (Wang et al., 2014b; Gong et al., 2016; Gong and Du, 2018; Wang et al., 2019). On the other hand, it has been noticed that a vehicle platooning control covering a long stretch of traffic stream will block mobility needs (Darren Cottingham 2020), if it cannot efficiently accommodate lane-change requests. This research gap will significantly limit the application of advanced CAV platooning control techniques in practice. Thus, motivated by bridging this gap, this study aims at developing a cooperative lane-change control, assuming that the target platoon is under a platoon-centered platooning control.

Third, we noticed that few existing lane-change control algorithm considers the time windows required by the lane-change requests and the associated feasibility issue, although Ni et al., (2020) addressed the lane-change feasibility problem from a different angle by proposing feasibility judgement criterion. However, it is possible that the target CAV platoon in reality under specific platooning control cannot accommodate lane-change requests within the required time window due to the traffic condition constraints. Thus, investigating the feasibility under this context is critical for developing a proper lane-change accommodation control. It will guide the platoon to accept or reject the lane-change requests appropriately. Moreover, the results will provide valuable insight into making subject vehicle's lane change decisions. This study intends to bridge this gap in the existing literature.

Last, the existing efforts mainly focused on lane-change decisions but overlooked the switching of different dynamic states that the target platoon experiences when it accommodates the lane-change requests. Specifically, it is unclear whether the lane-change decision can instruct a platoon to switch feasibly and smoothly from its original car-following control to lane-change accommodation control and finally restore the initial car-following control. For example, suppose a lane-change decision model uses safe spacing lane-change constraints that are more aggressive than the safety constraints under car-following control. In this case, the spacing between a subject vehicle and its immediate leading and following platoon vehicles may not satisfy the safety distance constraints under the car-following control right after the lane-change maneuver. Accordingly, the platoon may not be able to restore the initial car-following control. This research gap will raise the difficulty of integrating the lane-change control and platooning control in practice. This study will thoroughly address the switching feasibility and stability of the hybrid dynamic system.

Motivated by the abovementioned research gaps, this study is devoted to developing a platoon-based cooperative lane-change control (PB-CLC), seeking to instruct a long stretch and well-connected CAV platoon (e.g., more than 15 vehicles) under an MPC based platoon-centered car-following control to accommodate multiple lane-change requests (≥ 2 subject vehicles) smoothly and efficiently from the subject vehicles beside the platoon, within their required time windows. To achieve this research goal, we contribute the following modeling, hybrid system dynamic analysis, and solution approaches, which address the research challenges raised by the enhanced features of the proposed PB-CLC control.

First of all, this study develops an MINLP-MPC model to search the best timing and spacing for the platoon to accommodate the

lane-change requests without causing severe platoon stream fluctuations. To smoothly integrate the MINLP-MPC decision model into the PB-CLC control, we further conducted the mathematical analysis as follows. Considering the lane-change requests coming with time window requirements, the feasibility of the MINLP-MPC model becomes a critical issue. To address this challenge, we went through a structured proof from Lemma 1 to Lemma 5. The results summarized in Theorem 1 demonstrate that the lane-change requests can only be feasibly accommodated by the platoon if the prediction horizon *P* of the MINLP-MPC is no smaller than the derived time window lower bound. Moreover, the MINLP-MPC model is different from the common lane-change decision model since it should not only find the best lane-change spacing and timing but also consider the switching behaviors between car-following and lane-change accommodation states (see Appendix-II for technical details).

Next, we consider that the platoon will physically experience three dynamic traffic states: car-following state, spacing preparation state and restoration state during the entire lane-change process, which are mathematically carried out by three sequential MPC and forms a hybrid MPC system. Specifically, the platoon is initially under the MPC-based platoon-centered car-following control developed by Gong et al. (2016) with well-validated system performance. It will switch to the spacing preparation state once receiving the lane-change decision made by solving the MINLP-MPC model. After the subject vehicles cut in the platoon, the platoon will switch to the restoration state and eventually return to the initial car-following state. Based upon the feasibility of the MINLP-MPC model, we carefully designed the hybrid MPC system and mathematically proved its feasibility and stability. The theoretical proofs in Theorem 2 and Theorem 3 ensure the platoon runs smoothly and safely through the entire dynamic lane-change process under the provided hybrid MPC control.

Moreover, the MINLP-MPC decision model is NP-hard, which often does not have an efficient solver with a polynomial computation complexity. However, the real-time PB-CLC control requires solving the MINLP-MPC model within one control interval (< 1 sec) to ensure the practical implementation of the hybrid MPC system involving three dynamic states. To address this challenge, we developed a machine learning aided distributed branch and bound algorithm (ML-DBB) by taking advantage of the problem's unique features. Specifically, the ML-DBB algorithm employs a computer simulator and supervised machine learning approaches (Kotsiantis et al., 2007; James et al., 2013) to capture the candidate optimal lane-change spacings and timings, which reduce the solution searching space of integer variables relevant to lane-change decisions in the MINLP-MPC. Built upon the reduced solution space, a distributed branch and bound method (Androulakis and Floudas, 1999; Djamai et al., 2010) is further used to split the computation loads and solve the MINLP-MPC model efficiently. During the development of the ML-DBB algorithm, feature selection plays a critical role to ensure the effectiveness of the machine learning model. This study developed a customized feature processing approach to improve the applicability and prediction accuracy of the developed machine learning models.

Last, we carried out extensive numerical experiments to validate the effectiveness and merits of the ML-DBB algorithm in solving the MINLP-MPC model. Besides, our numerical experiments demonstrate that the platoon using PB-CLC control can quickly accommodate the lane-change requests within the required time window and significantly improve traffic smoothness and efficiency, compared with field traffic without platooning control and a recently developed cooperative lane-change control. Parameter sensitivity analysis of the MINLP-MPC model is also conducted to provide insights into the parameter settings.

The organization of the remaining of this paper is as follows. Following the Introduction, Section 2 provides the preliminary problem formulations and briefly introduces the hybrid MPC system. Section 3 mathematically develops the cooperative lane-change decision model (MINLP-MPC). Next, we analyze the feasibility of the MINLP-MPC model in Section 4 and design the hybrid MPC system, proving its feasibility and stability in Section 5. The solution approaches of the hybrid MPC system are discussed in Section 6. The main focus is given to the development of the ML-DBB algorithm for the MINLP-MPC model. Section 7 further conducts numerical experiments to validate the applicability and effectiveness of our approaches. The entire study and future work are summarized in Section 8.

2. Problem Statement

This research is devoted to developing the PB-CLC control. Vehicles mentioned hereafter in this paper refer to CAVs. To conduct this research rigorously, we first make the general clarifications and assumptions as follows, with more added along the development of the mathematical models. Mainly, this study considers a two-lane highway road segment with pure CAV traffic flow (this assumption can be relaxed, see Remark 1 in section 3). There are multiple CAVs on a subject lane requiring cutting in the adjacent target platoon due to discretionary or mandatory reasons\(^1\). The CAV platoon is under a MPC based platoon-centered platooning control (i.e., car-following) developed by Gong et al., (2016); Gong and Du (2018) because of its superior performance for sustaining traffic efficiency and smoothness while exposed to traffic disturbances, compared with the vehicle-centered reactive control such as ACC and CACC. If the spacing next to a subject vehicle is acceptable, the subject vehicle will smoothly shift in without extraneous assistance. Otherwise, the PB-CLC control will coordinate the movements of the platoon and the subject vehicles to complete the lane-change requests with the aim to minimize the negative impacts on the platoon. Once the subject vehicle is well positioned beside an acceptable target spacing, the lateral lane-change movements can be conducted quickly within a sample time interval $\tau < 1$ sec. Accordingly, this study mainly focuses on the longitudinal platooning control for accommodating lane-change requests and ignores subject vehicles' lateral movements during cut-in maneuvers. However, we should note that the vehicles' lateral cut-in dynamics can be easily incorporated into our current model using steering control, that will not affect the longitude constraints or increase the mathematical complexity of the

¹ The discretionary lane-change seeks to gain speed privilege, of which the time window is usually 6-11 seconds; The mandatory lane-change is required according to the trip plan, such as moving to off-ramp, of which the time window is usually 1-3 seconds.

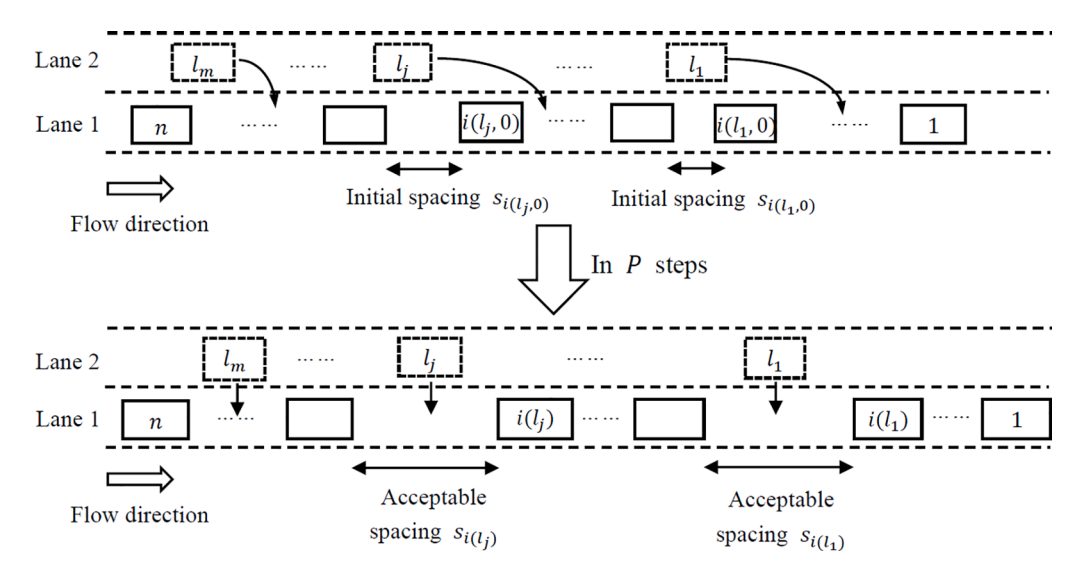


Fig. 1. Lane-change process.

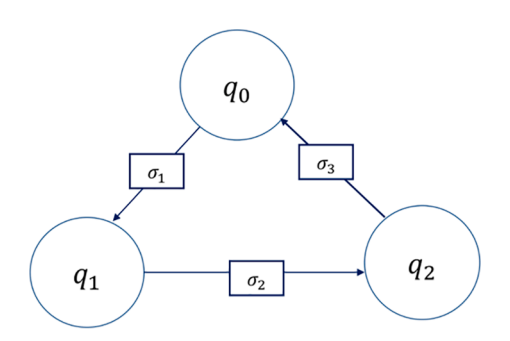


Fig. 2. Hybrid MPC system.

MINLP-MPC model and the hybrid MPC system. The developed lateral control law also demonstrates that the lateral movements can be fulfilled within a sample time interval (1 sec). Please see the mathematical demonstration in the Appendix-I.

It is also noticed that the neighborhood traffic around the subject vehicles or the platoon may cause the infeasibility for the platoon to accommodate lane-change requests within a given time window. For example, there may exist uncontrolled vehicles around subject vehicles or the platoon, which potentially limit the CAVs' trajectory control. As a result, the CAV platoon may not be able to yield spacings for the lane-change accommodation within a given time window. As the first attempt to integrate lane-change into platooning control, this study assumes that the traffic conditions around subject vehicles and platoon are suitable during the accommodation process so that the CAVs' trajectory control is not constrained by surrounding traffic (i.e., uncontrolled vehicles). These more complicated scenarios will be addressed in future work. In addition, we assume that no overtaking occurs between subject vehicles during the relatively short lane-change accommodation process for safety and efficiency. Lastly, this study assumes that wireless connections between all CAVs perform well, thus the communication delay and failures are neglected.

Using the example shown in Fig. 1, we formally introduce the problem setup as follows. We consider that it is very possible that multiple vehicles require lane-change simultaneously. Thus, without loss of generality, this study considers m subject vehicles, denoted by $l_1, l_2, ..., l_m$ respectively in Fig. 1 moving with the speed $v^1, v^2, ..., v^m$ and the acceleration $u^1, u^2, ..., u^m$ respectively on the subject Lane 2. They send lane-change requests to the platoon on the target lane which is Lane 1 in Fig. 1 simultaneously. Notation l is used to denote a subject vehicle while the set of the subject vehicles is denoted by $L = \{l_1, l_2, ..., l_m\}$. Besides, without confusion, notation l is also used to describe the index of a subject vehicle l = 1, 2, ..., m while the index set is also denoted by $L = \{1, 2, ..., m\}$.

We consider there are n many CAVs in the platoon, and let x_i , v_i u_i for $i \in I = \{1, ..., n\}$ respectively represent the longitudinal position, speed, and acceleration of the ith platoon vehicle. Accordingly, notation i(l, 0) for $i \in I$, $l \in L$ is used to indicate a particular platoon vehicle i that locates immediately in front of the subject vehicle i at step i0. Here i0 represents the time step when the platoon receives the lane-change requests, indicating the start of the lane-change accommodation control. The details of the notation i0 and relevant concepts will be fully discussed in next section. We then introduce i1 to label the spacings between two adjacent platoon vehicles. Additionally, the notation i1 for i2 for i3 is used to label a spacing between two adjacent platoon vehicles i3 and i4 to and i5 notation i6 represents a particular spacing between two platoon vehicles i6, i7 and i8 and i9 and i1, which is initially

Table 1 Notation list.

Notation	Description	Туре
τ	Sample time interval	Parameter
k	Control time step	Index
p	Lane-change time step	Index
i	Platoon vehicle's index	Index
I	Platoon vehicles index set	Set
x_i	Platoon vehicle i's longitudinal position	Continuous variable
$ u_i$	Platoon vehicle i's longitudinal speed	Continuous variable
u_i	Platoon vehicle i's longitudinal acceleration	Continuous variable
L_i	Platoon vehicle i's vehicle length	Continuous variable
$a_{min,i}/a_{max,i}$	Platoon vehicle i's acceleration/deceleration limits	Continuous variable
1	Subject vehicle's index & notation	Index & notation
L	Subject vehicles' index & notation set	Set
x^{l}	Subject vehicle l's longitudinal position	Continuous variable
v^l	Subject vehicle l's longitudinal speed	Continuous variable
u^l	Subject vehicle l's longitudinal acceleration	Continuous variable
L^l	Subject vehicle l's length	Continuous variable
a_{min}^l / a_{max}^l	Subject vehicle <i>l</i> 's acceleration/deceleration limits	Continuous variable
s_i	Spacing between platoon vehicle i and $i+1$	Index & value
i(l, 0)	A platoon vehicle located beside subject vehicle l at $p = 0$	Index
$S_{i(l,0)}$	A platoon spacing beside subject vehicle l at $p=0$	Index & value
$S_{i(l)}$	Subject vehicle l's target feasible lane-change spacing	Index
i(l)	Leading platoon vehicle ahead of spacing $s_{i(l)}$	Index
$y_{s,p}^l$	Subject vehicle l 's lane-change decision, i.e. spacing s , step p	Integer variable
s(l)	Subject vehicle l's target optimal lane-change spacing	Index
p(l)	Subject vehicle <i>l</i> 's target optimal lane-change time step	Index

beside the subject vehicle l at step p=0; notation $s_{i(l)}$ represents the feasible target spacing for subject vehicle l to cut in between platoon vehicles i(l) and i(l)+1. $s_{i(l)}$ is used in the feasibility proof for the MINLP-MPC model in section 4. In the meantime, notation s(l) and p(l) describe subject vehicle l's optimal lane-change spacing and timing respectively, which are employed in section 5 and section 6. Note that the notation s_i is abused in certain context to also denote the value of the spacing between two platoon vehicles i and i+1 to avoid extra notation. The labels of vehicles and spacings increase from downstream to upstream and the origin of the location coordinates is set at the tail of the platoon. The trajectory control is conducted at discrete time steps ($k \in \mathbb{Z}_+ := \{0,1,2,...\}$) with an uniform duration τ and the control variables u_i (i=1,...,n) keep constant during an interval τ . In addition, we use k to substitute τk for the notational simplicity hereafter.

Apart from the above-mentioned problem formulation, we formally introduce the hybrid MPC system, which is used to capture and control the entire lane-change accommodation process. Specifically, the hybrid MPC system in Fig. 2 consists of the following three dynamic states under sequential MPC control: car-following state under MPC- q_0 platooning control \rightarrow spacing preparation state under MPC- q_1 for preparing spacing to accommodate lane-change requests \rightarrow restoration state under MPC- q_2 for restoring the initial car-following control q_0 after lane-change. The three MPC states are well linked by three switching signals σ_1 , σ_2 and σ_3 and thus forms a closed-loop cycle, indicating the platoon can go through the entire lane-change process smoothly. Specifically, the completion of solving the cooperative lane-change decision model MINLP-MPC triggers the switching signal σ_1 to start the switching from car-following state q_0 to spacing preparation state q_1 . When the platoon under state q_1 finishes preparing the lane-change spacing, well-positioned subject vehicles will smoothly cut in the platoon, which triggers the switching signal σ_2 . Then the platoon switches to the restoration state q_2 and will not return to the initial car-following state q_0 until the car-following safe constraints are recovered (switching signal σ_3). The mathematical formulations of the hybrid MPC system and the proofs of the closed-loop cycle feasibility and stability are presented in Section 5

To facilitate the reading of the presented mathematical work, we summarize the notations introduced above as well as some commonly used notations in Table 1 which will be mentioned later in the model formulation section. We will also define other notations that are only used in some specific sections. To avoid a very long list, we do not include them in Table 1.

3. MINLP-MPC Mathematical Model for PB-CLC Control

This section first introduces the vehicle dynamics and constraints and then develops lane-change constraints. Built upon that, we formulate the MINLP-MPC model to implement the lane change decision for the PB-CLC control.

3.1. Vehicle dynamics and constraints

We first formulate the constraints related to vehicle dynamics and car-following safety. The longitudinal dynamics of CAVs are described by the double integrator model in Equations (1)-(4) for discrete time steps $\forall k \in \mathbb{Z}_+ := \{0,1,2,...\}$. Specifically, Equations (1) and (2) describe the subject vehicles' dynamics while Equations (3) and (4) describe the platoon vehicles' dynamics.

$$x^{l}(k+1) = x^{l}(k) + \tau v^{l}(k) + \frac{\tau^{2}}{2}u^{l}(k), \ l \in L$$
(1)

$$v'(k+1) = v'(k) + \tau u'(k), \ l \in L$$
(2)

$$x_i(k+1) = x_i(k) + \tau v_i(k) + \frac{\tau^2}{2} u_i(k), \ i \in I$$
(3)

$$v_i(k+1) = v_i(k) + \tau u_i(k), \ i \in I$$
 (4)

In addition, we consider that the CAVs in the problem are subject to important state and control constraints summarized as follows for any control sampling point $k \in \mathbb{Z}_+ := \{0, 1, 2, ...\}$

$$a_{min,i} \le u_i(k) \le a_{max,i}; \ a_{min}^l \le u^l(k) \le a_{max}^l, \ i \in I, \ l \in L$$
 (5)

$$v_{min} \le v_i(k) \le v_{max}; \ v_{min} \le v^l(k) \le v_{max}, \ i \in I, \ l \in L$$

$$\begin{cases}
 x_{i}(k) - x_{i+1}(k) \ge LB_{i+1} + \tau v_{i+1}(k) - \frac{\left[v_{i+1}(k) - v_{min}\right]^{2}}{2a_{min,i}}, & i \in I \\
 x'(k) - x^{l+1}(k) \ge LB^{l+1} + \tau v^{l+1}(k) - \frac{\left[v^{l+1}(k) - v_{min}\right]^{2}}{2a_{min}^{l+1}}, \{l, l+1\} \in L
\end{cases}$$
(7)

More exactly, Equation (5) limits vehicles' control inputs within given acceleration/deceleration bounds, respectively denoted by $a_{max,i}/a_{min,i}$ for platoon vehicle i and a_{max}^l/a_{min}^l for subject vehicle l. Equation (6) limits vehicles' longitudinal speeds within the predefined minimum and maximum speed, respectively denoted by v_{min} and v_{max} . Equation (7) presents the safety distance constraints. It is modified from the conflict-free car-following constraint. It ensures traffic safety under the extreme condition that the leading vehicle stops suddenly. Since the extreme condition barely occurs in reality, the conflict-free constraint is too conservative and cannot be used to improve road capacity. We adopt the less conservative constraint in Equation (7), which maintains traffic safety under the condition of $v_{min} = 0$, and allows a relatively small spacing to fully utilize the road capacity while ensuring the MPC's sequential feasibility. Notations LB_i and $LB^l > 0$ are constant values of platoon vehicle i and subject vehicle l respectively, which are related to the vehicle length and the minimum car-following buffer spacing when vehicles come to a stop.

3.2. Lane-change Constraints

We next provide the formulations to model the lane-change maneuvers. To do that, we introduce another notation p to represent the time step, at which a lane-change accommodation process proceeds. In addition, we consider the lane-change accommodation must be completed in next P steps. Thus, we have $p \in P = \{0, 1, ...P\}$. In addition, we assume several subject vehicles simultaneously send lane-change requests at control time step $k = k^*$ (i.e., p = 0), indicating the begin of the lane-change accommodation process. Accordingly, the control time step $(k^* + p) \in \mathbb{Z}_+$ is the same step with the lane-change time step p for $p \in P$.

To ensure safe and successful lane-change maneuvers, the PB-CLC control seeks to make lane-change decisions on two items: a) the best spacings ($s \in S = \{1, ...n-1\}$) in the platoon to accommodate the subject vehicles, and (b) the best time steps to perform the lane-change maneuvers. These two decisions should be optimally made with the aim to minimize the negative impact on the traffic efficiency and smoothness of the platoon, while ensuring the safety of completing the lane-change maneuvers within a given time window. Built upon the idea, this study considers the following constraints in Equations (8)-(11). Specifically, Equation (8) indicates that a lane-change request can only be accommodated by one platoon spacing at one time step.

$$\begin{cases}
\sum_{p=1}^{P} \sum_{s=1}^{n-1} y_{s,p}^{l} = 1, \ l \in L, \\
y_{s,p}^{l} = \{0,1\}, \ s \in S, \ p \in P,
\end{cases}$$
(8)

where the binary variables $y_{sp}^l = 1$ if the spacing s is selected for the subject vehicle l to cut in at time step $p \le P$. Otherwise, $y_{sp}^l = 0$. Next, this study notes that the lane-change requests should be served in a limited time window (τP), which can be relatively flexible for discretionary lane-changes but strict for mandatory lane-changes. For example, the mandatory lane-change request for exiting highway to an off-ramp must be completed before the vehicle passing the exit point. Accordingly, we introduce the constraints in Equation (9), which indicates that the acceptable spacings for lane-change have to be yielded within the time window τP .

$$\sum_{n=1}^{+\infty} p y_{s,p}^l \le P, \ l \in L \tag{9}$$

Considering the lane-change requests are accommodated and conducted in a relatively short time and the overtaking behavior is unsafe and inefficient during lane-change maneuvers, this study regulates that no overtaking occurs between subject vehicles once

they send the lane-change requests. Therefore, if the spacing s is selected for subject vehicle l, only the spacing after s (i.e., the spacing s, s+1,...n-1) can be selected for subject vehicle l+1. This idea is mathematically illustrated in Equation (10) below.

$$\sum_{p=1}^{P} \sum_{s=1}^{n-1} s y_{s,p}^{l} \le \sum_{p=1}^{P} \sum_{s=1}^{n-1} s y_{s,p}^{l+1}, \ \{l, l+1\} \in L$$
 (10)

Moreover, if the spacing s is selected for the subject vehicle l to conduct the lane-change at step p, namely $y_{sp}^l = 1$, then subject vehicle l should have arrived beside the target acceptable spacing s (i.e. s_i) between platoon vehicles i and i+1 at step p, ready to conduct the lane-change. Additionally, to ensure safe and smooth lane-change control (i.e., ensure the feasibility and stability of the hybrid system controller in Section 5), this study makes the regulations that the subject vehicle l will keep the safe distance h away from the immediate adjacent platoon vehicles after it cuts in the platoon until step P. These relationships are described in Equation (11) below. Note that Equation (11) is different from common lane-change safety distance constraints in a lane-change decision model. It is particularly designed when considering the feasibility of dynamic state switching under the hybrid MPC system. See Appendix-II for a more comprehensive discussion.

$$\begin{cases} x^{l}(p) - x_{i+1}(p) \ge h + M\left(\sum_{\mathfrak{p}=0}^{p} y_{s,\mathfrak{p}}^{l} - 1\right), \ s \in S, \ p \in P, \ l \in L, \\ x_{i}(p) - x^{l}(p) \ge h + M\left(\sum_{\mathfrak{p}=0}^{p} y_{s,\mathfrak{p}}^{l} - 1\right), \ s \in S, \ p \in P, \ l \in L, \end{cases}$$
(11)

where M is a large positive number and h represents the constant safe leading and following distance between the subject vehicle and its immediate leading and following platoon vehicles on the target lane so that a safe lane-change maneuver can be sustained. It is noted that Equation (11) is trivial when the spacing s and time steps $\mathfrak{p} \in \{0,1,...p\}$ are not selected as optimal lane-change decision for subject vehicle l (i.e., Equation (11) is always true if $\sum_{\mathfrak{p}=0}^p \mathcal{p}_{s,\mathfrak{p}}^l = 0$). Note that the lane-change study Roelofsen (2009) points out that the safe lane-change distance h for human-drive vehicles should be a variable closely related to the leading and following vehicles' speeds rather than a constant, aiming to ensure safe lane-change control even in extreme scenarios where the following uncontrolled vehicle's speed is far smaller than that of the leading uncontrolled vehicle. However, the rigorous mathematical formulation of safe lane-change distance h is unclear in the current literature. And in this study, the leading and following vehicles are CAVs under our platooning control. Therefore, this study adopts the constant safe lane-change distance and further regulates the safe lane-change distance h will hold after lane change, which avoids the extreme scenarios and thus ensures safe lane-change control. In fact, this regulation achieves the same safety performance as using a variable lane-change distance and will potentially facilitate the development of the hybrid system controller in Section 5.

3.3. Mixed Integer Nonlinear Programming Based Model Predictive Control

Based upon the constraints above, this section proposes the P-step MINLP-MPC model. Mainly, by taking vehicles' current states as initial inputs, the P-step MINLP-MPC model generates the optimal lane- change decisions along with the longitudinal vehicle trajectory instructions in next P steps, so that safe and smooth lane-change maneuvers are ensured to be completed at the best spacings and timings without significantly impairing the platoon's traffic efficiency and smoothness. Below, we present the MINLP-MPC model in detail. Note that according to the feasibility analysis and proofs in Section 4, the prediction horizon P of the MINLP-MPC model should be greater or equal to a lower bound \underline{P} of the lane-change time window. For discussion convenience, we let P equal to the lower bound P in this study.

Considering the potential insertion of lane-change subject vehicles, the spacing error at s_i and relative speed for platoon vehicle i at step p are modeled by Equation (12) and (13) respectively at lane-change time step $p \in P$: ={0, 1, ...P}, subject to the dynamics in Equations (1) and (4).

$$\Delta x_{s_i}(p) = x_i(p) - x_{i+1}(p) - s_d \left(1 + \sum_{l} \sum_{p=1}^{p} y_{i,p}^l \right), \ s_i \in S, \ p \in P,$$
(12)

$$\Delta v_i(p) = v_i(p) - v_{i+1}(p), \ i \in I \setminus \{n\}, \ p \in P,$$
(13)

where s_d is the constant desired spacing of the platoon on the target lane. Equation (12) indicates that if $\mathfrak m$ many subject vehicles cut in the same spacing s_i before the time step p (i.e. $\sum_i \sum_{\mathfrak p=1}^p y_{s_i,\mathfrak p}^l = \mathfrak m$), the desired spacing at s_i is $\mathfrak m s_d$ at step p.

According to Equations (12) and (13), the control dynamics during lane-change maneuvers are defined in Equations (14) and (15).

$$z(p) := (\Delta x_1(p), ..., \Delta x_{n-1}(p))^T \in \mathbb{R}^{n-1}$$
(14)

$$\mathbf{z}'(\mathbf{p}) := (\Delta \mathbf{v}_1(\mathbf{p}), \dots, \Delta \mathbf{v}_{n-1}(\mathbf{p}))^T \in \mathbb{R}^{n-1}$$

$$\tag{15}$$

Wrapping up the constraints above, the optimizer of the MPC at step p = 0 is given by the MINLP-MPC model below in Equations

(1)-(16), with the control variables $u = \{u_i(p), \ u^l(p), \ i \in I, \ l \in \mathscr{L}, \ p \in P\} \in \mathbb{R}^{n+m}, \ y = \{y_{s,p}^l \text{ for } s \in S, \ p \in P, l \in \mathscr{L}\} \in \mathbb{R}^{(n-1)^*P^*m}.$

$$\mathbf{Min} \ \Gamma(u,y) = \sum_{p=1}^{P} \left\{ \frac{1}{2} \left[z^{T}(p) Q_{z} z(p) + (z'(p))^{T} Q_{z'} z'(p) \right] + \omega_{1} \frac{\tau^{2}}{2} \| \ u(p-1) \|_{2}^{2} \right\} + \omega_{2} \sum_{l \in \mathcal{L}} \sum_{s=1}^{n-1} \sum_{p=1}^{P} p y_{s,p}^{l}$$

$$\tag{16}$$

Subject to: for each $p \in P$: ={1, ..., P}, Eq (1)-(15), where Q_z : = $\Omega^T D_\alpha \Omega$ and Q_x : = $\Omega^T D_\beta \Omega$ are symmetric and positive definite matrices and $u(p) = \{u_i(p), i \in I\} \in \mathbb{R}^n$. Ω is an orthogonal matrix which characterizes the interaction of the CAVs under the platooning control. The diagonal matrices $D_\alpha = \operatorname{diag}(\alpha_1, \ldots, \alpha_n)$ and $D_\beta = \operatorname{diag}(\beta_1, \ldots, \beta_n)$, where $\alpha_i > 0$ and $\beta_i > 0$ are penalty weights for each spacing error and relative speed term respectively (i.e., $i = 1, \cdots, n-1$). Let $\alpha : = (\alpha_1, \ldots, \alpha_{n-1})$ and $\beta : = (\beta_1, \ldots, \beta_{n-1})$. The selection of α and β will affect the stability performance of the platoon and has been fully investigated in Gong et al. (2016).

The objective function Γ seeks to make a balance between minimization of the traffic flow oscillations and the promptness of the lane-change accommodation by putting proper penalty weights Q_z , Q_z , ω_1,ω_2 respectively on the following four penalty terms: (i) the errors between desired vehicle spacings and actual spacings; (ii) the fluctuations of the spacings between adjacent platoon vehicles, i. e., the relative speed between adjacent vehicles; (iii) the variations of vehicle speeds, i.e., acceleration /deceleration; and (iv) the lane-change accommodation promptness. In reality, we can assign a relatively small penalty weight ω_2 for a discretionary lane-change request so that the control mainly focuses on platoon smoothness, whereas a large penalty weight ω_2 for a mandatory lane-change request such that the control gives higher priority to a prompt response. The constraints in Equations (1)-(11) represent the constraints related to vehicle dynamics and the lane-change maneuver. Equations (12)-(15) describe the control dynamics and the interdependent relationships between variables in the objective function. Note that the MINLP-MPC model is only activated at step p=0 when the platoon receives the lane-change requests.

Remark 1. The MINLP-MPC model can be easily extended to the case of three-lane highway. Specifically, consider lane-change requests are sent from both two side lanes beside the platoon, denoted by lane R_1 and R_2 respectively. In this case, we can apply the safety distance constraints in Equation (7) and the non-overtaking constraints in Equation (10) to subject vehicles on both lane R_1 and lane R_2 . Since no additional complicated variables or constraints are involved, it will not bring in new conceptual and computational challenges.

4. MINLP-MPC Model Feasibility

It is noticed that if the lane-change time window P is too small or the platoon and the subject vehicles are not properly positioned, the target platoon may not be able to yield spacings to accommodate the lane-change requests within the duration of the time window. This means that the MINLP-MPC model is infeasible. This section thus investigates a lower bound of the lane-change time window P by analyzing the feasibility of the MINLP-MPC model, charactering the initial states of the platoon and subject vehicles. The feasibility analysis will also facilitate the development of the hybrid MPC system and solution approaches later. In addition, this study observed that the presentation of the feasibility proof is tremendously complicated as more subject vehicles are involved. Thus, without loss of generality, this study first proves the MINLP-MPC model feasibility only considering two subject vehicles (m = 2), and then extends the proof to more general cases involving more subject vehicles (m > 2) using the same approaches. To simplify the proof process and better illustrate the key ideas of the proof, this section considers the homogenous case that all vehicles share the same vehicle length and buffer safe distance constant LB as well as deceleration/acceleration limits a_{min}/a_{max} , but our proof can be easily extended to the heterogeneous cases. Below we illustrate the main ideas of the proofs.

To prove the feasibility of the MINLP-MPC model, we essentially need to demonstrate the intersection of the constraint sets in Equations (1)-(15) is not empty at any lane-change time step $p \in P$, given that it starts from a feasible scenario at step p = 0. Note that the control dynamic constraints in Equations (12)-(15) are naturally feasible once the constraints in Equations (1)-(11) are feasible. Thus we omit Equations (12)-(15) and only consider Equations (1)-(11) in our following proofs. By analyzing the features of the MINLP-MPC model, we further recognized that it is hard to directly prove the feasibility of the constraints in Equations (1)-(11) due to the involvement of integer variables in the lane-change constraints in Equations (8)-(11). To solve this difficulty, we separate the constraint sets into two parts as follows.

- (i) $\mathscr{S}_1(u(p))$: It is the convex constraints set in Equations (1)-(7) for capturing the vehicle dynamics, acceleration, speed and safety constraints at step $p \in P$. Besides, $\mathscr{S}_1(u_i(p))$ and $\mathscr{S}_1(u^l(p))$ represent the platoon vehicle i and subject vehicle l's constraints set respectively in Equations (1)-(7) at step $p \in P$. Mathematically, $\mathscr{S}_1(u(p)) = \{\mathscr{S}_1(u_i(p)), \mathscr{S}_1(u^l(p)), i \in I, l \in L\}$.
- (ii) $\mathscr{S}_2(u(p),\ y_{s,p}^l)$: It is the lane-change related constraints set in Equations (8)-(11) involving integer variables at step $p \in P$.

Built upon the abovementioned two separate constraints sets, we prove the feasibility of the MINLP-MPC under the case with two subject vehicles by the idea as follows. First, we prove the constraints set $\mathscr{S}_1(u(p))$ is not empty at every step $p \in P$. Then, we prove that with a proper P, for every step $p \in P$, there exists at least one feasible solution in $\mathscr{S}_1(u(p))$, which also satisfies $\mathscr{S}_2(u(p), y_{sp}^l)$. Namely, for $\forall p \in P, \exists u(p) \in \mathscr{S}_1(u(p))$, and $\{u(p), y_{sp}^l\} \in \mathscr{S}_2(u(p), y_{sp}^l)$. This entire proof is structured and achieved by Lemma 1-Lemma 5 and then Theorem 1. Below we introduce Lemma 1 first, which proves the platoon's sequential feasibility, given it starts from a feasible initial state at step p=0.

Lemma 1. For $k \in \mathbb{Z}_+ := \{0, 1, 2, ...\}$ and $i \in I$, if $\mathscr{S}_1(u_i(k-1))$ is feasible, then $\mathscr{S}_1(u_i(k))$ is feasible and compact. In addition, the feasible control inputs profile $\mathbb{S}_1(u_i(k))$ for platoon vehicle i at step k is given below:

$$u_i(k) \in \mathbb{S}_1(u_i(k)) = \left[\max \left\{ a_{min}, \underline{a_{i,v}}(k) \right\}, \min \left\{ a_{max}, \overline{a_{i,v}}(k), \ \overline{a_{i,d}}(k) \right\} \right]$$

$$(17)$$

Where,

$$a_{i,v}(k) = \frac{v_{min} - v_i(k-1)}{\tau} \le 0 \tag{17.1}$$

$$\overline{a_{i,v}}(k) = \frac{v_{max} - v_i(k-1)}{\tau} \ge 0 \tag{17.2}$$

$$\overline{a_{i,d}}(k) = \frac{3}{2} a_{min} + \underline{a_{i,v}} - \frac{a_{min}}{\tau^2} \sqrt{B(k)}$$
(17.3)

$$B(k) = \frac{\left(v_i(k-1) - v_{min}\right)^2 \tau^2}{a_{min}^2} + \frac{\tau^3 \left(v_i(k-1) - v_{min}\right)}{-a_{min}} + \frac{9}{4}\tau^4 + \left(\frac{2\tau^2}{-a_{min}}\right) \left[\left(\frac{v_{i-1}(k-1) + v_{i-1}(k)}{2} - v_{min}\right)\tau + \mathcal{S}_1(u_i(k-1))\right] \ge 0$$
 (17.4)

Proof:

Lemma 1 has been proved and the mathematical representations in Equations (17) and 17.1)-(17.4) are accordingly formulated by the lemma 4.1 of Gong and Du (2018). The main idea of the proof is to show the intersection of the constraints in Equations (1)-((7) is nonempty at control step k if the platoon is running under the feasible constraints at control step k-1, $k \in \mathbb{Z}_+$.

Using the results in Lemma 1, this study wants to further prove that there exsits feasible control inputs which satisfies both $\mathcal{S}_1(u(p))$ and $\mathcal{S}_2(u(p), y_{s,p}^l)$ for $\forall p \in P$. It is equivalent to saying that we are able to find feasible control inputs for the platoon to adjust its spacings so that the lane-change requests can be successfully completed within the lane-change time window P. To do that, it is noticed that the numerical value of the lane-change time window P will affect the feasibility. For example, a short time window may not provide enough time for the platoon to adjust its spacings and then accommodate the lane-change requests. Built upon this note, the main idea of the following proof is to find a lower bound for the lane-change time window P, denoted by P_E , so that the feasibility of the MINLP-MPC model can be sustained if the platoon and subject vehicles are initially under general feasible scenarios ($\mathbb E$). Lemma 2-Lemma 5 below complete this proof. Mainly, we first define an extreme scenario (E) for the platoon and subject vehicles, and then Lemma 2 proves that any other general scenario ($\mathbb E$) can be transferred to this extreme scenario (E) in finite steps (say $J(\mathbb E(k^*) \to E)$), using the feasible control input from $\mathbb S_1(u(k))$. Here k^* represents the control time step when lane change requests are received (at P = 0) and E = 0 which ensures the feasibility of the MINLP-MPC model under the extreme scenario (E). Then we can induce that there exists a lower bound E = 0 and E = 0, which ensures the feasibility of the MINLP-MPC under general scenario (E = 0). This study first formally defines the scenario (E = 0) and then introduce Lemma 2.

(E): $v_{min} \leq v_i \& v^l \leq v_{max}$, $\mathfrak{g}_i \leq 0$ and $\mathfrak{g}^l \leq 0$, $\forall i \in I$, $l \in L$, which are equivalent to the speed and safety distance constraints in Equations (6) and (7). Specifically, \mathfrak{g}_i and \mathfrak{g}^l are derived from Equation (7): $\mathfrak{g}_i = LB_{i+1} + \tau v_{i+1} - \frac{[v_{i+1} - v_{min}]^2}{2a_{min,i+1}} - (x_i - x_{i+1})$, $\mathfrak{g}^l = LB^{l+1} + \tau v^{l+1} - \frac{[v^{l+1} - v_{min}]^2}{2a^{l+1}} - (x^l - x^{l+1})$.

(E): $v_i \& v^l = v_{\min}, \ g_i \leq 0 \text{ and } g^l \leq 0 \quad \text{ for } \forall i \in I, l \in L.$

Mainly, a general scenario (\mathbb{E}) represents a feasible car-following scenario satisfying the constraint set $\mathcal{S}_1(u(p))$, whereas the extreme scenario (E) indicates that all platoon vehicles and subject vehicles are running at minimum speed with safe inter-vehicle spacings.

Lemma 2. For $k^* \in \mathbb{Z}_+ := \{0, 1, 2, ...\}$, there exists a control input profile $u(\mathbb{E}(k^*) \to E) \in \mathbb{S}_1(u(k))$ so that a platoon and subject vehicles under the scenario $\mathbb{E}(k^*)$ can be converted to the extreme scenario (E) in the number of time steps: $J(\mathbb{E}(k^*) \to E) = \left| \frac{v_{max} - v_{min}}{-\tau a_{min}} \right|$.

Proof. This study proves that any other scenario $\mathbb{E}(k^*)$ at step k^* can be transferred to this extreme scenario (E) using the feasible control inputs in $\mathbb{E}(u(k))$ for $k \in \{k^*, ...k, k^* + P\}$ within the number of steps $\left\lfloor \frac{v_{max} - v_{min}}{-\tau a_{min}} \right\rfloor$. Below we can construct a control input profile $u(\mathbb{E}(k^*) \to E) = \{u_i(\mathbb{E}(k^*) \to E), u^l(\mathbb{E}(k^*) \to E) \text{ for } i \in I, \ l \in L\} \in \mathbb{S}_1(u(k))$ to make all vehicles simultaneously decelerate, which transfers the scenario $\mathbb{E}(k^*)$ to (E).

$$u_i(\mathbb{E}(\boldsymbol{k}^*) \to E) = \left\{ \begin{aligned} a_{\min}, & \text{if } v_i(k) \geq v_{\min} - \tau a_{\min} \\ \frac{v_{\min} - -v_i(k)}{\tau}, & \text{if } v_{\min} \leq v_i(k) < v_{\min} - \tau a_{\min} \end{aligned} \right\} \in \mathbb{S}S_1(u(k)),$$

$$u^{l}(\mathbb{E}(k^{*}) \to E) = \begin{cases} a_{min}, & \text{if } v^{l}(k) \ge v_{min} - \tau a_{min} \\ \frac{v_{min} - - v^{l}(k)}{\tau}, & \text{if } v_{min} \le v^{l}(k) < v_{min} - \tau a_{min} \end{cases} \in sS_{1}(u(k)),$$

where $k \in \left\{k^*, k^*, ..., k^* + \left\lfloor \frac{v_{max} - v_{min}}{-\tau a_{min}} \right\rfloor\right\}$ When the vehicle's speed at step k ($v_i(k)$ or $v^l(k)$) is larger than $v_{min} - \tau a_{min}$, the vehicle decelerates at the maximum deceleration a_{min} . As the speed gets close to v_{min} , specifically when $v_{min} \le v_i(k)$ or $v^l(k) < v_{min} - \tau a_{min}$, the vehicle cannot sustain the maximum deceleration a_{min} so that it will decelerate with $u_i = \frac{v_{min} - -v_i(k)}{\tau}$ or $u^l = \frac{v_{min} - -v^l(k)}{\tau}$.

Accordingly, the maximum number of the deceleration time steps needed for a platoon and subject vehicles under a general scenario $\mathbb{E}(k^*)$ converting to the extreme scenario E is given in Equation (18).

$$J(\mathbb{E}(k^*) \to E) = \begin{vmatrix} v_{max} - v_{min} \\ -\tau a_{min} \end{vmatrix}$$
 (18)

With the results above, we complete the proof for Lemma 2. ■

Built upon the results of Lemma 2, this study next seeks to find the feasible lower bound $\underline{P_E}$ under the extreme scenario (*E*). To achieve this goal, we start from Lemma 3, which introduces a sequential acceleration strategy to ensure the platoon has target lane-change spacings large enough to accommodate subject vehicles' lane change, utilizing the feasible control inputs. Then we investigate a simple case with only one subject vehicle requiring for lane change in Lemma 4. Lemma 5 further extends the results to the case involving two subject vehicles and the following Theorem 1 summarize the results. Remark 2 finally generalizes the results to the cases involving more than two subject vehicles. Note that Lemma 2 above is applied under scenario $\mathbb{E}(k^*)$ at control time step $k^* \in \mathbb{Z}_+$: $= \{0,1,2...\}, \text{ when the lane-change requests are received. Accordingly, any general scenario } \mathbb{E}(k^*) \text{ which starts at control step } k^* \text{ has been transferred to extreme scenario } (E) \text{ at step } k^* + \left\lfloor \frac{v_{max} - v_{min}}{-\tau \alpha_{min}} \right\rfloor. \text{ For simplicity, we drop the control time step index } k^* + \left\lfloor \frac{v_{max} - v_{min}}{-\tau \alpha_{min}} \right\rfloor \text{ but use the lane change time step } p \in P := \{0, 1...P\} \text{ for extreme scenario } (E) \text{ in the following proofs.}$

Lemma 3. Assume that the platoon and m subject vehicles are under extreme scenario (E) at p=0, and subject vehicles intend to cut in different target spacings, a sequential acceleration strategy $\widetilde{u} \in \mathbb{S}_1(u)$ in Equation (19) can be constructed for platoon vehicles to yield safe spacings $s_i(p^*) \geq 2h$ (for $\forall i \in I \setminus \{n\}, p^* \in \{(i+1)^*\mathfrak{m}, ...P\}$) to accommodate subject vehicles' lane-change requests, where $m=\left\lfloor \frac{v_{\max}-v_{\min}}{\tau a_{\max}} \right\rfloor$.

$$\widetilde{u} = \{u_i(p), p \in P, i \in I \} \in \mathbb{S}_1(u(k)), \ u_i(p) = \begin{cases} a_{max} & \text{if } p \in [(i-1)^*\mathfrak{m}, \ i^*\mathfrak{m}] \cap \mathbb{Z} \\ 0 & \text{otherwise} \end{cases}$$

$$(19)$$

Proof. Recall that all vehicles are initially under the extreme scenario (E), $v_i = v_{min}$, $\mathfrak{q}_i \leq 0$, $\forall i \in I \cup L$. By applying the \widetilde{u} , the platoon vehicles will sequentially accelerate their speed from v_{min} to v_{max} by the acceleration a_{max} in the order of i=1,2,...n. More exactly, it means that the first leading vehicle in the platoon labeled as i=1 will accelerate first. After its speed reaches v_{max} , the second vehicle i=2 start to accelerate, and the same acceleration process continues until the last vehicle i=n reaches speed v_{max} . Note that the time steps needed for a vehicle accelerating from v_{min} to v_{max} with the acceleration a_{max} is measured by $m=\left\lfloor \frac{v_{max}-v_{min}}{va_{max}} \right\rfloor$. As a result, the speed profile of the platoon vehicles can be described by Equation (20).

$$\forall i \in I, \ v_i(p) = \begin{cases} v_{min} & \text{if } p \in [0, \ (i-1)*\mathfrak{m}] \cap \mathbb{Z} \\ v_{min} + (p - (i-1)*m)\tau^*a_{max} & \text{if } p \in [(i-1)*\mathfrak{m}, \ i^*\mathfrak{m}] \cap \mathbb{Z} \\ v_{max} & \text{if } p \in [i^*\mathfrak{m}, \ P] \cap \mathbb{Z} \end{cases}$$

$$(20)$$

Specifically, by the definition of \widetilde{u} , for any platoon vehicle $i \in I$, $u_i(p) = 0$ at time steps $\forall p \in [0, (i-1)^*\mathfrak{m}] \cap \mathbb{Z}$, vehicle i maintains v_{min} and will not accelerate until all the leading vehicles reach v_{max} at time step $p = (i-1)^*\mathfrak{m}$. After that vehicle i takes \mathfrak{m} -many time steps to make its speed reach v_{max} at $p = i^*\mathfrak{m}$. Afterwards, platoon vehicle i keeps its speed at v_{max} constantly for the time steps $p \in [i^*\mathfrak{m}, P] \cap \mathbb{Z}$.

Based upon Equation (20), we first prove that $s_i(p^*) \ge 2h$ for $\forall i \in I \setminus \{n\}, \forall p^* \in \{(i+1)^*\mathfrak{m}, ...P\}$. To conduct the proof, we define $\Delta s_i(p^*)$ as the increased inter-vehicle spacing s_i between vehicles i and i+1 resulted from the control input \widetilde{u} by the time step p^* . Then $s_i(p^*)$ can be described in Equation (21):

$$s_i(p^*) = s_i(0) + \Delta s_i(p^*)$$
 (21)

Notice that by the step $p^* \in \{(i+1)^*\mathfrak{m},...P\}$, the platoon vehicles i and i+1 both have finished acceleration process sequentially. According to Equation (20), during the time interval $[(i-1)^*\mathfrak{m},\ i^*\mathfrak{m}]$, vehicle i accelerates from v_{min} to v_{max} with a_{max} while vehicle i+1 keeps speed v_{min} . During the time interval $[i^*\mathfrak{m},\ (i+1)^*\mathfrak{m}]$, vehicle i drives at speed v_{max} while vehicle i+1 accelerates from v_{min} to v_{max} with a_{max} . During other time intervals, vehicle i and i+1 have the same speed profile. Besides, platoon vehicles i and i+1 share the same acceleration dynamics and thus run the same distance during acceleration. Therefore, the increased inter-vehicle spacing

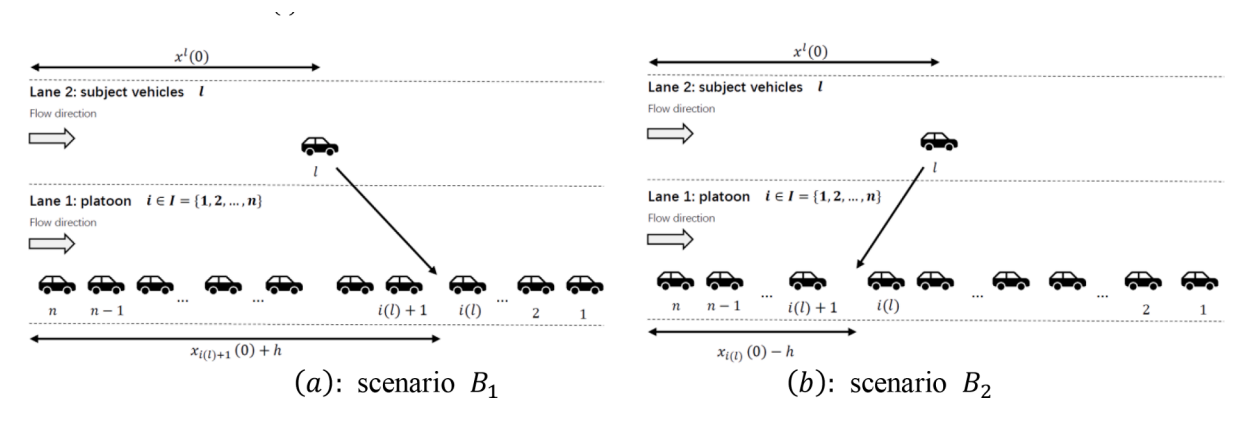


Fig. 3. Two scenarios B_1 , B_2 of one subject vehicle lane-change case.

 $\Delta s_i(p^*)$ between platoon vehicles i and i+1 is induced by the dynamic difference that vehicle i drives at speed ν_{max} during $[i^*\mathfrak{m},\ (i+1)^*\mathfrak{m}]$ for \mathfrak{m} time steps whereas vehicle i+1 drives at speed ν_{min} during the time interval $[(i-1)^*\mathfrak{m},\ i^*\mathfrak{m}]$ for another \mathfrak{m} time steps. Then we have

$$\Delta s_i(p^*) = \text{mtr}(v_{max} - v_{min}) \tag{22}$$

Under extreme scenario (*E*), $s_i(0) \ge LB_{i+1} + \tau v_{min}$ is derived from the definition of (*E*) and the safety distance constraints in Equation (7). Then combining Equations (21) and (22) above, immediately we have:

$$s_i(p^*) \ge LB_{i+1} + \tau v_{min} + \operatorname{int} \tau(v_{max} - v_{min})$$
 (23)

According to the references Manual (2000), Roelofsen (2009) and Bokare and Maurya (2017), we examine this distance is safe for a lane-change maneuver by considering the practical numerical values of the parameters as follows. $h \le 35m$; $v_{max} = 33$ m/s; $v_{min} = 21m/s$; $a_{max} \le 3.7m/s^2$; $-a_{min} \ge 3m/s^2$; $3m \le LB_i \le 5.9m$, $\tau = 1s$. Then $m = \begin{bmatrix} v_{max} - v_{min} \\ \tau a_{max} \end{bmatrix} \ge 4$; $2h \le 70m$. From the Equation (23) and the parameters above, we have $s_i(p^*) \ge 72m \ge 2h$.

Recall that we want to show the sequential acceleration strategy \widetilde{u} is feasible, namely it satisfies constraints in Equations (1)-(7) (i.e. $\widetilde{u} \in \mathbb{S}_1(u)$). It suffices to prove the safety constraints in Equation (7) can be satisfied in \widetilde{u} because all the other constraints in Equation (1)-(6) are naturally satisfied in the construction process of \widetilde{u} . Mathematically, we need to prove $s_i(p^*) \geq LB_{i+1} + \tau v_{i+1}(p^*) - \frac{(v_{i+1}(p^*) - v_{min})^2}{2a_{min,i+1}}$. Notice that under our assumptions, $LB_{i+1} + \tau v_{i+1}(p^*) - \frac{(v_{i+1}(p^*) - v_{min})^2}{2a_{min,i+1}} \leq LB_{i+1} + \tau v_{max} - \frac{(v_{max} - v_{min})^2}{2a_{min,i+1}} \leq 62.9m \leq 72m \leq s_i(p^*)$. Therefore, we complete the proof for Lemma 3.

Using the sequential acceleration strategy \widetilde{u} defined in Lemma 3, this study next investigates the feasible lower bound $\underline{P_{1,E}}(l)$ of the lane-change time window by Lemma 4, considering the case with only one subject vehicle $l=l_1$ or l_2 requiring for a lane change (m=1) under the extreme scenario (E).

Lemma 4. Assume that the platoon and two subject vehicles $\{l_1, l_2\}$ are under extreme scenario (*E*) at p = 0 and only one subject vehicle requires to cut in the target spacing $s_{i(l)} \in S$ between the platoon vehicle i(l) and i(l) + 1, $\underline{P_{1,E}}(s_{i(l)}|B)$ defined below can ensure the model feasibility.

$$\underline{P_{1,E}}(s_{i(l)}|B) = \begin{cases}
\max\left\{ (i(l)+1)m, \frac{(x_{i(l)+1}(0)+h)-x^l(0)}{\tau(v_{max}-v_{min})} + \frac{m}{2} + m\delta(l) \right\} & \text{if } B = B_1: \ x_{i(l)+1}(0) + h \ge x^l(0) \\
\max\left\{ (i(l)+1)m, \frac{(x^l(0)+h)-x_{i(l)}(0)}{\tau(v_{max}-v_{min})} + \left(i(l) - \frac{1}{2} \right)m \right\} & \text{if } B = B_2: \ x^l(0) \ge x_{i(l)}(0) - h
\end{cases}$$

where $\delta(l_2) = 1$ and $\delta(l_1) = 0$; B_1 and B_2 define two scenarios respectively that the subject vehicle l cuts in the spacing $s_{i(l)}$ which is before and after the subject vehicle l (see Fig. 3 (a) and (b)).

Proof. This proof considers that a lane-change maneuver consists of two procedures, which are respectively defined by \mathfrak{l}_1 and \mathfrak{l}_2 as follows.

 l_1 : The platoon adjusts the target spacing at $s_{i(l)}$ and make it larger than 2h so that it can accommodate the lane-change maneuver. We denote the number of the time steps needed to finish the procedure of l_1 as $J_1(s_{i(l)} \to 2h)$.

 l_2 : The subject vehicle l adjusts its speed to approach the target spacing $s_{i(l)}$. We denote the number of the time steps needed to finish l_2 as $J_2(\to s_{i(l)})$.

Notice that the two procedures \mathfrak{l}_1 and \mathfrak{l}_2 are conducted simultaneously to complete a lane change maneuver. Therefore, the lower bound of the lane-change time window equals to the larger number of steps of completing \mathfrak{l}_1 or \mathfrak{l}_2 , i.e., $\underline{P_{1,E}}(s_{i(l)}B) = \max\{J_1(s_{i(l)} \to 2h), J_2(\to s_{i(l)})\}$ According to Lemma 3, by applying the sequential acceleration strategy \widetilde{u} , we can ensure a safe spacing $s_{i(l)} \in S$ for the lane change at the time step $p^* \in \{(i(l)+1)^*\mathfrak{m}, ...P\}$. Correspondingly, the number of time steps needed for the procedure \mathfrak{l}_1 is bounded by Equation (24). Namely, the platoon needs $(i(l)+1)\mathfrak{m}$ time steps to enlarge the spacing $s_{i(l)}$ to be larger than 2h.

$$J_1(s_{i(l)} \to 2h) \ge (i(l) + 1)\mathfrak{m}$$
 (24)

Next, this study analyzes the number of the time steps $J_2(\to s_{i(l)})$ for a subject vehicle to approach the target spacing $s_{i(l)}$ (i.e., complete the procedure I_2). To do it, we consider two scenarios, B_1 and B_2 separately, in which the subject vehicle l is initially running behind or ahead of the target spacing $s_{i(l)}$. We use different acceleration strategies for B_1 and B_2 . More exactly, the subject vehicle l under scenario B_1 tends to accelerate to catch up the platoon vehicle i(l) + 1 ahead of it, while under scenario B_2 , the subject vehicle l tends to maintain the v_{min} speed to wait for the platoon vehicle i(l) to catch up.

We first discuss the number of time steps $J_2(\to s_{i(l)}|B_1)$ under scenario B_1 . To finish the lane-change maneuver, the subject vehicle l is required to arrive $s_{i(l)}$ and run ahead of the platoon vehicle i(l)+1 on the target lane with a safe lane change distance h by the time step $J_2(\to s_{i(l)}B_1)$. Notice that the procedure of \mathfrak{l}_1 guarantees that the target spacing $s_{i(l)}$ has double safe lane change spacing 2h. Therefore, once the subject vehicle l can run ahead of the platoon vehicle i(l)+1 with a safe lane change spacing h by time step $J_2(\to s_i)$, we ensure that the subject vehicle l can simultaneously run behind of the platoon vehicle i(l) with a safe lane change spacing h by the time step $J_2(\to s_{i(l)}B_1)$. Mathematically, this consideration is presented by Equation (25).

$$x^{J}(J_{2}(\to s_{i(l)}B_{1})) \ge x_{i+1}(J_{2}(\to s_{i(l)}B_{1})) + h$$
 (25)

Combining Equation (25) and the vehicle dynamics in Equations (1)-(4), the following deductions in Equation (26) provides the lower bound of the needed time steps $J_2(\rightarrow s_{i(1)}B_1)$ by applying the strategy \widetilde{u} to platoon vehicles 1, 2..., i(1), and $l=l_1$:

$$x^{l}(J_{2}(\rightarrow s_{i(l_{1})}|B_{1})) \geq x_{i+1}(J_{2}(\rightarrow s_{i(l_{1})}|B_{1})) + h \Leftrightarrow x^{l}(0) - (x_{i+1}(0) + h) + m\tau \frac{v_{max} + v_{min}}{2} + (J_{2}(\rightarrow s_{i(l_{1})}|B_{1}) - m)\tau v_{max} - J_{2}(\rightarrow s_{i(l)}|B_{1})\tau v_{min} \geq mJ_{2}(\rightarrow s_{i(l_{1})}|B_{1}) \geq \frac{(x_{i(l_{1})+1}(0) + h) - x^{l_{1}}(0)}{\tau(v_{max} - v_{min})} + \frac{m}{2}$$

$$(26)$$

To facilitate the articulation hereafter, we denote the sequential acceleration strategy applied by the platoon vehicles 1, 2, ..., i(l) and subject vehicle l above as $\widetilde{u}_{B_1} \in \widetilde{u}$. Mathematically, $\widetilde{u}_{B_1}(l) : \widetilde{u} \to \{1, 2, ..., i(l) \cup l\}$, which indicates that \widetilde{u}_{B_1} is applied to the subject vehicle l and the leading platoon vehicles 1, 2, ... i(l), not to the following platoon vehicles i(l) + 1, ... n. Therefore, the platoon vehicle i(l) + 1 and its following vehicles maintain the speed v_{min} for the subject vehicle l to catch up. In addition, Equation (26) considers that the subject vehicle l is the leading subject vehicle l_1 so that subject vehicle l can start to accelerate the speed at time step l in steps by which the subject vehicle l reaches the speed of l in steps by which the subject vehicle l reaches the speed of l in the subject vehicle l in the subject vehi

$$J_2(\rightarrow s_{i(l_2)}B_1) \ge \frac{(x_{i(l_2)+1}(0)+h)-x^{l_2}(0)}{\tau(v_{max}-v_{min})} + \frac{3}{2}\pi$$
(27)

Combining Equation (24) for $J_1(s_{i(l)} \to 2h)$ and Equations (26), (27) for $J_2(\to s_{i(l)}B_1)$, $\underline{P_{1,E}}(s_{i(l)}B_1)$ is calculated under situation B_1 mathematically by the Equations (28) and (29) respectively for the subject vehicle $l = l_1$ and $l = l_2$.

$$\underline{P_{1,E}}(s_{i(l_1)}B_1) = \max\{J_1(s_{i(l_1)} \to 2hB_1), \ J_2(\to s_{i(l_1)}B_1)\} = \max\left\{(i(l_1) + 1)\mathfrak{m}, \frac{(x_{i_1+1}(0) + h) - x^{l_1}(0)}{\tau(v_{max} - v_{min})} + \frac{\mathfrak{m}}{2}\right\}$$
(28)

$$\underline{P_{1,E}}(s_{i(l_2)}|B_1) = \max\{J_1(s_{i(l_2)} \to 2hB_1), \ J_2(\to s_{i(l_2)}B_1)\} = \max\left\{(i(l_2) + 1)\mathfrak{m}, \frac{(x_{i(l_2) + 1}(0) + h) - x^{l_2}(0)}{\tau(v_{max} - v_{min})} + \frac{3}{2}\mathfrak{m}\right\}$$
 (29)

Using the similar approach, we study the number of the time steps needed $J_2(\to s_{i(l)}|B_2)$ under B_2 scenario, using the acceleration strategy $\widetilde{u}_{B_2} \in \widetilde{u}$. The details of the analysis can be seen in Appendix-III. Then, $\underline{P_{1,E}}(s_{i(l)}|B_2)$ under scenario B_2 can be mathematically determined by the following Equation (49).

$$\underline{P_{1,E}}(s_{i(l)}|B_2) = \max\{J_1(s_{i(l)} \to 2hB_2), \ J_2(\to s_{i(l)}B_2)\} = \max\{(i(l)+1)\mathfrak{m}, \frac{(x^l(0)+h)-x_{i(l)}(0)}{\tau(v_{max}-v_{min})} + \left(i(l)-\frac{1}{2}\right)\mathfrak{m}\}$$
(30)

Wrapping the results in Equations (28), (29) and (30), we complete the proof for Lemma 4.

Built upon the results in Lemma 4, we next construct the lower bound $\underline{P_{2,E}}$ for the case involving two-subject vehicles requiring for lane change in Lemma 5 to ensure the feasibility of the MINLP-MPC model. To develop this lemma, we consider four scenarios regarding the lane-change maneuvers of two subject vehicles.

 $C_1: x_{i(h)+1}(0) + h \ge x^{l_1}(0); x_{i(l_2)+1}(0) + h \ge x^{l_2}(0),$ which represents the case that both the subject vehicles l_1 and l_2 cut in front (i.

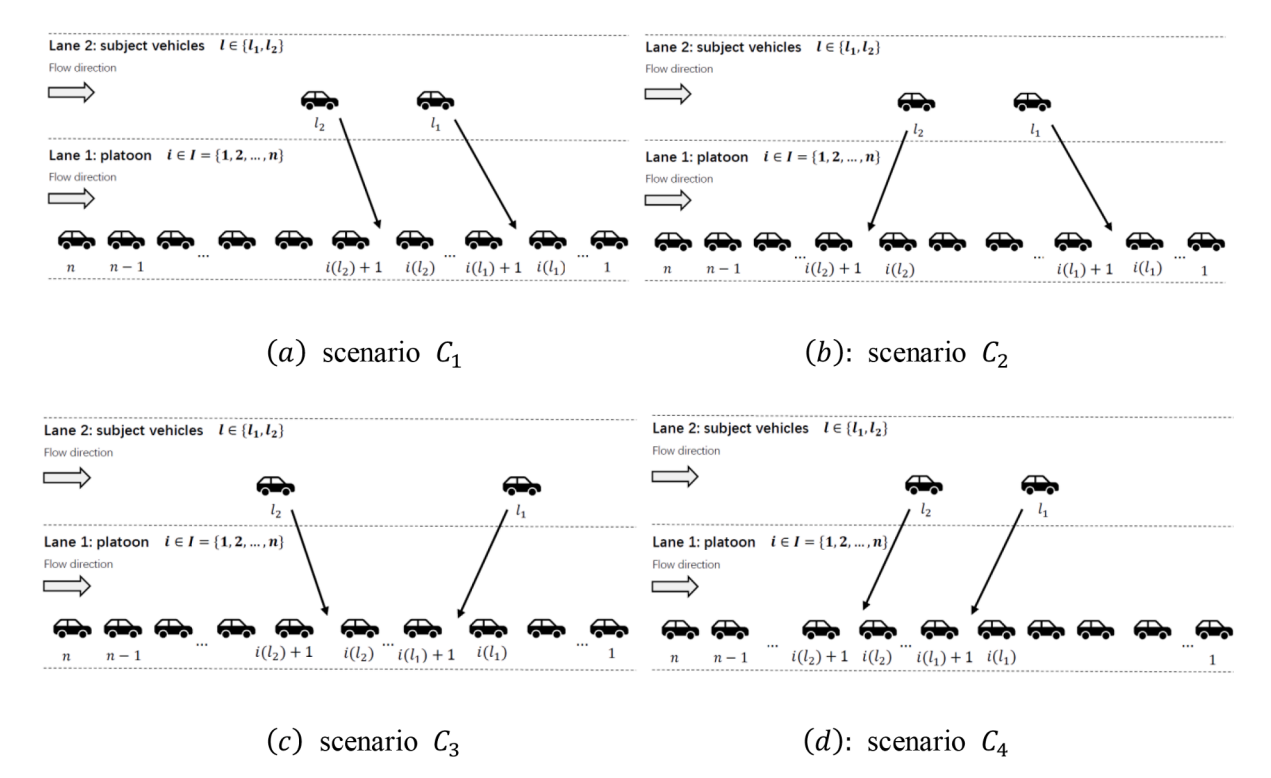


Fig. 4. Four scenarios C_1, C_2, C_3, C_4 of two subject vehicles lane-change case.

e., under scenario B_1), see Fig. 4 (a);

 $C_2: x_{i(l_1)+1}(0) + h \ge x^{l_1}(0); \ x^{l_2}(0) \ge x_{i(l_2)}(0) - h$, which represents the case that the subject vehicle l_1 cuts in front (under B_1), while the subject vehicle l_2 cuts in back (under B_2), see Fig. 4 (b);

 $C_3: x^{l_1}(0) \ge x_{i(l_1)}(0) - h; x_{i(l_2)+1}(0) + h \ge x^{l_2}(0)$, which represents the case that the subject vehicles l_1 cuts in back (under B_2), while the subject vehicle l_2 cuts in front (under B_1), see Fig. 4 (c);

 $C_4: x^{l_1}(0) \ge x_{i(l_1)}(0) - h; \ x^{l_2}(0) \ge x_{i(l_2)}(0) - h$, which represents the case that both the subject vehicles l_1 and l_2 cut in back (under B_2), see Fig. 4 (d).

Lemma 5. Assume that (i) the platoon and the lane change subject vehicles are under extreme scenario (*E*) at p=0; (ii) two subject vehicles l_1, l_2 , which intend to cut in the spacing $s_{i(l_1)}$ respectively between platoon vehicles $i(l_1)$ and $i(l_1)+1$ and $s_{i(l_2)}$ between platoon vehicles $i(l_2)$ and $i(l_2)+1$ in the platoon on the target lane, $s_{i(l_1)} < s_{i(l_2)}$, $s_{i(l_1)} & s_{i(l_2)} \in S$. Then we have the lower bound of $\underline{P_{2,E}}$ as follows to ensure the model feasibility.

$$\underline{P_{2,E}}(s_{i(l_1)}, s_{i(l_2)}|C) = \begin{cases} \max \left\{ \begin{array}{l} \underline{P_{1,E}}(s_{i(l_1)}|B_1), \ \underline{P_{1,E}}(s_{i(l_2)}|B_1) \right\} + \varepsilon(C_1) \ \ \text{if} \ \ C = C_1 \\ \max \left\{ \begin{array}{l} \underline{P_{1,E}}(s_{i(l_1)}|B_1), \ \underline{P_{1,E}}(s_{i(l_2)}|B_2) \right\} + \varepsilon(C_2) \ \ \text{if} \ \ C = C_2 \\ \max \left\{ \begin{array}{l} \underline{P_{1,E}}(s_{i(l_1)}|B_2), \ \underline{P_{1,E}}(s_{i(l_2)}|B_1) \right\} + \varepsilon(C_3) \ \ \text{if} \ \ C = C_3 \\ \max \left\{ \begin{array}{l} \underline{P_{1,E}}(s_{i(l_1)}|B_2), \ \underline{P_{1,E}}(s_{i(l_2)}|B_2) \right\} + \varepsilon(C_4) \ \ \text{if} \ \ C = C_4 \\ \end{cases} \end{cases} ,$$

where $\varepsilon(C_1)$, $\varepsilon(C_2)$, $\varepsilon(C_3)$, and $\varepsilon(C_4)$ are the delay terms to fix the conflicts caused by applying acceleration strategies \widetilde{u}_{B_1} , $\widetilde{u}_{B_2} \in \widetilde{u}$ from Lemma 4 so that we can construct $P_{2,E}$. The mathematical representations of $\varepsilon(C_1)$, $\varepsilon(C_2)$, $\varepsilon(C_3)$, $\varepsilon(C_4)$ are shown below.

$$\varepsilon(C_1) = \left\{ \begin{array}{c} \Delta J_1(s_{i(l_1)} \to 2h|B_1) = 0 \\ \Delta J_2(v^{l_1} \to \widetilde{v}|B_1) = 0 \\ \Delta J_1(s_{i(l_2)} \to 2h|B_1) = \max\left\{J_2(v^{l_1} \to \widetilde{v}|B_1) - J_1(s_{i(l_1)} \to 2h|B_1), 0\right\} \\ \Delta J_2(v^{l_2} \to \widetilde{v}|B_1) = 0 \end{array} \right\}$$

$$\varepsilon(C_2) = \left\{ \begin{array}{c} \Delta J_1(s_{i(l_1)} \to 2h|B_1) = 0 \\ \Delta J_2(v^{l_1} \to \widetilde{v}|B_1) = 0 \\ \Delta J_1(s_{i(l_2)} \to 2h|B_2) = \max\left\{J_2(v^{l_1} \to \widetilde{v}|B_1) - J_1(s_{i(l_1)} \to 2h|B_1), 0\right\} \\ \Delta J_2(v^{l_2} \to \widetilde{v}|B_2) = \max\left\{J_2(v^{l_1} \to \widetilde{v}|B_1) - J_1(s_{i(l_1)} \to 2h|B_1), 0\right\} \end{array} \right\},$$

$$\varepsilon(C_3) = \left\{ \begin{array}{l} \Delta J_1(s_{i(l_1)} \to 2h|B_2) = 0 \\ \Delta J_2(v^{l_1} \to \widetilde{v}|B_2) = 0 \\ \Delta J_1(s_{i(l_2)} \to 2h|B_1) = 0 \\ \Delta J_2(v^{l_2} \to \widetilde{v}|B_1) = J_2(v^{l_1} \to \widetilde{v}|B_2) \end{array} \right\} \text{ and } \varepsilon(C_4) = \left\{ \begin{array}{l} \Delta J_1(s_{i(l_1)} \to 2h|B_2) = 0 \\ \Delta J_2(v^{l_1} \to \widetilde{v}|B_2) = 0 \\ \Delta J_1(s_{i(l_2)} \to 2h|B_2) = 0 \\ \Delta J_1(s_{i(l_2)} \to 2h|B_2) = 0 \\ \Delta J_2(v^{l_2} \to \widetilde{v}|B_2) = 0 \end{array} \right\}$$

Proof. Notice that $\underline{P_{1,E}}$ in Lemma 4 is developed for the case that only one of the two subject vehicles requires lane-change accommodation. To find the time window lower bound $\underline{P_{2,E}}$ for the scenarios involving two subject vehicles' requests, we can use a naïve approach. If there are two subject vehicles simultaneously using the same acceleration strategies as those in Lemma 4 without conflicts, then the $\underline{P_{2,E}}$ is equal to the maximum one of the lower bounds $\underline{P_{1,E}}$ for the two subject vehicles. Thus according to Lemma 4, we have

$$\underline{P_{2,E}}(s_{i(b)}, s_{i(c)}|C) = \begin{cases} \max \left\{ \underline{P_{1,E}}(s_{i(l_1)}|B_1), \ \underline{P_{1,E}}(s_{i(l_2)}|B_1) \right\} & \text{if } C = C_1, \\ \max \left\{ \underline{P_{1,E}}(s_{i(l_1)}|B_1), \ \underline{P_{1,E}}(s_{i(l_2)}|B_2) \right\} & \text{if } C = C_2, \\ \max \left\{ \underline{P_{1,E}}(s_{i(l_1)}|B_2), \ \underline{P_{1,E}}(s_{i(l_2)}|B_1) \right\} & \text{if } C = C_3, \\ \max \left\{ \underline{P_{1,E}}(s_{i(l_1)}|B_2), \ \underline{P_{1,E}}(s_{i(l_2)}|B_2) \right\} & \text{if } C = C_4 \end{cases}$$

$$= \begin{cases} \max\{J_{1}(s_{i(l_{1})} \rightarrow 2h|B_{1}), J_{2}(\rightarrow s_{i(l_{1})}|B_{1}), J_{1}(s_{i(l_{2})} \rightarrow 2h|B_{1}), J_{2}(\rightarrow s_{i(l_{2})}|B_{1})\} & \text{if } C = C_{1}, \\ \max\{J_{1}(s_{i(l_{1})} \rightarrow 2h|B_{1}), J_{2}(\rightarrow s_{i(l_{1})}|B_{1}), J_{1}(s_{i(l_{2})} \rightarrow 2h|B_{2}), J_{2}(\rightarrow s_{i(l_{2})}|B_{2})\} & \text{if } C = C_{2}, \\ \max\{J_{1}(s_{i(l_{1})} \rightarrow 2h|B_{2}), J_{2}(\rightarrow s_{i(l_{1})}|B_{2}), J_{1}(s_{i(l_{2})} \rightarrow 2h|B_{1}), J_{2}(\rightarrow s_{i(l_{2})}|B_{1})\} & \text{if } C = C_{3}, \\ \max\{J_{1}(s_{i(l_{1})} \rightarrow 2h|B_{2}), J_{2}(\rightarrow s_{i(l_{1})}|B_{2}), J_{1}(s_{i(l_{2})} \rightarrow 2h|B_{2}), J_{2}(\rightarrow s_{i(l_{2})}|B_{2})\} & \text{if } C = C_{4} \end{cases}$$

However, in traffic reality, the acceleration strategies of the two subject vehicles adopted in Lemma 4 may cause conflicts. Below we demonstrate the conflicts, and then derive the mathematical formulation for the corrections: $\varepsilon(C_1)$, $\varepsilon(C_2)$, $\varepsilon(C_3)$, $\varepsilon(C_4)$ so that we can fix the solution in Equation (31) which uses the naïve approach.

Notice that each delay term ε (.)has four components $\{\Delta J_1(s_{i(l_1)} \to 2h|B), \Delta J_2(v^{l_1} \to \widetilde{v}|B), \Delta J_1(s_{i(l_2)} \to 2h|B), \Delta J_2(v^{l_2} \to \widetilde{v}|B)\}$, which are respectively the delays corresponding to four lane-change procedures $\{J_1(s_{i(l_1)} \to 2h|B), J_2(\to s_{i(l_1)}|B), J_1(s_{i(l_2)} \to 2h|B), J_2(\to s_{i(l_2)}|B)\}$ in the maximum function in the Equation (31), where $B = B_1$ or B_2 .

For the scenario C_1 , both the subject vehicles l_1 and l_2 tend to cut in front. They are under scenario B_1 defined in Lemma 4. Thus we consider they respectively apply the acceleration strategy $\widetilde{u}_{B_1}(l_1): \widetilde{u} \to \{1, 2, ..., i(l_1), l_1\}$ and $\widetilde{u}_{B_1}(l_2): \widetilde{u} \to \{1, 2, ..., i(l_2), l_1, l_2\}$ to complete the cut-in maneuvers simultaneously. From Equation (9) and the assumptions in Lemma 5, we have the target spacing of the subject vehicle l_1 is ahead of the subject vehicle l_2 's target spacing: $s_{i(l_1)} < s_{i(l_2)}$. It also indicates that $i(l_1) < i(l_2)$. Namely, the platoon vehicle $i(l_1)$ is running before platoon vehicle $i(l_2)$.

The conflicts will potentially arise at the platoon vehicles denoted by $i(l_1 \leftrightarrow l_2) \in \{i(l_1)+1, \dots i(l_2)\}$ if the platoon yields a lane-change spacing for subject vehicle l_1 earlier than it arrives at the target spacing, i.e., $J_2(\to s_{i(l_1)}|B_1) > J_1(s_{i(l_1)} \to 2h|B_1)$. Specifically, to accommodate the subject vehicle l_1 's lane-change request by following $\widetilde{u}_{B_1}(l_1)$, platoon vehicles $i(l_1 \leftrightarrow l_2)$ are required to stay speed ν_{min} until the subject vehicle l_1 reaches the target spacing $s_{i(l_1)}$ by the time step $J_2(\to s_{i(l_1)}|B_1)$. However, to accommodate the subject vehicle l_2 's lane change by following $\widetilde{u}_{B_1}(l_2)$, platoon vehicles $i(l_1 \leftrightarrow l_2)$ are required to sequentially accelerate to prepare the spacing $s_{i(l_2)}$ for accommodating vehicle l_2 starting from the end of the time step $J_1(s_{i(l_1)} \to 2h|B_1)$. Consequently, if $J_2(\to s_{i(l_1)}|B_1) > J_1(s_{i(l_1)} \to 2h|B_1)$, the conflict takes place. More exactly, platoon vehicles $i(l_1 \leftrightarrow l_2)$ are required to stay speed ν_{min} by $\widetilde{u}_{B_1}(l_1)$ since subject vehicle l_1 has not reached the target spacing $s_{i(l_1)}$ yet. On the other hand, they are also instructed by $\widetilde{u}_{B_1}(l_2)$ to accelerate since the process to prepare a spacing for subject vehicle l_2 's lane-change request has been triggered by the end of the time step $J_1(s_{i(l_1)} \to 2h|B_1)$. Therefore, during the time steps $\{J_1(s_{i(l_1)} \to 2h|B_1), \ldots, J_2(\to s_{i(l_1)}|B_1)\}$, any platoon vehicle $i(l_1 \leftrightarrow l_2)$ will receive two conflict instructions.

To resolve the conflict, we let the platoon vehicles $i(l_1 \hookrightarrow l_2) \in \{i(l_1) + 1, \dots i(l_2)\}$ first stay speed v_{min} from time step $J_1(s_{i(l_1)} \to 2h|B_1)$ until the time step $J_2(v^{l_1} \to \widetilde{v}|B_1)$ by which the subject vehicle l_1 arrives at target spacing $s_{i(l_1)}$. This leads to a time delay $\Delta J_1(s_{i(l_2)} \to 2h|B_1) = J_2(\to s_{i(l_1)}|B_1) - J_1(s_{i(l_1)} \to 2h|B_1)$ for the subject vehicle l_2 's lane-change procedure \mathfrak{l}_1 . Notice that if $J_2(\to s_{i(l_1)}|B_1) \leq J_1(s_{i(l_2)} \to 2h|B_1)$, $\Delta J_1(s_{i(l_2)} \to 2h|B_1) = 0$. Namely, no such conflict and there is no time delay in the subject vehicle l_2 's procedure \mathfrak{l}_1 . Combine these two together, $\Delta J_1(s_{i(l_2)} \to 2h|B_1) = \max\{J_2(\to s_{i(l_1)}|B_1) - J_1(s_{i(l_1)} \to 2h|B_1), 0\}$. Furthermore, we can examine and find that no time delay exists in the other three lane-change procedures under $B_1:\{J_1(s_{i(l_1)} \to 2h|B_1), J_2(\to s_{i(l_1)}|B_1), J_2(\to s_{i(l_2)}|B_1)\}$.

Specifically, subject vehicle l_1 's original lane-change acceleration strategy $\widetilde{u}_{B_1}(l_1)$ is not sacrificed to address the conflicts, thus there is no delay term in subject vehicle l_1 's two lane-change procedures \mathfrak{l}_1 , \mathfrak{l}_2 . Namely, $\Delta J_1(s_{i(l_1)} \to 2h|B_1) = 0$; $\Delta J_2(\to s_{i(l_1)}|B_1) = 0$. For the subject vehicle l_2 's lane change procedures \mathfrak{l}_2 , according to the acceleration strategy $\widetilde{u}_{B_1}(l_2)$, subject vehicle l_2 accelerates after subject vehicle l_1 in order to catch up with the platoon vehicle $i(l_2) + 1$, which keeps speed v_{min} all the time. Therefore, the modification we made above has no impact on the subject vehicle l_2 's lane change procedures \mathfrak{l}_2 . There is no time delay term. Namely, $\Delta J_2(\to s_{i(l_2)}|B_1) = 0$. We have the delay term $\mathfrak{e}(C_1)$ in Equation (32):

$$\varepsilon(C_{1}) = \left\{ \begin{array}{c} \Delta J_{1}(s_{i(l_{1})} \to 2h|B_{1}) = 0\\ \Delta J_{2}(\to s_{i(l_{1})}|B_{1}) = 0\\ \Delta J_{1}(s_{i(l_{2})} \to 2h|B_{1}) = \max\{J_{2}(\to s_{i(l_{1})}|B_{1}) - J_{1}(s_{i(l_{1})} \to 2h|B_{1}), 0\}\\ \Delta J_{2}(\to s_{i(l_{2})}|B_{1}) = 0 \end{array} \right\}$$

$$(32)$$

Recall that these four components above corresponds to the formulation of scenario C_1 in Equation (31):max $\{J_1(s_{i(l_1)} \to 2h|B_1), J_2(\nu^{l_1} \to \widetilde{\nu}|B_1), J_1(s_{i(l_2)} \to 2h|B_1), J_2(\nu^{l_2} \to \widetilde{\nu}|B_1)\}$. For the next three scenarios C_2 , C_3 , C_4 , we will discuss the conflict terms $\varepsilon(C_2)$, $\varepsilon(C_3)$, $\varepsilon(C_4)$ in the similar way. Here, we directly give the results, but provide detailed analysis in Appendix-IV.

$$\varepsilon(C_{2}) = \left\{ \begin{array}{c} \Delta J_{1}(s_{i(l_{1})} \rightarrow 2h|B_{1}) = 0 \\ \Delta J_{2}(\rightarrow s_{i(l_{1})}|B_{1}) = 0 \\ \Delta J_{1}(s_{i(l_{2})} \rightarrow 2h|B_{2}) = \max\{J_{2}(\rightarrow s_{i(l_{1})}|B_{1}) - J_{1}(s_{i(l_{1})} \rightarrow 2h|B_{1}), 0\} \\ \Delta J_{2}(\rightarrow s_{i(l_{2})}|B_{2}) = \max\{J_{2}(\rightarrow s_{i(l_{1})}|B_{1}) - J_{1}(s_{i(l_{1})} \rightarrow 2h|B_{1}), 0\} \end{array} \right\}$$

$$(33)$$

$$\varepsilon(C_3) = \begin{cases} \Delta J_1(s_{i(l_1)} \to 2h|B_2) = 0\\ \Delta J_2(\to s_{i(l_1)}|B_2) = 0\\ \Delta J_1(s_{i(l_2)} \to 2h|B_1) = 0\\ \Delta J_2(\to s_{i(l_2)}|B_1) = J_2(\to s_{i(l_1)}|B_2) \end{cases}$$
(34)

$$\varepsilon(C_4) = \begin{cases} \Delta J_1(s_{i(l_1)} \to 2h|B_2) = 0\\ \Delta J_2(\to s_{i(l_1)}|B_2) = 0\\ \Delta J_1(s_{i(l_2)} \to 2h|B_2) = 0\\ \Delta J_2(\to s_{i(l_2)}|B_2) = 0 \end{cases}$$
(35)

Wrapping up the discussions above, we complete the proof for Lemma 5. •

Notice that we assume the two subject vehicles l_1 and l_2 cut in different target spacings, which is the most common case of lane change maneuver. For the case where the two subject vehicles l_1 and l_2 cut in the same spacing, similar strategies can be utilized and we do not show the detailed proof here.

Lemma 5 provides the lower bound $P_{2,E}(s_{i(l_1)}, s_{i(l_2)}|C)$ needed for the case with two subject vehicles requiring for lane change under extreme scenario (*E*). Finally, by summarizing the results from **Lemma 1** to **Lemma 5**, we present the lower bound $P_{2,E}$ in **Theorem 1** to ensure the feasibility of the MINLP-MPC model, considering a platoon is running under a general scenario (\mathbb{E}).

Theorem 1. Assume that (i) a platoon and two subject vehicles l_1, l_2 are under a general scenario \mathbb{E} at control time step k^* (ii) subject vehicles l_1, l_2 intend to cut in the spacing $s_{i(l_1)}$ and $s_{i(l_2)}$ respectively, $s_{i(l_2)} \neq s_{i(l_1)}$, $s_{i(l_1)} \& s_{i(l_2)} \in S$. Then the lower bound of $\underline{P_{2,\mathbb{E}}}$ under scenarios C_1 to C_4 are summarized as follows.

$$\underbrace{P_{2,\overline{\epsilon}}(s_{i(l_1)},s_{i(l_2)}|C_1)}_{\text{max}} \left\{ \begin{aligned} \max \left\{ \frac{(x_{i(l_1)+1}(0)+h)-x^{l_1}(0)}{\tau(v_{max}-v_{min})} + \left(i(l_2)-i(l_1)+\frac{1}{2}\right)m, \\ \frac{(x_{i(l_2)+1}(0)+h)-x^{l_2}(0)}{\tau(v_{max}-v_{min})} + \frac{m}{2} \right\} \end{aligned} \right\} + \underbrace{\frac{v_{max}-v_{min}}{-\tau a_{min}}}_{\text{otherwise}} \text{ if } \widetilde{J},$$

$$\max \left\{ \frac{(x_{i(l_2)+1}(0)+h)-x^{l_2}(0)}{\tau(v_{max}-v_{min})} + \frac{m}{2} \right\} + \underbrace{\frac{v_{max}-v_{min}}{-\tau a_{min}}}_{\text{otherwise}} \text{ otherwise} \right\}$$

$$\begin{split} & P_{2,\mathbb{E}}(s_{i(l_1)},s_{i(l_2)}|C_2) = \begin{cases} \frac{(x_{i(l_1)+1}(0)+h)-x^{l_1}(0)}{\tau(v_{max}-v_{min})} + \left(i(l_2)-i(l_1)+\frac{1}{2}\right)m, \\ \frac{(x^{l_2}(0)+h)-x_{i(l_2)}(0)+(x_{i(l_1)+1}(0)+h)-x^{l_1}(0)}{\tau(v_{max}-v_{min})} \end{cases} + \frac{v_{max}-v_{min}}{-\tau a_{min}} \text{ if } \widetilde{J} \\ & + \frac{(i(l_2)-i(l_1))m}{\tau(v_{max}-v_{min})} \\ & + \frac{(x_{i(l_1)+1}(0)+h)-x^{l_1}(0)}{\tau(v_{max}-v_{min})} + \frac{m}{2}, \\ & \frac{(x^{l_2}(0)+h)-x_{i(l_2)}(0)}{\tau(v_{max}-v_{min})} + \left(i(l_2)-\frac{1}{2}\right)m \end{cases} + \frac{v_{max}-v_{min}}{-\tau a_{min}} \text{ otherwise} \\ & \frac{(x^{l_1}(0)+h)-x_{i(l_2)}(0)}{\tau(v_{max}-v_{min})} + \left(i(l_1)-\frac{1}{2}\right)m, \\ & \frac{(x_{i(l_2)+1}(0)+h)-x^{l_2}(0)+(h)-x_{i(l_1)}(0)}{\tau(v_{max}-v_{min})} + \left(i(l_1)-\frac{1}{2}\right)m, \\ & \frac{(x_{i(l_2)+1}(0)+h)-x^{l_2}(0)+(h)-x_{i(l_1)}(0)}{\tau(v_{max}-v_{min})} + \left(i(l_1)-1\right)m \end{cases} \right\} + \begin{bmatrix} v_{max}-v_{min}\\ -\tau a_{min} \end{bmatrix}, \\ & \frac{(x^{l_1}(0)+h)-x_{i(l_2)}(0)}{\tau(v_{max}-v_{min})} + \left(i(l_2)-\frac{1}{2}\right)m \\ & \frac{(x^{l_1}(0)+h)-x_{i(l_2)}(0)}{\tau(v_{max}-v_{min})} + \left(i(l_1)-\frac{1}{2}\right)m \\ & \frac{(x^{l_1}(0)+h)-x_{i(l_2)}(0)}{\tau(v_{max}-v_{min})} + \left(i(l_1)-\frac{1}{2}\right)m \\ & + \begin{bmatrix} v_{max}-v_{min}\\ -\tau a_{min} \end{bmatrix}, \end{aligned}$$

where condition \widetilde{J} : $J_2(\rightarrow s_{i(l_1)}|B_1) > J_1(s_{i(l_1)} \rightarrow 2h|B_1)$.

Proof. According to Equation (18) in Lemma 2, a general scenario (\mathbb{E}) can be transferred into extreme scenario (E) within $\left\lfloor \frac{v_{max}-v_{min}}{-\tau a_{min}} \right\rfloor$ time steps. Therefore, $\underline{P_{2,E}}(s_{i(l_1)},s_{i(l_2)}|C) = \underline{P_{2,E}}(s_{i(l_1)},s_{i(l_2)}|C) + \left\lceil \frac{v_{max}-v_{min}}{-\tau a_{min}} \right\rceil$, where the mathematical descriptions of $\underline{P_{2,E}}(s_{i(l_1)},s_{i(l_2)}|C)$ are given in Lemma 5. Since $\underline{P_{2,E}}(s_{i(l_1)},s_{i(l_2)}|C)$ is derived from the maximum functions, we compare the elements in the maximum functions with given information and present the results in **Theorem 1**. We omit the detailed discussions here.

Theorem 1 above finds a conservative lower bound of the P value: $\underline{P_{2,\mathbb{E}}}$ to ensure the feasibility of the MINLP-MPC model so that two subject vehicles l_1 and l_2 can complete lane changes at different target spacings while the platoon is initially under a general feasible scenario. Therefore, if we pick a time window $P \ge \underline{P_{2,\mathbb{E}}}$, the MINLP-MPC model is able to find a feasible trajectory control solution to complete this task for two subject vehicles cutting in different spacings. For the case where the subject vehicles l_1 and l_2 cut into the same target spacing, modified similar strategies could be applied and we need to accordingly modify the results in Lemma 4, Lemma 5 and Theorem 1. We do not present the detailed results here.

Remark 2. Our proofs above can be extended to analyze the feasibility of the cases involving more than two subject vehicles: $l \in \{l_1, l_2, ..., l_m\}$, m > 2. Note that Lemma 1-Lemma 4 can be directly applied for more than two subject vehicles cases. Recall that Lemma 4 investigates two different lane-change maneuvers (B_1, B_2) of one subject vehicle case. Lemma 5 considers the interferences of the lane-change maneuvers between two subject vehicles, differentiate them into four different scenarios C_1, C_2, C_3, C_4 , and then introduces the corresponding delay terms $\varepsilon(C_1), \varepsilon(C_2), \varepsilon(C_3)$, $\varepsilon(C_4)$, which are integrated into the results in Lemma 4 to find out the lane-change time window. When it comes to m subject vehicles cases (m > 2), utilizing the similar analysis approach used in Lemma 5, there are 2^m different scenarios $C_1, C_2, \ldots, C_{2^m}$ involved and 2^m corresponding delay terms $\varepsilon(C_1), \varepsilon(C_2), \ldots, \varepsilon(C_{2^m})$. Using the same approach as we analyze $\varepsilon(C_1), \varepsilon(C_2), \varepsilon(C_3)$, $\varepsilon(C_4)$ in Lemma 5, we can determine the mathematical representations of the delay terms $\varepsilon(C_1), \varepsilon(C_2), \ldots, \varepsilon(C_{2^m})$. Due to the complexity resulted from the high dimensionality, we omit these detailed discussions here. More importantly, it is not common in real traffic to have many individual subject vehicles simultaneously requiring for lane-change accommodation for a platoon in a short time period. If this occurs, it is equivalent to the problem that one subject platoon (not individual vehicle) cuts in another target platoon. We propose to develop new approach to address this complicated case in the future work. #

The mathematical formulation of the $\underline{P}_{2,\mathbb{E}}$ in Theorem 1 indicates that $\underline{P}_{2,\mathbb{E}}$ will increase when the two elements increase: the required safe distance to accommodate lane-change requests (i.e., h), and the initial distance between subject vehicle l and its target lane-change spacing (i.e., $|x_{i(l)+1}(0)-x^l(0)|$). Specifically, if a larger safe lane-change spacing h is required, then it takes the platoon more time steps to generate the acceptable spacings to accommodate the lane-change requests. On the other hand, if the subject vehicle

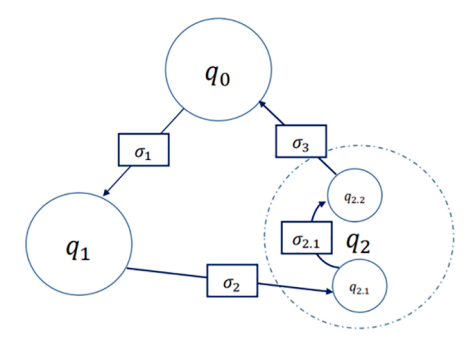


Fig. 5. Hybrid MPC system (m = 2).

l is instructed to cut in a target spacing that is far away from its initial location, naturally it needs more time for coordinating the movements of a subject vehicle l and the platoon. Therefore, it can only be done within a larger time window. Our numerical experiments find that the optimal spacings for subject vehicles to cut in are often selected near subject vehicles' initial locations. Therefore, we may choose a smaller time window P, which helps reduce the computation loads. Moreover, by plugging well-accepted values for the parameters in the mathematical formulation in Theorem 1, we find that $P_{2,E} \le 15$ often holds. Thus, P = 15 is a proper lane-change time window to ensure the MINLP-MPC model feasibility. We validate it by our extensive numerical experiments as well. In addition, this experimental time window also gives an instruction for the lead time of requiring mandatory lane-change accommodation. Wrapping the thoughts above, the model feasibility analysis and Theorem 1 provide us good insights to set up the value of the lane-change time window P in this PB-CLC control so that we can balance the model feasibility and computation load. In the meantime, the feasibility proof further facilitates the development of the hybrid system controller and solution approach. We will discuss the details in the corresponding sections.

5. Hybrid MPC System

This section formally presents the mathematical formulations of the hybrid MPC system and proves the hybrid control feasibility and stability. It is noted that the hybrid MPC system will get very complicated as the number of subject vehicles increases. Thus without loss of generality, we first construct a hybrid MPC system considering two subject vehicles l_1, l_2 requiring for lane-change (m = 2) and then proves the feasibility and stability of this m = 2 hybrid MPC system. Finally, this study generalizes the m = 2 hybrid MPC system to make it applicable for the case of more subject vehicle (m > 2).

5.1. Hybrid System construction

As two subject vehicles are involved in the PB-CLC, the corresponding hybrid MPC system initially illustrated in Fig. 2 will be further complicated shown in Fig. 5, where q_i (i = 0, 1, 2) represent three different states illustrated in the problem formulation section, $q_{2.1}$ and $q_{2.2}$ are sub-states of restoration state q_2 . σ_i (i = 1, 2, 3) represents the switching signal between different states and $\sigma_{2.1}$ represents the switching signal between sub-states $q_{2.1}$ and $q_{2.2}$. More exactly, q_0 is the state that the CAVs in the platoon (not including the subject vehicles $l \in L$) follow the car-following movements under the control instruction from the MPC- q_0 given below for the control time step $k \in Z_+(q_0) = \{0, 1, ..., k^* - 1\}$.

 $MPC-q_0$:

$$\mathbf{Min} \; \Gamma(u(k)) = \frac{1}{2} \left[z^{T}(k+1)Q_{z}z(k+1) + (z^{'}(k+1))^{T}Q_{z^{'}}z^{'}(k+1) \right] + \frac{\Delta t^{2}}{2} \| \; u(k) \; \|_{2}^{2}$$

s.t. Constraints in Equations (1)-(7) \cap { $i \in I$ }, (12)-(15)

Note that MPC- q_0 can be obtained by removing integer variables y that are relevant to lane-change maneuvers from the MINLP-MPC model. After removing y, the prediction time horizon P can be set to 1 and thus the MINLP-MPC turns to a systematical carfollowing (platooning) control which was first adopted in Gong et al. (2016). Once the platoon under MPC- q_0 receives the lane-change requests from subject vehicles at time step k^* , they cooperatively determine the optimal cut-in timing and spacing for each subject vehicle (i.e., determine s(l) and p(l), $l \in \{l_1, l_2\}$) through solving the MINLP-MPC model within one sample time interval. The end of this process activates the switching signal σ_1 , which instructs the system to switch from the state q_0 to the new state q_1 starting from the step k^* .

Accordingly, the state q_1 describes the process that the target platoon manages its spacings to accommodate the lane-change requests with given optimal lane-change decisions in timing and spacing generated by the MINLP-MPC model. The state q_1 starts from the time step k^* until one of the subject vehicles shifts in the time step min $\{p(l_1),p(l_2)\}$. Accordingly, the platoon control model under the state q_1 is given by MPC- q_1 , which is implemented at every control step $k \in Z_+(q_1) = \{k^*, ..., k^* + \min \{p(l_1),p(l_2)\}\}$.

 $MPC-q_1$:

$$\mathbf{Min} \; \Gamma(u, y) = \sum_{p=1}^{P} \left\{ \frac{1}{2} \left[z^{T}(p) Q_{z} z(p) + (z'(p))^{T} Q_{z'} z'(p) \right] + \frac{\Delta t^{2}}{2} \| \; u(p-1) \; \|_{2}^{2} \right\}$$

s.t. for time steps $p \in P$: Constraints in Equations (1)-(7) $\cap \{i \in I, l \in \{l_1, l_2\}\}, (12)$ -(15)

$$y_{s(l),\widetilde{p}(l)}^{l} = 1, \ y_{s,p}^{l} = 0; \ l \in \{l_1, l_2\}, \ \forall s \in S, s \neq s(l), \ p \in P, p \neq \widetilde{p}(l)$$
 (36)

$$x^{l}(p) - x_{i(l)+1}(p) \ge h, \ x_{i(l)}(p) - x^{l}(p) \ge h; \ \forall p \in \left\{ \widetilde{p}(l), ..., \widetilde{P} \right\}, \ l \in \{l_1, l_2\},$$
(37)

where $\tilde{p}(l) = p(l) - (k - k^*)$ is the dedicated time step of the lane-change maneuver at each platoon control step k after k^* . Namely, as the control under $\mathbf{MPC-q_1}$ proceeds, the dedicated time step of the lane-change maneuver decreases. Equation (36) and Equation (37) are obtained by respectively integrating the optimal lane change decisions (i.e., the optimal solutions of $y_{s,p}^l \forall s \in S, p \in P$) into Equation (8) and Equation (11). $\tilde{P} = P - (k - k^* - 1)$ in Equation (37) is the updated lane-change time window P. Note that Equation (37) is only activated when a safe lane-change spacing is ready and will force the safe lane-change spacing keep active until the end of the updated lane-change time window \tilde{P} . Thus, $\mathbf{MPC-q_1}$ is derived from the MINLP-MPC model but specifies the lane-change decision values P0 which are relevant to the lane change maneuvers.

Next, the state q_2 including $q_{2.1}$ and $q_{2.2}$ in the hybrid system functions as an intermediate state for the platoon to smoothly switch from state q_1 back to state q_0 . The state q_2 is necessary for two reasons. First, neither q_0 nor q_1 fits the state that only one of the subject vehicles has cut in the platoon, but the other is still proceeding the lane-change maneuver. Therefore, we design the substate $q_{2.1}$, which is trigged by the switching signal σ_2 when one of the subject vehicles finishes the lane-change maneuver at the time step $k^* + \min \{p(l_1), p(l_2)\}$. Second, it is not feasible for the system to directly switch to state q_0 from state q_1 since \mathbf{MPC} - q_0 and \mathbf{MPC} - q_1 use different types of safety constraints. Specifically in \mathbf{MPC} - q_0 , at control time step $k \ge k^* + p(l)$, the subject vehicle l, which has cut in the spacing between vehicles i(l) and i(l) + 1 in the platoon, should satisfy the safety distance constraints in Equations (38) and (39), which are derived from Equation (7). But this cannot happen automatically. More exactly, when the subject vehicle l just finishes the lane change at the time step $k^* + p(l)$, the spacings between the subject vehicle l and its neighbors are only ensured to be larger than the safe lane-change distance h (see Equation (11) or Equation (37)). However, the lane-change safe distance h is usually smaller than the safety distance, which is the right-hand side of the Equations (38) and (39) below.

$$x^{J}(k) - x_{i(l)+1}(k) \ge LB_{i(l)+1} + \tau v_{i(l)+1}(k) - \frac{\left[v_{i(l)+1}(k) - v_{min}\right]^{2}}{2a_{min,i(l)+1}}$$
(38)

$$x_{i(l)}(k) - x^{l}(k) \ge LB^{l} + \tau v^{l}(k) - \frac{\left[v^{l}(p^{*}) - v_{min}\right]^{2}}{2a^{l}}$$
(39)

Therefore, the safety feasibility is not secured for the platoon to directly switch from the state q_1 to state q_0 . We need the intermediate state q_2 , which consists of two sub-states $q_{2,1}$ and $q_{2,2}$. The first sub-state $q_{2,1}$ describes the state, when one of the subject vehicles has finished the lane change while the other subject vehicle has not. The second sub-state $q_{2,2}$ describes the following state when both two subject vehicles have finished lane-change maneuvers. More exactly, denote the subject vehicle $\bar{l} \in l$ is the first one to finish the lane-change maneuver at control time step $k^* + p(\bar{l})$ in the target spacing $s(\bar{l})$, which is between the platoon vehicles $i(\bar{l})$ and $i(\bar{l}) + 1$. Mathematically, $\bar{l} = \arg\min_{l=\{l_1,l_2\}}\{p(l_1),p(l_2)\}$. Then the other subject vehicle is denoted by $\underline{l} = l \setminus \bar{l}$, with its corresponding optimal lane change spacing and timing denoted by $\underline{s(l)}, k^* + p(\underline{l})$ respectively. In summary, the first sub-state $q_{2,1}$ describes the state during control time steps $\{k^* + p(\bar{l}) + 1, ..., k^* + p(\underline{l})\}$, whereas the second sub-state $q_{2,2}$ describes the situation starting from the control time step $k^* + p(\underline{l}) + 1$ until the system receives the switching signal σ_3 .

Correspondingly, the platoon control model under sub-state $q_{2.1}$ is given by MPC- $q_{2.1}$, which is implemented at the control time step $k \in Z_+(q_{2.1}) = \left\{k^* + p(\overline{l}) + 1, ..., k^* + p(\underline{l})\right\}$.

 $MPC-q_{2,1}$

$$\mathbf{Min} \; \Gamma(u, y) = \sum_{p=1}^{P} \left\{ \frac{1}{2} \left[z^{T}(p) Q_{z} z(p) + (z^{'}(p))^{T} Q_{z^{'}} z^{'}(p) \right] + \frac{\Delta t^{2}}{2} \| \; u(p-1) \; \|_{2}^{2} \right\}$$

s.t. for time steps $p \in P$: Constraints in Equations (1)-(6) $\cap \{i \in I, l \in \{l_1, l_2\}\}, (7) \cap \{i \in I\}, (12)$ -(15), Equations (36) and (37) for l = l;

$$x^{l}(k) - x_{i(l)+1}(k) \ge h, \ l = \bar{l},$$
 (40)

$$x_{i(l)}(k) - x^l(k) \ge h, \ l = \bar{l},$$
 (41)

where Equations (40) and (41) applied to subject vehicle \bar{l} are the spacing constraints for safe lane-change, which are formulated

according to the Equation (37). Accordingly, the safety constraints in Equation (7) are not employed for the spacing $s(\bar{l})$. Equations (36) and (37) describe the lane-change process of subject vehicle \underline{l} . In summary, **MPC-** $q_{2.1}$ is derived from the **MPC-** q_1 but removes one subject vehicle's lane-change decision variable γ since it has finished the lane-change maneuver.

The platoon control model under sub-state $q_{2.2}$ is given by MPC $-q_{2.2}$, which is implemented at the control time step $k \in Z_+(q_{2.2}) = 0$

$$\left\{k^* + p(\underline{l}) + 1, ..., k^* + p(\sigma_3)\right\}.$$

$$\mathbf{Min} \; \Gamma(u, y) = \sum_{p=1}^{P} \left\{ \frac{1}{2} \left[z^{T}(p) Q_{z} z(p) + (z^{'}(p))^{T} Q_{z^{'}} z^{'}(p) \right] + \frac{\Delta t^{2}}{2} \| \; u(p-1) \; \|_{2}^{2} \right\}$$

s.t. for time steps $p \in P$: Constraints in Equations (1)-(6) $\cap \{i \in I, l \in \{l_1, l_2\}\}$, (7) $\cap \{i \in I\}$, (12)-(15), Equations (40) and (41) for $l = \overline{l}, l$, where $k^* + p(\sigma_3)$ represents the control time step when the system receives the switching signal σ_3 ; Equations (40) and (41) for $l = \overline{l}, l$ indicate that both two subject vehicles employ the lane-change spacing constraints right after the lane change maneuver. Thus, **MPC**- $q_{2,2}$ is also derived from the **MPC**- q_1 but completely removes the lane-change decision variable y since both two subject vehicles have finished the lane-change maneuvers.

The control instruction of MPC- $q_{2.2}$ will enlarge the immediate preceding and following spacings of each subject vehicle (will show it in persistent feasibility proof later). Once the safety distance constraints in Equations (38) and (39) are re-satisfied for all subject vehicles, the system triggers the switching signal σ_3 for the switch from intermediate sub-state $q_{2.2}$ to the car-following state q_0 . Up to this time step, the platoon completes a PB-CLC control cycle to accommodate the lane change requests.

Notice that it is possible that the two subject vehicles simultaneously finish the lane change at the same step. In this situation, the system should directly switch from state q_1 to sub-state $q_{2.2}$, skipping the sub-state $q_{2.1}$. To simplify the hybrid system, we do not introduce new switching signal to describe this switching. Instead, we consider the system still goes through sub-state $q_{2.1}$ but will immediately switch to sub-state $q_{2.2}$. Besides, if the platoon is under stable condition and the desired spacing s_d is very large, then the safety distance constraints in Equations (38) and (39) are likely to be directly satisfied after two subject vehicles finish the lane-change maneuvers, so that both sub-state $q_{2.1}$ and $q_{2.2}$ should be skipped. We can apply the same abovementioned trick to simplify the hybrid system.

5.2. Persistent feasibility analysis of the hybrid system

This study notes the importance to prove the persistent feasibility of the MPC-based hybrid system since each state of the hybrid system corresponds to a MPC model (Bridgeman et al., 2016, Zhang et al., 2016). Mainly, the persistent feasibility of a hybrid system consists of two parts: (i) Each state of the hybrid system is individually feasible; (ii) The switchings between states are feasible. Along with the feasibility analysis, the closure property of the cycle in the hybrid system (such as $q_0 \rightarrow q_1 \rightarrow q_{2.1} \rightarrow q_{2.2} \rightarrow q_0$ in this study) is often discussed. This sub-section first proves the feasibility of the hybrid system and further proves the cycle of the hybrid system is closed in Theorem 2.

Theorem 2. The hybrid system is feasible and the cycle $q_0 \rightarrow q_1 \rightarrow q_{2.1} \rightarrow q_{2.2} \rightarrow q_0$ is closed, if the following three conditions hold. (i) State q_0 is initially feasible at control time step k = 0; (ii) Theorem 1 holds, which ensures the feasibility of the MINLP-MPC; (iii) The prediction horizon $P > p(\sigma_3)$.

Proof. To prove this theory, we first show the feasibility of each individual state in the hybrid system and then prove that each necessary switching from one state to another is feasible. Combining these two results, we conclude the feasibility of the hybrid system. To do that, we note that the sequential feasibility of state q_0 was proved in Gong et al., 2016, given that the condition (i) holds: q_0 is initially feasible at k = 0. Besides, the feasibility of the state q_1 , sub-states $q_{2.1}$ and $q_{2.2}$ are all indicated by the feasibility analysis of the MINLP-MPC model in Section 4. Namely, if the MINLP-MPC model can determine a feasible solution to conduct the lane change maneuvers when the prediction horizon P satisfies the inequalities in Theorem 1, then the sequential feasibility of the state q_1 , sub-states $q_{2.1}$ and $q_{2.2}$ are secured. Following this idea, we provide the proof in detail as follows.

Recall that the MINLP-MPC model predicts the vehicles' trajectories for next P steps, i.e. the control time step $k \in Z_+(\text{MINLP} - \text{MPC}) = \{k^*, ... k^* + P\}$, where k^* is the time step that the lane-change accommodation is required. Given the condition (iii) $P > p(\sigma_3)$, we have $Z_+(q_1)$, $Z_+(q_{2.1})$, $Z_+(q_{2.2}) \in Z_+(\text{MINLP} - \text{MPC})$, which indicates that the P-step trajectory predictions given by the MINLP-MPC model completely cover the control time steps of the state q_1 and sub-states $q_{2.1}$, $q_{2.2}$.

Next, we show that the constraints sets in q_1 , $q_{2.1}$ and $q_{2.2}$ are all derived from Equations (1)-(15), which are the constraints of the MINLP-MPC model. Specifically, state q_1 has the constraints in Equations (36) and (37), apart from the other constraints contained in Equations (1)-(15). Note that Equations (36) and (37) are derived from the lane-change constraints in Equations (8)-(11). Thus, the constraints set in state q_1 is derived from the constraints set of the MINLP-MPC model. Taking the same idea, sub-states $q_{2.1}$ and $q_{2.2}$ have constraints in Equations (40) and (41) that are different from Equations (1)-(15) and (36), (37). Notice that Equations (40) and (41) are the safe lane-change constraints derived from Equation (11), which is designed in particular to ensure that the subject vehicle keeps the safe distances h with the adjacent platoon vehicles after lane change. Wrapping above, the constraints sets of q_1 , $q_{2.1}$, $q_{2.2}$ are all subsets derived from the constraints set of the MINLP-MPC model. Consequently, given that the second condition (ii) Theorem 1

holds, which means the MINLP-MPC model is feasible, state q_1 and sub-states $q_{2,1}$, $q_{2,2}$ are all feasible.

Then, we show that the switchings between states are feasible. The switching signal σ_1 : $q_0 \rightarrow q_1$ is feasible because states q_0 and q_1 share the same constraint set at the switching time step k^* . The state switchings such as σ_2 : $q_1 \rightarrow q_{2.1}$, $\sigma_{2.1}$: $q_{2.1} \rightarrow q_{2.2}$ are all feasible for the same reason that two states share the same constraint sets at the switching time step. The feasibility of the switching signal σ_3 : $q_{2.2} \rightarrow q_0$ is proved next together with the proof of the cycle closure property.

To prove the cycle of the hybrid system $q_0 o q_1 o q_{2.1} o q_{2.2} o q_0$ is closed, which means that the hybrid system will go through the cycle in finite time steps. Notice that the hybrid system is state-dependent. That is to say, the state switchings will happen when certain conditions are satisfied. According to the hybrid system construction process in Section 5.1, the state switchings $q_0 o q_1 o q_{2.1} o q_{2.2}$ always hold. Specifically, the switching $q_0 o q_1$ takes place when the lane-change requests are received and the lane-change decisions y are specified by the MINLP-MPC model at step k^* . The switching $q_1 o q_{2.1}$ and $q_{2.1} o q_{2.2}$ happen respectively when one subject vehicle first finishes lane-change and both two subject vehicles finish lane-change.

Therefore, to prove the cycle of the hybrid system is closed, we only need to show the switching $q_{2.2} \rightarrow q_0$ will finish in finite time steps. Note that the switching $q_{2.2} \rightarrow q_0$ completes if the safety distance constraint in Equation (7) \cap { $i \in I$ } are re-satisfied from the lane-change safe constraints in Equations (40) and (41). Given that the sub-state $q_{2.2}$ is stable (Gong and Du, 2018), the sub-state $q_{2.2}$ will enter the steady-state below in finite steps such as at the time step \tilde{k} , according to the MPC- $q_{2.2}$ model.

$$\Delta x_1(\widetilde{k}) = \Delta x_2(\widetilde{k}) = \dots = \Delta x_{i(l)}(\widetilde{k}) = \Delta x^l(\widetilde{k}) = \Delta x_{i(l)+1}(\widetilde{k}) = \dots = \Delta x_{n-1}(\widetilde{k}) = s_d,$$

$$\Delta v_1 \Big(\widetilde{k}\Big) = \Delta v_2 \Big(\widetilde{k}\Big) = \ldots = \Delta v_{i(l)} \Big(\widetilde{k}\Big) = \Delta v^l \Big(\widetilde{k}\Big) = \Delta v_{i(l)+1} \Big(\widetilde{k}\Big) = \ldots = \Delta v_{n-1} \Big(\widetilde{k}\Big) = 0,$$

If we make the desired spacing s_d satisfy $s_d \geq LB + \tau v_{max} - \frac{[v_{max} - v_{min}]^2}{2a_{min,l}}$, then consequently $s_d \geq LB + \tau v_{i+1}(k^*) - \frac{[v_{i+1}(k^*) - v_{min}]^2}{2a_{min,l}}$, for $\forall i \in I \cup I$. At step \widetilde{k} , we have that $\Delta x_{i(l)}(\widetilde{k})$ and $\Delta x^l(\widetilde{k}) = s_d$ will satisfy the safety distance constraints in Equations (38) and (39) (i.e. Equation (7)) for $\forall l \in \{l_1, l_2\}$ at the time step \widetilde{k} . Then, sub-state $q_{2.2}$ switches to state q_0 triggered by switching signal σ_3 . With this, we prove the feasibility of the switching $q_{2.2} \rightarrow q_0$. Wrapping the arguments above, we conclude that the hybrid system is feasible and the cycle $q_0 \rightarrow q_{2.1} \rightarrow q_{2.2} \rightarrow q_0$ is closed. It completes the proof for Theorem 2.

5.3. Stability analysis of the hybrid system

The stability of a hybrid system is another important aspect to evaluate the applicability of the PB-CLC control in practice. A system is stable if it can reach and stay the steady-state after it got affected by undesired disturbances. In this sub-section, the stability of the hybrid system is proved by Theorem 3 below.

Theorem 3. If each state in the hybrid system is asymptotically stable, then the whole hybrid system is asymptotically stable.

Proof. Suppose states q_0 , q_1 and sub-states $q_{2.1}$ and $q_{2.2}$ are asymptotically stable (AS), and the CAV platoon is initially in state q_0 with an arbitrary feasible condition. Since state q_0 is AS, the trajectory along state q_0 is bounded over all steps $k \le k^*$ (when there is no switching). At control time step $k^* + 1$, state q_0 switches to state q_1 and thus q_1 starts from a finite initial condition at step $k^* + 1$. Since q_1 is AS, it follows from the same argument that the trajectory along state q_1 is bounded over all step $k^* + 1 \le k \le k^* + p(\underline{l})$. Suppose q_1 switches to $q_{2.1}$ at control time step $k^* + p(\underline{l}) + 1$ and further switches to $q_{2.2}$ at control time step $k^* + p(\underline{l})$. We can repeat the above argument for sub-states $q_{2.1}$ and $q_{2.2}$. Finally, when $q_{2.2} \to q_0$, state q_0 starts from some finite initial condition at step $k^* + p(\sigma_3)$. Since q_0 is AS, this state converges to zero in (z, z') as control time step k tends to be infinity. Hence, a trajectory of the entire process is bounded and converges to zero. This gives rise to the asymptotic stability of the entire process. We complete the proof for Theorem 3.

Notice that the stability of state q_0 has been discussed in Gong et al. (2016) and the stability of states q_1 and q_2 have been discussed in Section 6 in Gong and Du (2018). Together Theorem 3, we prove the stability of the whole hybrid system.

Remark 3. We can construct a MPC-based hybrid system (m > 2) for more than two subject vehicles lane-change cases using the similar approaches. The MPC-based hybrid system (m > 2) shares the same structure with two subject vehicles (m = 2) case in Fig. 5, where state q_2 has more sub-states such as $q_{2,1}$, $q_{2,2}$,..., $q_{2,m}$ to describe the m subject vehicles' sequentially finished lane-change maneuvers. Then the feasibility and stability of the hybrid system (m > 2) can be proved using the same strategies in **Theorem 2** and **Theorem 3** with the MINLP-MPC model feasibility (m > 2) discussions in **Remark 2**.#

The rigorous proofs for feasibility and stability analysis above indicate that the MINLP-MPC model (function as switching signal σ_1) needs to be solved within a sample time interval τ (< 1sec) to ensure the control smoothness and safety. Besides, the desired platoon spacing s_d should be larger than the upper bound of the conservation safe distance in constraint Equation (7) to sustain the feasibility and cycle closure property of the MPC-based hybrid system. It is also observed that the feasible switching from the lane-change accommodation state to the car-following state may not occur naturally in general. Therefore, it is significantly important to introduce a well-designed hybrid system controller to facilitate the feasible state restoration. Built upon the MINLP-MPC model in Section 3 and its feasibility proof in Section 4, we provided a well-designed MPC-based hybrid system controller and proved its persistent feasibility and

Table 2Summary of the features and target variables.

Feature Set SI	$s \in S, i \in I, l \in S$	\mathscr{L}				
Platoon Subject vehicles	$\Delta x_s(0)$ $s_{i(l,0)}$	$v_i(0)$ $v^l(0)$	$LB_i \\ LB^l$	$a_{max,i} \ a_{max}^l$	$a_{min,i} \ a_{min}^l$	n
Target variables	s(l)			p(l)		

Table 3 Parameter settings for sampling.

Parameters	Values	
MPC prediction horizon P	15 (steps)	
Lane-change safe distance h	30 (m)	
Desired distance s_d	50 (m)	
Sample time interval τ	1 (s)	
Minimum speed v_{min}	22 (m/s)	
Maximum speed v_{max}	31(m/s)	
Penalty weight ω_1	1	
Penalty weight ω ₂	$n^{2}*P$	
Penalty weight α_i	$0.1*n^2 - 0.6*(n+1-i)$	
Penalty weight β_i	$0.3*n^2 - 1.2*(n+1-i)$	

stability in this section. All these insights reinforce the effectiveness and merits of our MINLP-MPC model from the perspective of the mathematical rigorousness.

6. Solution Approach

This section develops efficient distributed optimization algorithms to solve the optimizers in the hybrid MPC system. Note that the MPC- q_0 , MPC- q_1 and MPC- q_2 are convex optimization problems, and can be efficiently solved by the distributed optimization approaches developed in Gong et al., (2016) and Gong and Du, (2018). Hence, the research challenge of the solution approach for the hybrid MPC system is to solve the large-size MINLP-MPC model within a very short time interval τ (< 1sec) so that we can ensure the continuity and smoothness of the real-time hybrid MPC control. Traditional algorithms (e.g., branch and bound algorithm (Wolsey, 1998; Morrison et al., 2016) apparently cannot meet the real-time computation requirement. By taking advantages of the unique features of the MINLP-MPC model, this study develops a machine-learning aided distributed branch and bound approach (ML-DBB) to address this difficulty. We present the key idea as follows.

The main computation obstacle for solving the MINLP-MPC model is to determine the values of integer variables. Once these values are known, the MINLP reduces to a convex optimization problem, which can be solved efficiently by the existing algorithms. Moreover, the integer variables represent the proper timing and spacing for the platoon to accommodate the lane-change requests, which are closely related to the initial states of the platoon and subject vehicles. For example, if a subject vehicle is close to the head of the platoon, it will not be considered to cut in a spacing near the tail of the platoon, due to the traffic smoothness and the efficiency. Hence, spacings not pertaining to this subject vehicle can be removed from the solution space to improve computation efficiency without impacting on the solution optimality.

Inspired by these observations, this study develops a machine-learning aided distributed branch and bound approach (ML-DBB) by integrating the unique features mentioned above. Mainly, we develop machine learning models to predict good candidate lane-change spacings and time steps for accommodating the lane-change requests, based on the features such as the initial relative positions of the subject vehicles to the platoon, and the initial states of the platoon and subject vehicles. Note that these predicted candidate lane-change spacings and time steps refer to a reduced solution space containing a set of candidate optimal binary solutions of *y* in the MINLP-MPC model. Next, the distributed branch and bound method (DBB) will assign these candidate optimal binary solutions to different 'workers' (such as each platoon vehicle) and thus split the computation loads. With the given solutions of the binary variables, the MINLP is reduced to a convex programming, which can be solved by each worker efficiently. Combining the local optimal solution from each worker, the DBB algorithm can quickly find the global optimal (or near optimal) solution within the short sample time interval. We present the technical details as follows.

6.1. Supervised machine learning

The optimal lane-change decisions obtained by solving the MINLP-MPC model are closely related to the initial states of the target platoon and subject vehicles, such as vehicle length constants, acceleration /deceleration limits and initial spacing, speeds. Hence, this study considers the input variables (also named as features) and output variables (also named as target variables) defined in the set of *SI* in Table 2 to develop the machine learning models.

Specifically, the features regarding the initial states of the platoon are captured by the platoon size n, spacing $\Delta x_s(0)$, vehicle speed $v_i(0)$, vehicle length LB_i and the acceleration/deceleration limits $a_{max,i}$, $a_{min,i}$ for $s \in S$, $i \in I$. The features associated with the

initial states of the subject vehicles are described by speed $v^l(0)$, longitudinal relative position to the target platoon $s_{i(l,0)}$, acceleration/ deceleration limits a^l_{max} , a^l_{min} and length LB^l for $l \in L$. The features of the platoon and the subject vehicles together form the feature set SI. Recall that $s_{i(l,0)}$ represents a spacing between the platoon vehicles i(l,0) and i(l,0)+1 that longitudinally covers the position of the subject vehicle l at step p=0. Thus, it characterizes the initial relative position between subject vehicle l and the target platoon.

We consider s(l), p(l) for $l \in L$ (see them in Table 2), the optimal spacing and time step, at which subject vehicle l will conduct the lane-change maneuver, as the target variables. Accordingly, for each subject vehicle l, there are two individual machine learning models that need to be developed, which respectively predict lane-change spacings s(l) and time steps p(l) for $l \in L$, using the input features. With the solutions of $\{s(l), p(l), l \in L\}$, we can easily refer the solution of the binary variable set $y = \{y_{s,p}^l, s \in S, p \in P, l \in L\}$ in the MINLP-MPC model. Note that the physical values of $\{s(l), p(l), l \in L\}$ are bounded by the platoon size n and the lane-change time window p. Thus, using the bounded integer variables sets $\{s(l), p(l), l \in L\}$ rather than the binary variable set p with the size equal to $p(l) \in L$ as the target variables will help to reduce the dimensionality and then facilitate the development of the machine learning models.

On the other hand, the MINLP-MPC also involves some engineering parameters (see them in Table 3). Even though these parameters also affect the target variables, some of them are pre-determined by the engineering experiences and others have the same setup for the platooning control under different platoon conditions. For example, the sample time interval τ of the MPC often takes a value less than human's reaction time; minimum speed ν_{min} and maximum speed ν_{max} are determined by the speed limit of the highway road. Moreover, the penalty weight α_i , β_i are carefully designed to ensure the control stability and smoothness according to the formulations developed in Gong et al. (2016). The penalty weight ω_2 is chosen to make a trade-off between the traffic smoothness and the lane-change promptness. These penalty weights are only related with the specific feature: platoon size n, Therefore, this study will not consider these parameters as the features in our machine learning models. Instead, our numerical experiments in Section 7.3 will test the influence of these parameters on optimal lane-change decisions and traffic smoothness by analyzing the parameter sensitivity.

Based upon the features, target variables and parameter settings above, this study develops supervised machine learning models using the following techniques. First, it is noticed that no existing sample data for the features and target variables are available. To address this issue, the MINLP-MPC model-based computer simulator is employed to scientifically generate sample data for the features and target variables using the c-LHS sampling technique. Next, this study further processes the feature set SI to generate selective features so that we can generalize the usage of the machine learning models and improve the prediction performance. Lastly, different machine learning models are established to explore the best-fit relationships between the target variables and features. Adjusted R^2 , cross-validated mean square error (CV-MSE) and accuracy are used as performance metrics to examine the fitting goodness of the candidate models. The following sub-sections discuss the technical details to build up the machine learning models, including data sampling, feature processing and machine learning model development.

6.1.1. c-LHS Sampling

To develop the machine learning models, our first task is to collect the sample data for the input features and corresponding target variables. However, it is very expensive (or impossible) to get either field data or simulation data for these variables. This is because the CAV platooning control is still an emerging technology and it is hard to do either field experiments or simulation by existing simulators. To address this difficulty, this study uses the computer experimental simulator based upon the MINLP-MPC model to do the data sampling. In the meantime, it is observed that numerous features are involved in this problem and each feature has innumerable choices within their lower & upper bounds. A scientific computer experiments design technique is thus critical to ensure all essential scenarios are sampled, using a limited amount of the sample data, according to the existing study Santner et al., 2003). Moreover, given that some features are involved in constraints in Equations (6) and (7), the constrained simple random sampling technique (c-SRS) is a potential sampling approach. However, it is known that c-SRS has poor space filling properties: it may leave large empty space and generate very close data points. According to Petelet et al., (2010), the constrained Latin hypercube sampling technique (c-LHS) avoids the disadvantage of c-SRS and requires fewer data samples to explore the whole data space. Holistically considering these factors, this study adopts c-LHS sampling technique to generate the sample data for the features of the platoon and subject vehicles. For completeness, we introduce the steps to do c-LHS in Appendix-V. Specifically, this study uses the c-LHS algorithm to do the sampling for the features in Table 1 with sample data size N = 1000 for each platoon size $n \in \{16, 17, ..., 23, 24\}$ with two subject vehicles case (m=2). Next, the sample data of the features combined with the engineering parameters in Table 3 are implemented as the initial inputs to the MINLP-MPC model so that we can find the corresponding optimal lane-change decisions $\{s(l), p(l), l \in L\}$, which are used as the sample data of the target variables to develop the machine learning models. Putting together these 9000 sample data for the features and target variables, we move further to do the feature processing in next sub-section.

6.1.2. Feature processing

The c-LHS sampling data is generated for a platoon with specific size (n). This study noticed that if the full set of features within SI are used for developing the machine learning models, we will have to train different machine learning models for every scenario with possible platoon size for each subject vehicle. Besides, the number of features can become tremendously large when the value of n increases. The machine learning models will have the difficulty in generalization.

To address this limitation, we further process the sample data by the following two procedures. First, it is observed that those platoon vehicles and spacings in the vicinity of the subject vehicles have stronger impacts on the lane-change decision on s(l) and p(l) than others do. Motivated by this view, this study considers only selecting the features of a sub-platoon near the subject vehicle to

develop the machine learning models. Namely, we use the pruned features set: \widetilde{Sl} : $\widetilde{S}(l) \subset S$, $\widetilde{I}(l) \subset I$, $l \in L$, where $\widetilde{S}(l)$ and $\widetilde{I}(l)$ respectively represent the sets of the spacing and platoon vehicles near subject vehicle l's initial location $s_{i(l)}$. Note that \widetilde{SI} is initially selected as a large set, which includes features of eight neighboring platoon vehicles and seven spacings around subject vehicle l. If there are not enough neighboring platoon vehicles making some features unavailable, for example, the subject vehicle is located at the head or the tail of the platoon, we will manually assign large values, such as 200 m, to the missing spacing features and zeros to the speed, acceleration/deceleration features, in view of the fact that there is no platoon vehicle there. In next Section 6.1.3, we will justify that it is enough to include these many features in \widetilde{SI} , by using the feature selection technique. Briefly, the feature selection technique will select the most important features in \widetilde{SI} . The selection results in Table 4 indicate that only features of five platoon vehicles and four spacings nearby have significant impacts on the lane-change decisions (target variables).

Next, we introduce the second feature processing procedure. To differentiate notations, $s^*(l)$, $p^*(l)$ are used to describe the machine learning models' predicted results on optimal lane-change spacing s(l) and time step p(l) respectively. Our experiments show that the pruned features in \widetilde{SI} work well to predict s(l), $l \in L$, but not p(l), $l \in L$. Note that p(l) is strongly correlated with the selected s(l). Therefore, this study considers using the predicted optimal spacings $s^*(l)$, $l \in L$ as one additional feature to predict optimal p(l). Moreover, this study considers a new feature $\widehat{p}(l)$, which represents the least time steps needed to accommodate a lane-change request if only considering the subject vehicle and its immediate adjacent vehicles on the target lane. Mathematically, $\widehat{p}(l)$ is obtained by solving a small size optimization program, in which only a subject vehicle l ($l = l_1$, l_2 ... or l_m) and two immediate adjacent platoon vehicles $i^*(l)$ and $i^*(l) + 1$ around the predicted optimal spacing $s^*(l)$ are considered. Our study indicates that \widehat{p} is a significant factor to improve the prediction accuracy of the optimal lane-change time step. Besides, it only takes a very short time (~ 0.002 sec) to solve the optimization model.

$$\begin{aligned} & \text{Min } \widehat{p}(l) = \sum_{p=1}^{p} y_{s^*(l),p}^{l} *p \\ & \text{Subject to: Equations (1)-(7) for } i = i^*(l), i^*(l) + 1; l = l_1 \quad \text{or} \quad l_2 \quad \text{or} \quad \dots \quad \text{or} \quad l_m \\ & \sum_{p=1}^{p} y_{s^*(l),p}^{l} = 1; \; y_{s^*(l),p}^{l} \in \{0,1\}, \; p \in P \\ & x^{l}(p) - x_{i^*(l)+1}(p) \geq h + M \Big(y_{s^*(l),p}^{l} - 1 \Big) \\ & x_{i^*(l)}(p) - x^{l}(p) \geq h + M \Big(y_{s^*(l),p}^{l} - 1 \Big) \end{aligned}$$

Taking these new features $(\widehat{p}(l), s^*(l))$ into consideration, we have another selective feature set \widehat{SI} : $\widehat{S}(l) \subset S$, $\widehat{I}(l) \subset I$, $l \in L$, where $\widehat{S}(l)$ and $\widehat{I}(l)$ respectively represent the sets of the neighboring spacings and platoon vehicles around the optimal $s^*(l)$ predicted by \widetilde{SI} . Note that \widehat{SI} is also a large enough set which includes features of eight platoon vehicles and seven spacings. Using the features set \widehat{SI} and the extra feature $\widehat{p}(l)$, the optimal lane-change step $p^*(l)$ can be predicted much more accurately.

In short, this section further processes the c-LHS sampling data and obtains two pruned feature sets \widetilde{SI} and \widehat{SI} to improve the prediction performance of the machine learning approach. These procedures also make the machine learning model applicable for general scenarios with different sizes of platoons. More exactly, the optimal lane-change spacing (i.e., s(l), $l \in L$) is first predicted using the feature set \widetilde{SI} , whereas the optimal lane-change time steps (i.e., p(l), $l \in L$) are predicted using the feature set \widehat{SI} combined with the new features $s^*(l)$ and $\widehat{p}(l)$.

6.1.3. Machine learning models

We test six different machine learning models, including linear regression, linear discriminant analysis, random forests regression, random forests classification, support vector machine, and support vector regression. The test results show that linear regression gives the best performance from a combined view of simplicity, interpretability, accuracy to generate prediction interval. For the paper length concern, we mainly introduce the development of the linear regression models in this section.

To develop the linear regression models, we first do the feature selection using the forward stepwise selection algorithm, which is a computationally efficient alternative to the best subset selection method². Built upon the selected features, we developed the linear regression models $\mathfrak{s}(l)$ and $\mathfrak{p}(l)$ respectively for $\mathfrak{s}(l)$ and $\mathfrak{p}(l)$, $l \in \{l_1, l_2\}$. For illustration, we take subject vehicle l_1 as an example and show the corresponding linear regression models $\mathfrak{s}(l_1)$ and $\mathfrak{p}(l_1)$ as well as the models' performance in Table 4, where the selected features and their coefficients, standard error, t-test, p value (Pr(>|t|)) as well as adjusted R^2 , 10 fold cross-validated mean square error (CV-MSE) and accuracy are presented. For completeness, we put subject vehicle l_2 's linear regression models $\mathfrak{s}(l_2)$, $\mathfrak{p}(l_2)$ in Appendix-VI. The CV-MSE and the accuracy are calculated using the following Equations.

² The best subset method is not used due to its low efficiency in this application with a large number of features. The forward stepwise selection method demonstrates satisfying performance, although it has theoretical drawbacks.

Table 4 Linear regression models $s(l_1)$, $p(l_1)$.

Selected features $(s(l_1))$	Coefficients	Standard Error	t value	Pr(> t)
(Intercept)	-7.275e-01	7.645e-02	-9.515	< 2e-16
$\Delta \widetilde{x}_{l_1,0}$	-5.273e-03	3.036e-04	-17.364	< 2e-16
$\Delta \widetilde{x}_{l_1,1}$	-1.741e-03	1.919e-04	-9.073	< 2e-16
$\Delta \widetilde{x}_{l_1,-1}$	-1.635e-03	3.272e-04	-4.996	5.98e-07
$\Delta \widetilde{x}_{l_1,-2}$	-1.422e-04	1.802e-05	-7.891	3.34e-15
$\widetilde{m{ u}}_{l_1,-1}$	9.082e-03	1.385e-03	6.558	5.76e-11
$\widetilde{m{ u}}_{l_1,-2}$	1.156e-02	1.350e-03	8.564	< 2e-16
$\widetilde{oldsymbol{ u}}_{l_1,-3}$	6.532e-03	1.383e-03	4.721	2.38e-06
$S_{i(l_1,0)}$	9.990e-01	9.994e-04	999.594	< 2e-16
v^{l_1}	-3.409e-02	1.347e-03	-25.308	< 2e-16
Performance of $\mathfrak{s}(l_1)$		Adjusted R^2 0.9923	CV-MSE 0.0972	Accuracy 0.9032
Selected features $(p(l_1))$	Coefficients	Standard Error	t value	Pr(> t)
(Intercept)	3.054e+00	1.853e-01	16.486	< 2e-16
$\Delta \widehat{x}_{l_1,0}$	-1.231e-02	8.153e-04	-15.101	< 2e-16
$\Delta \widehat{x}_{l_1,-1}$	-1.052e-02	8.237e-04	-12.769	< 2e-16
$\Delta \widehat{x}_{l_1,-2}$	-7.090e-03	8.199e-04	-8.646	< 2e-16
$\widehat{oldsymbol{ u}}_{l_1,1}$	-2.709e-02	3.603e-03	-7.518	6.10e-14
$\widehat{m{v}}_{l_1,2}$	-2.161e-02	3.636e-03	-5.944	2.88e-09
$\widehat{a}_{max,l_1,-2}$	-5.003e-02	1.665e-02	-3.005	2.66e-03
$S_{i(l_1,0)}$	-2.661e-03	2.784e-04	-9.560	< 2e-16
$s*(l_1)$	-9.710e-02	1.394e-02	-6.968	3.45e-12
$\widehat{m{p}}(m{l}_1)$	1.070e+00	6.910e-03	154.858	< 2e-16
Performance of $p(l_1)$		Adjusted R^2 0.7568	CV-MSE 0.7891	Accuracy 0.4253

$$CV - MSE = \frac{1}{N_t} * \sum_{i=1}^{N_t} \left(r_i - \hat{r}_i \right)^2; \text{ accuracy} = \frac{N}{N_t},$$

where N_t is the testing data sample size (i.e., $N_t = 900$); r_i represents the actual value of the target variable, whereas \hat{r}_i represents the linear regression model's prediction value of the target variable. $[\hat{r}_i]$ is the value by rounding \hat{r}_i to the nearest integer since \hat{r}_i is likely to be a decimal. $N_{r=\widehat{r}_i|}$ represents the number of the testing data where $r_i = [\hat{r}_i]$: the prediction result $[\hat{r}_i]$ accords with the actual value r_i .

Table 4 presents the linear regression models $\mathfrak{s}(l_1)$ and $\mathfrak{p}(l_1)$ for predicting $\mathfrak{s}(l_1)$ and $\mathfrak{p}(l_1)$ respectively. More exactly, $\Delta \widetilde{x}_{l_1,j}, \widetilde{v}_{l_1,j}, \widetilde{a}_{max,l_1,j}$ belong to the pruned feature set \widetilde{SI} and represent jth-unit neighboring platoon vehicle's initial states around subject vehicle l_1 's predicted lane-change spacing $s^*(l_1)$. It is observed that after using the forward stepwise feature selection technique, only five platoon vehicles' initial states (j=-3,-2,-1,-1,-2) and four spacings (j=-1,-2,-1,-1) and seven spacings $(j=\pm 3,\pm 2,\pm 1,0)$. This observation validates that platoon vehicles and spacings that are more than 3 units far away from the subject vehicle l have few impact on subject vehicle l's lane-change decisions. It also demonstrates the effectiveness and correctness of setting up the pruned feature sets \widetilde{SI} and \widehat{SI} in Section 6.1.2.

Apart from the observations above, it is observed that in model $\mathfrak{s}(l_1)$, the p value of the feature $s_{i(l_1,0)}$ is small (< 2e-16) and its t value equals to 999.594, which is extraordinarily larger than other features' t values. This indicates that subject vehicle l_1 's lane-change spacing $s(l_1)$ is strongly influenced by the subject vehicle l_1 's initial location $s_{i(l_1,0)}$. Similarly in model $\mathfrak{p}(l_1)$, the t value of the feature $\hat{p}(l_1)$ is 154.858 greater than the other t values, which implies that subject vehicle l_1 's lane-change time step $p(l_1)$ is strongly affected by the newly introduced feature $\hat{p}(l_1)$. These results also justify the importance of the feature processing in Section 6.1.2. Besides, using the similar method to analyze the t values and p values of the other features, we find that subject vehicle l_1 's speed v^{l_1} and its neighboring platoon vehicles' spacings, speeds such as $\Delta \tilde{x}_{l_1,0}$, $\Delta \tilde{x}_{l_1,1}$, $\tilde{v}_{l_1,-2}$ have some impacts on $s(l_1)$, whereas subject vehicle l's initial location $s_{i(l_1,0)}$ and spacing like $\Delta \hat{x}_{l_1,0}$, $\Delta \hat{x}_{l_1,-1}$, $\Delta \hat{x}_{l_1,-2}$ can influence the lane-change decision on $p(l_1)$. It is noted that other features such as vehicle length L_i or L^{l_1} , acceleration/deceleration limit $a_{max,i}$ ($a_{max}^{l_1}$), $a_{min,i}$ ($a_{min}^{l_1}$) and platoon size n are mostly ruled out using the feature selection technique in Table 4, which shows that these types of features have minor impacts on lane-change decisions.

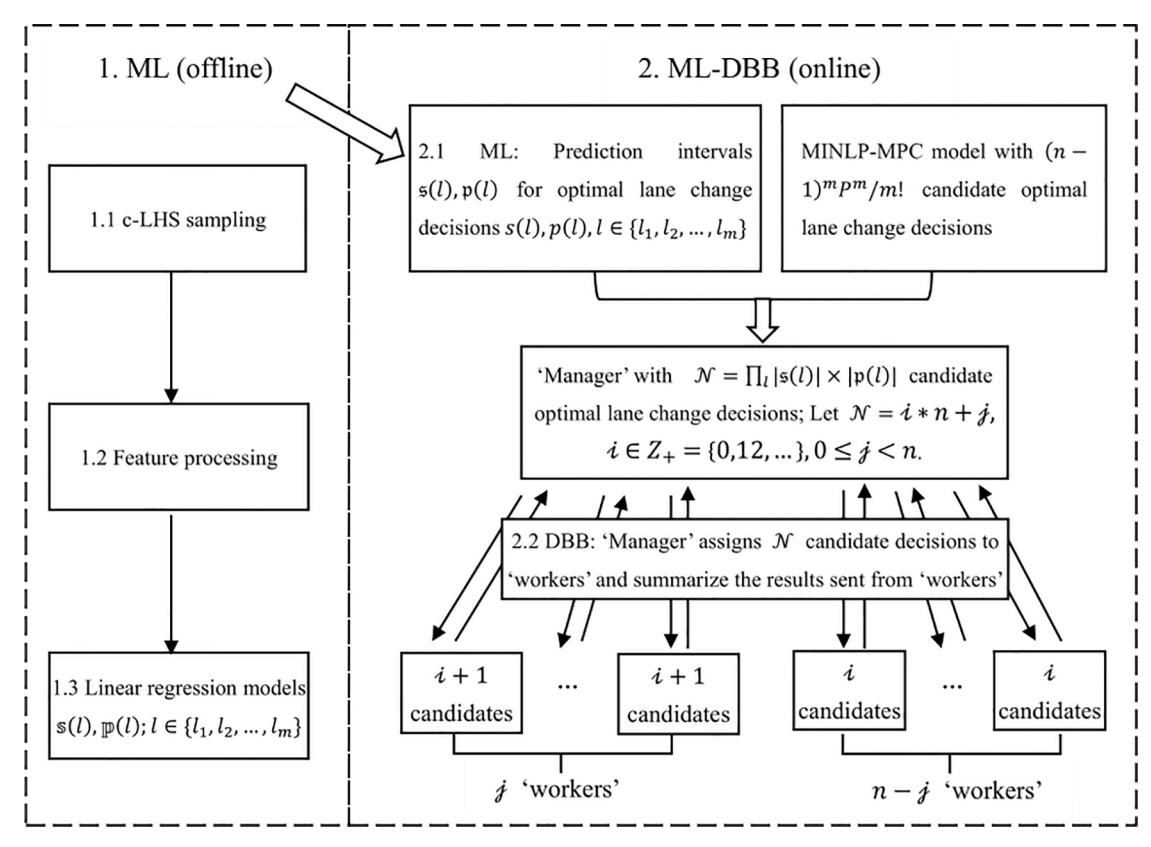


Fig. 6. ML-DBB framework.

As for the model performance in Table 4, the adjusted R^2 of linear regression model $\mathfrak{g}(l_1)$ reaches 0.99, which is strongly perfect, whereas the adjusted R^2 of linear regression model $\mathfrak{p}(l_1)$ is substantially good as 0.75. Moreover, CV-MSE and accuracy values of $\mathfrak{s}(l_1)$ also validate the model's performance. Although the accuracy of model $\mathfrak{p}(l_1)$ as 0.42 is not high, the CV-MSE which is less than 1 indicates that the average prediction error for lane-change step $p(l_1)$ is within 1 time step. Besides, to obtain global optimal or improved solutions, the prediction interval³ given by the linear regression models are used in our ML-DBB approach to further mitigate the minor effect of the low accuracy on model $\mathfrak{p}(l_1)$. We will illustrate the details in next sub-section.

Our experiments also found that using the random forests (classification) model improves the accuracy of predicting lane-change time step $p(l_1)$ significantly to 0.6702. However, it is hard to use the classification models to generate the prediction intervals, which are needed for the ML-DBB algorithm. As for the other machine learning regression models, minor improvements can be achieved compared with the linear regression models. Apart from the reasons above, linear regression model has many other advantages. For example, it has good interpretability and needs less storage space compared with non-parametric machine learning models. This study thus adopts the linear regression models (i.e., $\mathfrak{s}(l)$, $\mathfrak{p}(l)$) to generate the prediction intervals denoted by $\mathfrak{s}(l)$, $\mathfrak{p}(l)$ in the ML-DBB algorithm.

6.2. Machine learning based distributed branch and bound (ML-DBB)

The ML-DBB algorithm in this study integrates the prediction intervals generated online using the offline-built linear regression models into the distributed branch and bound algorithm (DBB), aiming to address the computation challenges of the MINLP-MPC. Specifically, the DBB algorithm is a modified version of the branch and bound algorithm to realize the distributed computation, which includes 'manager' and 'workers'. The 'manager' assigns branches (computation loads) to each 'worker' and then summarizes the computation results from the 'workers'. This study considers one of the subject vehicles as the 'manager' and platoon vehicles as the 'workers'. Fig. 6 presents the framework of the ML-DBB.

Mainly, once the lane-change requests are received, the platoon will send its initial states to the subject vehicles. One of the subject vehicles ('manager') uses the well-established offline machine learning models such as linear regression models (see in Section 6.1.3)

³ The prediction is given by the following general formula: prediction point \pm (t-multiplier \times standard error of the prediction). Prediction interval is an estimate of an interval where a future observation may fall, with a certain probability. It is similar in spirit to confidence interval, but considers more uncertainty of new random target variable and thus fits better in predicting a new target variable.

to quickly generate the prediction intervals $\S(l)$, $\[pi(l), l \in L$ for the optimal lane-change decisions. And then the ML-DBB integrates the prediction intervals into the MINLP-MPC model. More exactly, it removes those lane-change decisions outside the prediction intervals considering they are not good candidates to be selected by the MINLP-MPC. This step significantly reduces the searching space of the feasible lane-change decisions from the number of $(n-1)^m P^m/m!$ to $\mathscr{N} = \prod_i |\S(l)| \times |\mathfrak{p}(l)|$, where $|\S(l)|$, $|\mathfrak{p}(l)|$, $|\mathfrak{p}(l$

number of integers in the intervals $\mathfrak{S}(l)$, $\mathfrak{p}(l)$ respectively. Following that, the 'manager' enumerates the lane-change decisions in the prediction intervals and uniformly assigns these \mathscr{N} many candidate lane-change decisions to the 'workers' for further evaluation. Note that each lane-change decision corresponds to a set of integer variable solutions for the MINLP-MPC. Given one set of integer variable solutions, the MINLP is degraded to a convex NLP, which can be solved efficiently. Therefore, each 'worker' accomplishes its job by repeatedly referring one set of the integer variable solutions (i.e., lane-change decision), solving the corresponding NLP and finally sending the computational results back to the 'manager', including the vehicle trajectory instructions, the objective value and the referred lane-change decision. Last, the 'manager' compares the objective values from the 'workers' and finds the best local optimal lane-change decision with the vehicle trajectory instructions as the final solution. In summary, the offline-built machine learning models help lock a reduced searching space for the integer variables in the MINLP-MPC. Then the DBB uses the distributed computation resources to enumerate the integer variable solutions in the reduced search space and then solves the degraded MINLP (convex NLP) efficiently.

Note that the computation time of using the ML-DBB algorithm will be larger than the sample time interval (such as 1 sec) when the platoon size and subject vehicles size get very large to some extent. Under this situation, rather than using the ML-DBB, we will directly use the machine learning models to estimate the optimal lane-change decision, such as using the linear regression prediction on $\{s^*(l), l \in L\}$ and random forest (classification) prediction on $\{p^*(l), l \in L\}$. We will discuss its details in numerical experiments in Section 7.1.

7. Numerical Experiments

This section conducts three sets of numerical experiments: Experiment-I, Experiment-II and Experiment-III to verify the performance of our approaches from the following three aspects. (i) Validate the efficiency and merits of the ML-DBB algorithm, including the solution optimality and computation performance (Experiment-I). (ii) Demonstrate the effectiveness of the PB-CLC control to accommodate the lane-change requests while ensuring traffic efficiency and smoothness (Experiment-II, Experiment-III and Experiment-IV). (iii) Conduct the parameter sensitivity analysis on lane-change decisions and traffic smoothness (tuning parameters based on Experiment-II and Experiment-III).

Specifically, using the sampling approaches introduced in Section 6.1.1, Experiment-I generates two sets of sample data: each with 9000 scenarios for the case of two subject vehicles (m = 2) and the case of three subject vehicles (m = 3). The platoon size for each case varies from 16 to 24, i.e., $n \in \{16, ..., 24\}$. Experiment-II chooses a case including 2 subject vehicles and a platoon with 21 vehicles to implement the PB-CLC control, while Experiment-III further extends the test to a case involving 3 subject vehicles and a platoon with 24 vehicles. The initial states of the platoons and subject vehicles in the Experiment-III and Experiment-III are obtained from the NGSIM field data, which was collected on the eastbound of the I-80 in San Francisco Bay at Emeryville, California, 4:00 pm to 4:15 pm on April 15, 2005. It is noted that the platoons in Experiment-II and Experiment-III using the field data are not in steady-state. Hence, this study conducts Experiment-IV, which uses two subject vehicles and a stabilized platoon with 22 vehicles. Furthermore, we compare the proposed PB-CLC control with the cooperative lane-change control developed in Ni et al., (2020) in this scenario. The physical parameters of Experiment-II, Experiment-III and Experiment-IV follow the same in Table 3. Besides, the acceleration /deceleration limits are set as $a_{max,i}(a^l_{max}) = 5$ (m/s²), $a_{min,i}(a^l_{min}) = -6$ (m/s²), according to the NGSIM field data and Acceleration Parameters, Police Radar Information Center 2020. Based on the original parameter setting above, various parameters are tuned to test the parameter sensitivity on the lane-change decisions and traffic smoothness. We will present the parameter tuning details in Section 7.3.

7.1. Solution Optimality and Computation performance

To examine the computation performance of the ML-DBB, Experiment-I solved all the scenarios of the case with two subject vehicles and the case with three subject vehicles, using four different solution approaches, including commercial solver Gurobi 8.0 (BB algorithm), the ML-DBB algorithm integrating $\alpha=90\%$ and $\alpha=99\%$ machine learning prediction interval, (they are labeled by ML-DBB-90 and ML-DBB-99 respectively), and the direct machine learning point prediction based approach (it is labeled by ML-PP). Mainly, the ML-PP approach directly uses the predicted lane-change decision (i.e., $s^*(l)$, $p^*(l)$) as the optimal decision and then degrades the MINLP-MPC model to a NLP model, which can be solved efficiently to provide the corresponding trajectory control instructions by a distributed algorithm developed in Gong and Du (2018). Experiment-I is implemented on the computer with the following processor: Intel(R) Core (TM) i7-7700K CPU @4.20GHz and Ram: 16.0GB. The DSRC communication time refers to the existing study in Kenney, (2011). The solution optimality and computation performance for the case of two subject vehicles are summarized in Table 5.

We first discuss the performance of the ML-DBB using the prediction intervals with different confidence levels (i.e., $\alpha = 90\%$, $\alpha = 99\%$). The results in Table 5 show that both the ML-DBB-90 and ML-DBB-99 can efficiently solve the MINLP-MPC and provide a satisfactory solution by a computation time (0.1904sec or 0.3292sec) less than the sample time interval ($\tau = 1$ sec). They both significantly reduce the computation time as compared with that using the solver Gurobi 8.0 (3.011sec). In addition, Table 5 shows that using the ML-DBB-90 has 84.80% chance to end with global optimal solutions and this probability can be further increased to

Table 5 Solution Optimality and Computation Performance of Experiment-I for $l \in \{l_1, l_2\}$.

Solution optimality	ML-PP		ML-DBB-90	ML-DBB-99
Global optimal	38.79%		84.80%	94.00%
0-5% optimal	46.82%		10.60%	5.98%
5-10% optimal	8.91%		2.83%	0.02%
10-20% optimal	1.08%		0.40%	0.00%
Infeasible	4.40%		1.37%	0.00%
Total	100%		100%	100%
Computation performance	Gurobi 8.0	ML-PP	ML-DBB-90	ML-DBB-99
Computation time(s)	3.011	0.0632	0.1904	0.3292

The time includes both DSRC communication time (Kenney, 2011) and the computation time.

94.00% by using the ML-DBB-99. This solution optimality gain accompanies with a computation cost increment from 0.1904sec to 0.3292sec. Therefore, using wider prediction intervals in the ML-DBB algorithm improves the solution optimality but sacrifices the computation time. This is reasonable since a wider prediction interval includes more solution candidates for exploring optimal lane-change decision. Accordingly, it will reduce the chance of missing the optimal solution but incur more computation loads to the ML-DBB algorithm. In addition, our study noticed that the ML-DBB algorithm is applicable for the cases where the platoon size is less than 30 (i.e., n < 30) and the subject vehicles size is less than 5 (i.e., m < 4), which covers most of the general traffic conditions.

For the extreme cases involving a long platoon (n > 30) and many subject vehicles (m > 4), we suggest directly using the ML prediction point results (i.e., s*(l), p*(l)) as the lane-change decision (ML-PP). The results in Table 5 demonstrate the merits of this ML-PP approach. It has 38.79% chance to obtain the global optimal solutions and 46.82% chance to end with good solutions within 5% optimal gap, while the average computation time is only 0.0632sec. Thus, we conclude that the ML-PP approach will work reasonably well for a case that involves a long platoon and many subject vehicles requiring lane-change accommodation simultaneously. It is aware that the limitation of this approach is that it has relatively low chance to end with global optimal solutions and has certain risk (4.40%) to end with infeasible solutions.

The experiment results in Experiment-I for the case involving three subject vehicles are summarized in Table 6 below.

The results in Table 6 indicate that the ML-DBB approaches still show superior performance in the solution optimality and computation time, though slightly inferior as compared with the results in Table 5. This is mainly because three subject vehicles cases involve one extra subject vehicle's lane-change uncertainties and prediction results, which will naturally have negative impacts on the overall solution optimality. It is foreseeable that as the number of subject vehicles increases, the solution optimality performance will keep going down, especially the chances of obtaining global optimal solutions. However, we also noted that the chances of achieving good solutions within 5% optimal gap increase a lot to make up the losses of the chances to get global optimal solutions. In other words, the chances of obtaining global optimal solutions or good solutions within 5% optimal gap for three subject vehicles cases are comparable to that for two subject vehicles cases.

As for the computation performance, it is observed that involving one extra subject vehicle in the problem will increase the computation time from 3.011 seconds to 10.273 seconds by using the branch and bound method in Gurobi 8.0. This is because one extra subject vehicle will lead to (n-1)*P many extra integer variables, which greatly complicates the branching process. However, by using the ML-DBB-90 and ML-DBB-99, the computation time can be reduced to 0.3720 second and 0.5482 second respectively. When using the ML-PP approach, the computation time further decreases to 0.0656 second. They all outperform the solver Gurobi 8.0, but are slightly worse than the result in Table 5. It is foreseeable that as the number of subject vehicles increases, the computation time of ML-DBB will finally increases out of the control sampling time interval (1 second). In this situation, we would suggest using ML-PP approach to quickly find a good reasonable solution rather than global optimal solution.

Table 6 Solution Optimality and Computation Performance of Experiment-I for $l \in \{l_1, l_2, l_3\}$.

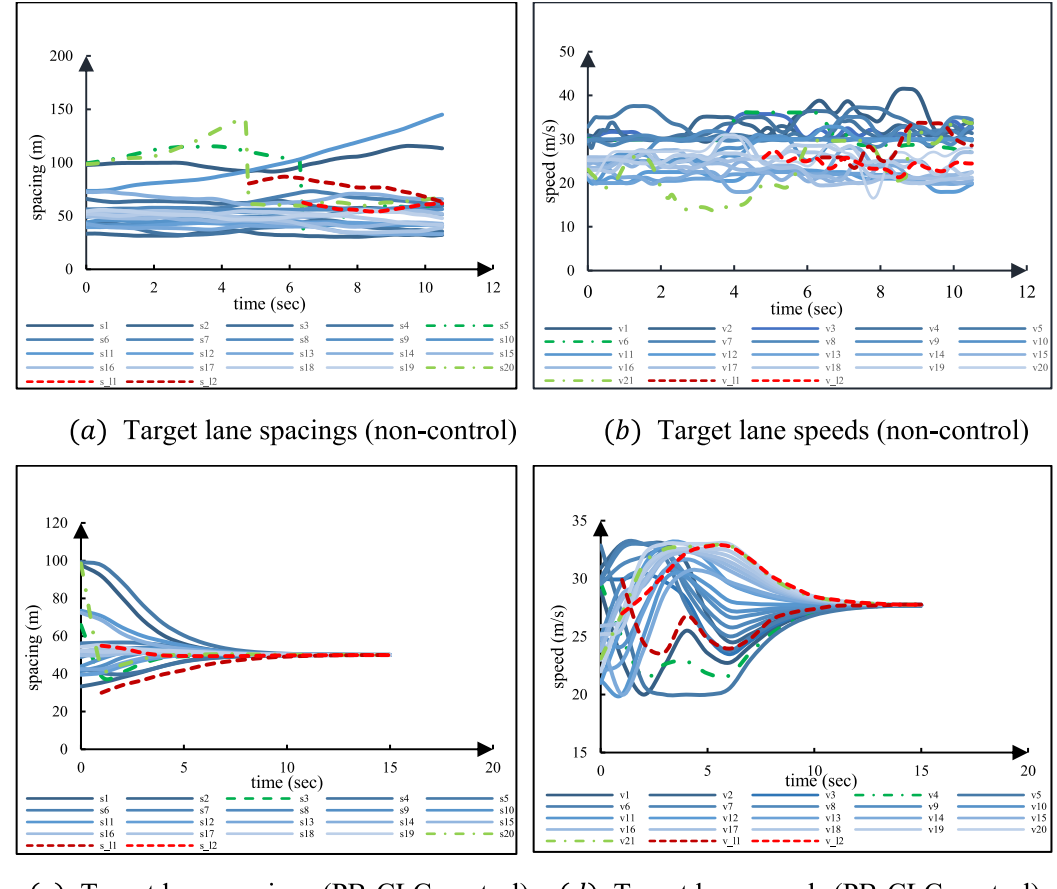
Solution optimality	ML-PP		ML-DBB-90	ML-DBB-99
Global optimal	22.27%		78.00%	90.10%
0-5% optimal	58.66%		14.70%	7.96%
5-10% optimal	11.93%		4.92%	1.94%
10-20% optimal	1.34%		0.83%	0.00%
Infeasible	5.80%		1.55%	0.00%
Total	100%		100%	100%
Computation performance	Gurobi 8.0	ML-PP	ML-DBB-90	ML-DBB-99
Computation time(s)	10.273	0.0656	0.3720	0.5482

The time includes both DSRC communication time (Kenney, 2011) and the computation time.

7.2. Cooperative platoon control effectiveness

Next, this study examines the traffic efficiency and smoothness under the PB-CLC control as it is specifically implemented by the hybrid MPC system in Experiment-II, Experiment-III and Experiment-IV. Fig. 7, Fig. 8 and Fig. 9 respectively demonstrate their results, where Fig. 7 and Fig. 8 plot the corresponding NGSIM field data with 0.1 second resolution as a benchmark and Fig. 9 compares the proposed PB-CLC control with a cooperative lane-change control in Ni et al., (2020). Additionally, Fig. 7, Fig. 8 and Fig. 9 all use the red (or orange-red) dashed lines to represent subject vehicles' speeds and following spacings after cutting in the platoon. And the green dashed-dotted lines are employed to represent the target spacings as well as the speeds of the platoon vehicles that are immediately behind the target spacings. All the other platoon vehicles are represented by blue lines. The emergence of a red dashed line indicates that a subject vehicle just cuts in the platoon.

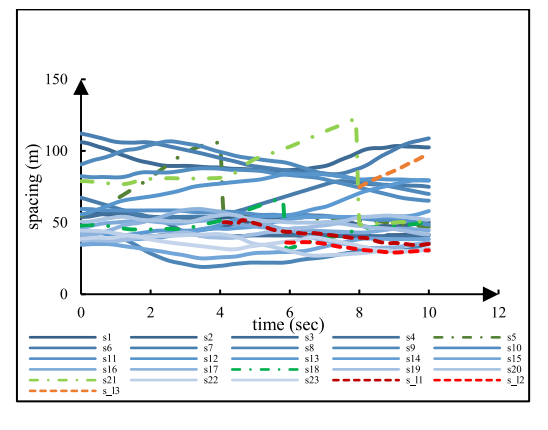
Fig. 7 demonstrates that the PB-CLC control can smoothen the lane-change accommodation as compared with the field traffic without control. Specifically, it is observed from Fig. 7 (a), (b) that the lane-change maneuvers can be accommodated in 7 time steps in field traffic without lane-change and platooning coordination control, whereas Fig. 7 (c), (d) show that the PB-CLC control accelerates the lane-change accommodation process so that two subject vehicles can cut in the platoon safely within the first time step (1 second after the request). Moreover, Fig. 7 (a) and (c) demonstrate that the PB-CLC control significantly mitigates the spacing fluctuations as compared with field traffic without lane-change and platooning coordination control. More exactly, the spacings under the PB-CLC control vary approximately from 30 (m) to 100 (m) and quickly converge to the desired spacing s_d in 15 seconds. Besides, the

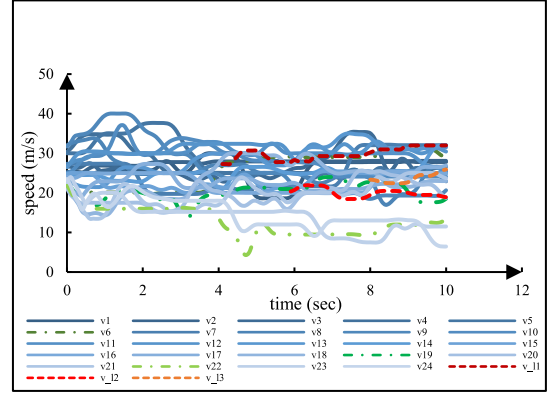


(c) Target lane spacings (PB-CLC control) (d) Target lane speeds (PB-CLC control)

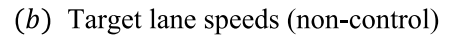
Fig. 7. Non-control vs. PB-CLC control of Experiment-II.

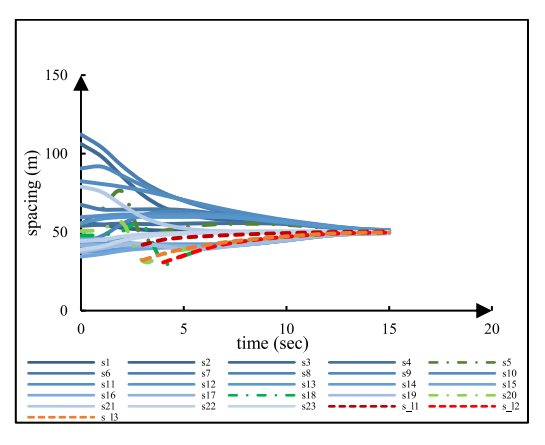
⁴ The field traffic also indicates that the target lane takes about 5-6 seconds to yield the lane-change spacing, while the subject vehicles only take about 1 second to conduct lateral movements and cut in (see spacing changes on target lanes). This observation supports our assumption about the lateral movement in Section 2.

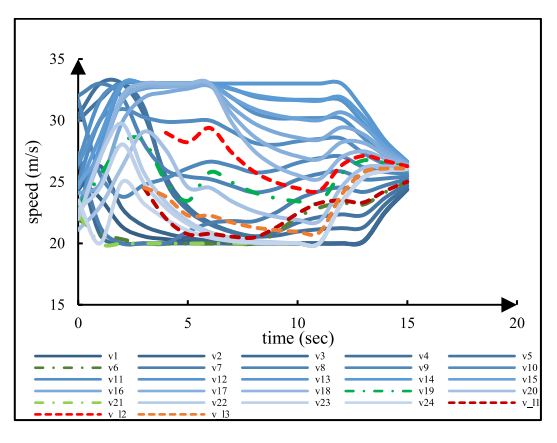




(a) Target lane spacings (non-control)







(c) Target lane spacings (PB-CLC control)

(d) Target lane speeds (PB-CLC control)

Fig. 8. Non-control vs. PB-CLC control of Experiment-III.

spacing fluctuations dampen along the control steps. In contrast, the spacings of field traffic range from 30 (m) to 150 (m) and fluctuate widely. On the other hand, Fig. 7 (b) and (d) indicate that vehicles' speeds under the PB-CLC control vary from 20 (m/s) to 34 (m/s), but quickly converge to a certain speed in 15 seconds. Although the initial speed fluctuations are large for adjusting the target spacings to accommodate lane-change requests, the following speed fluctuations are reduced smoothly and quickly until the convergence. The PB-CLC control significantly improves the traffic smoothness as compared with the chaotic uncontrolled field traffic.

Fig. 8 shows the same merits of the PB-CLC control as Fig. 7 in Experiment-III. The results in Fig. 8 indicate that the lane-change requests are accommodated a lot earlier by the PB-CLC control as compared with the filed data. Besides, the spacing and speed fluctuations are tremendously mitigated under the PB-CLC control. An interesting observation in Fig. 8 (d) is that vehicles' speeds cannot converge to a certain speed within the experimental time interval: 15 seconds. This is because one extra subject lane-change vehicle is involved in Experiment-III so that it needs more time for the platoon to adjust and go back to a stable speed. However, it is foreseeable that the speeds will converge within several extra steps.

Fig. 9 validates the effectiveness and merits of the PB-CLC control under the scenario that the platoon is initially in a stable state and two subject vehicles send lane-change requests at the 4th second in the experiments. Built upon this scenario, we also compared the performance of the PB-CLC with an existing study Ni et al., (2020), which develops a simple reactive cooperative lane change. Fig. 9 (a), (c) and (e) shown that the platoon under the PB-CLC control needs 3 seconds (from the 4th second to the 7th second) to adjust spacings and accommodate the lane-change requests. After that, it takes 13 seconds to fully re-stabilize the whole platoon. On the other hand, Fig. 9 (b), (d) and (f) show that platoon under the reactive lane-change control developed by Ni et al., (2020) takes 4 seconds (from the 4th second to the 8th second) to finish lane-change maneuvers and then spends more than 90 seconds to re-stabilize the whole platoon. Note that the reactive lane-change control by Ni et al., (2020) computes several neighboring platoon vehicles' optimal movements around subject vehicles to accommodate lane change and uses an optimum velocity ACC system for the other platoon vehicles. Although individual CAV's mobility and safety can be ensured, the traffic stream performance under this reactive control is not as good as the PB-CLC control.

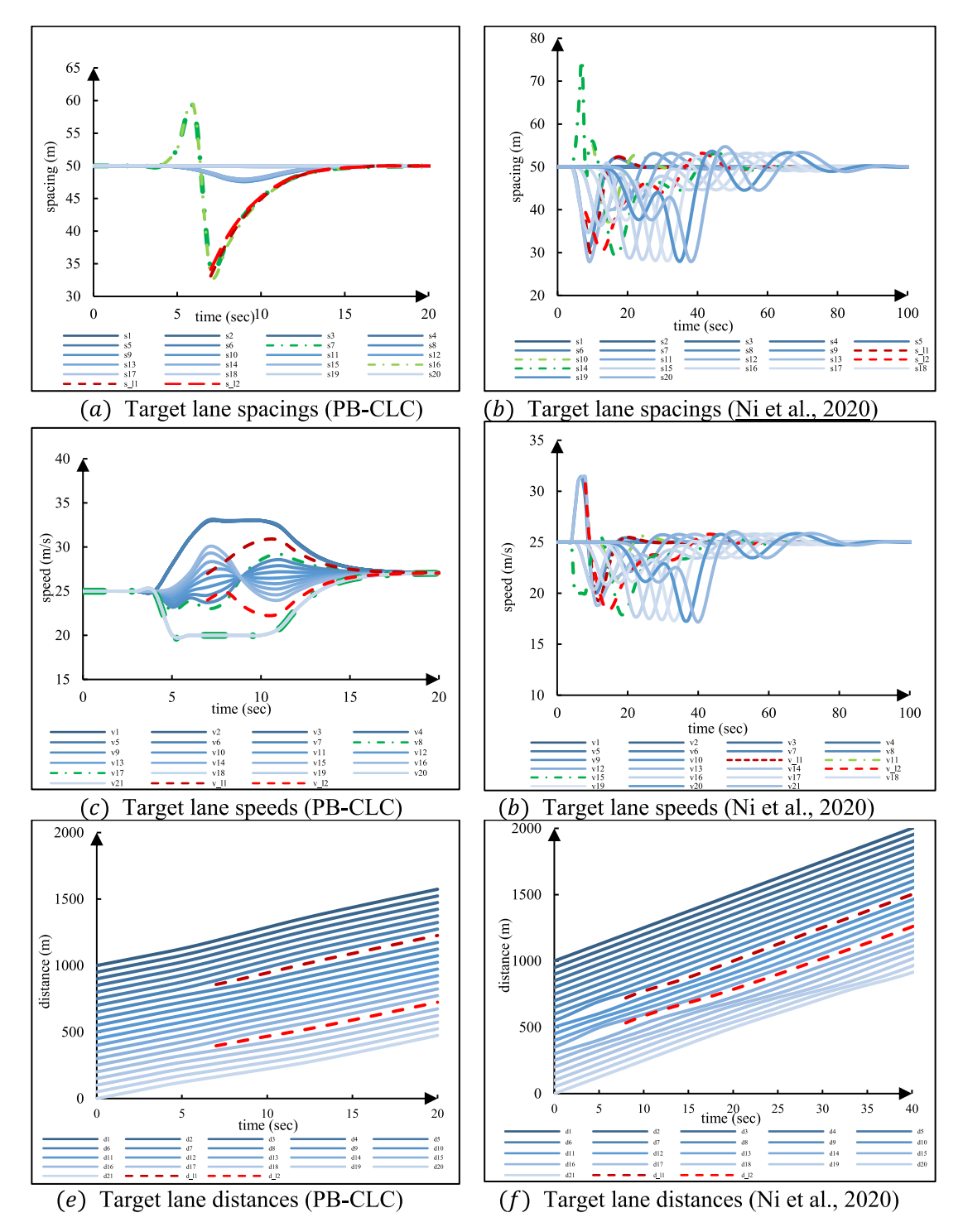


Fig. 9. Ni et al., (2020) vs. PB-CLC control of Experiment-IV.

7.3. Parameter sensitivity analysis

This study noticed that the optimal lane-change decisions are significantly influenced by some parameters in Table 3, which may vary widely if only to ensure the MINLP-MPC model feasibility and PB-CLC control stability. However, improper parameter settings may either weaken the safety of lane-change maneuvers, delay the lane-change maneuvers, or reduce the traffic smoothness if lane-change requests are accommodated too hastily. This study thus conducts the sensitivity analysis to investigate the parameter tuning

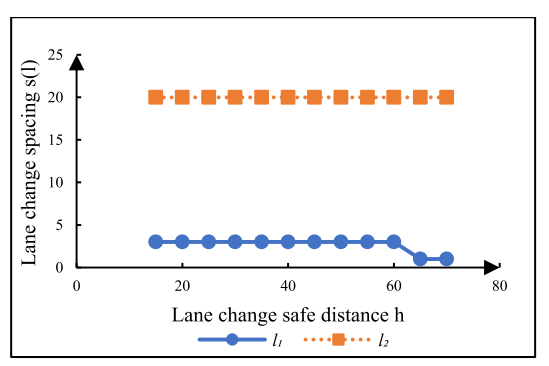
effects on the performance of the PB-CLC control based on the Experiment-II and Experiment-III. The insights will help us to set up proper parameter settings for accommodating lane-change requests under the PB-CLC control.

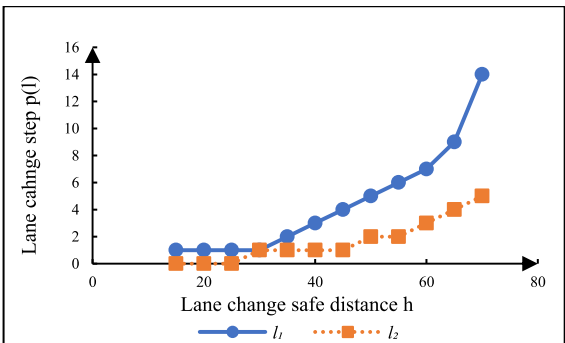
7.3.1. Sensitivity analysis on lane-change decisions

This study finds that the optimal lane-change decisions including both spacings s(l) and time steps p(l) are strongly affected by the lane-change safe distance h and penalty weight ω_2 compared with other parameters in Table 3. Specifically, the lane-change safe distance h is tuned in an ascending sequence {15, 20, 25, ..., 65, 70} (m). Recall that the penalty weight ω_2 corresponds to the penalty term: the lane-change promptness and is set as $\omega_2 = n^{2*}P$ in Table 3. Therefore, $u = P*n^2$ is set as a tuning unit and then the penalty weight ω_2 is tuned in an ascending sequence {0.01u, 0.05u, 0.1u, 0.2u, 0.4u, 0.6u, 0.8u, 1u, 2u, 5u} to see how the lane change decisions are influenced. The results of tuning the lane-change safe distance h and penalty weight ω_2 are shown in Figs. 10 and 11 respectively.

The results in Fig. 10 (a) and (c) indicate that the optimal lane-change spacing s(l) only varies slightly when the lane-change safe distance h is tuned. It is always around the spacing where the subject vehicle is initially located. Thus, the optimal lane-change spacing is also not sensitive to the selection of the lane-change safe distance h. On the other hand, Fig. 10 (b) and (d) demonstrate that the optimal lane-change time steps increase as the lane-change safe distance h increases. This is reasonable because the platoon needs more time to adjust spacing for lane-change accommodation with larger lane-change safe distance h. Apart from above, although large lane-change safe distance h may delay the lane-change maneuvers, h is supposed to be large enough (such as $h \ge 30m$) to sustain safe lane-change maneuvers according to Roelofsen (2009).

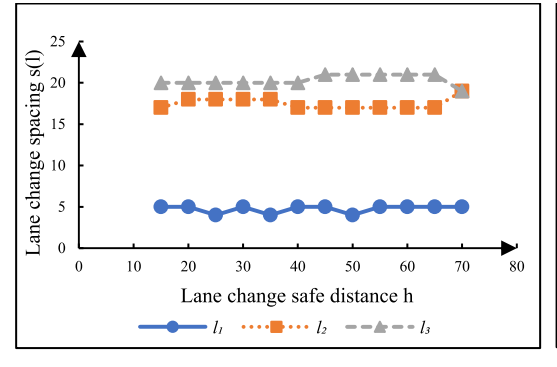
The results in Fig. 11 (a) and (c) indicate that the optimal lane-change spacing s(l) is also not sensitive to the selection of the penalty weight ω_2 . In fact, s(l) is insensitive to other parameters in Table 3 as well. This observation is consistent to our intuition. Spacings near the subject vehicle are naturally good candidates for the platoon to accommodate a lane-change request quickly, if these spacings are reasonably large such as in Experiment II and III. On the other hand, the results in Fig. 11 (b) and (d) demonstrate that the optimal lane-change time steps p(l) increase as the penalty weight ω_2 increases. Therefore, by tuning the penalty weight ω_2 , the MINLP-MPC can work efficiently for both short (such as mandatory lane-change) and long lane-change (discretionary lane-change) time window. Specifically, for the mandatory lane-change, penalty weight ω_2 can be tuned larger such as to $5*P*n^2$ which forces the platoon to quickly accommodate lane-change maneuvers. Whereas for discretionary lane-change, penalty weight ω_2 may be tuned smaller to $0.1*P*n^2$ so that lane-change maneuvers will not be accommodated too hastily to harm the traffic smoothness. It is interesting to observe that in Fig. 11 (a) and (b), subject vehicle l_2 's optimal lane-change spacing and time step keep unchanged at s = 20 and p = 1

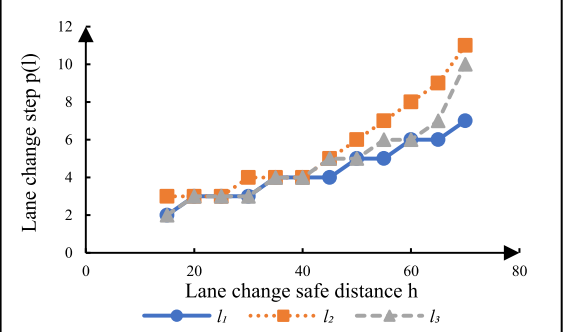




(a) Experiment-II: Lane change spacing s



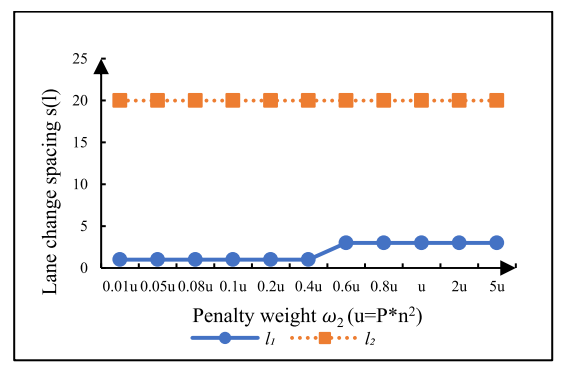


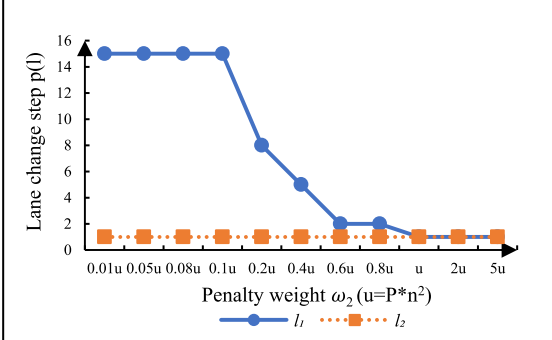


(c) Experiment-III: Lane change spacing s

(d) Experiment-III: Lane change step p

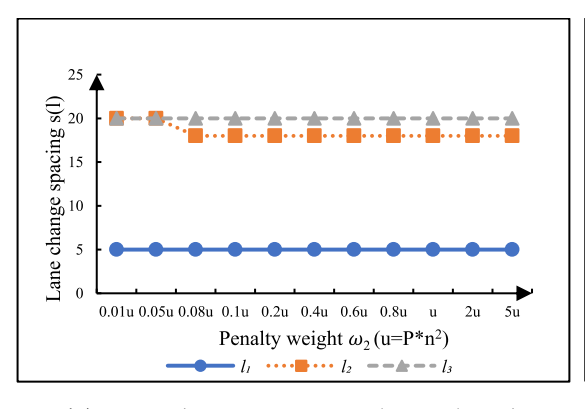
Fig. 10. Sensitivity analysis of the lane-change safe distance h.

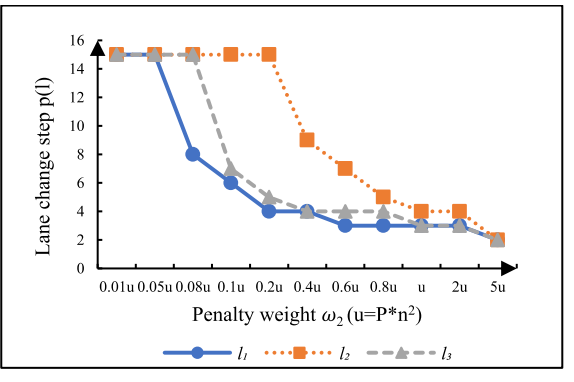




(a) Experiment-II: Lane change location s







(c) Experiment-III: Lane-change location s

(d) Experiment-III: Lane-change step p

Fig. 11. Sensitivity analysis of the penalty weight ω_2 .

respectively. It is because the initial platoon's spacing at s = 20 in Experiment-II is extremely large (about 100 m) so that this spacing near subject vehicle l_2 is always preferred and the lane-change request can be accommodated very soon.

7.3.2. Sensitivity analysis on traffic smoothness

Next, this study examines the sensitivity of traffic smoothness based on Experiment-II. According to the parameters given in Table 3, four Tests are set up as follows. Test (a) uses the same parameters setup in Section 7.2 (setup in Table 3). It will be used as the benchmark. Test (b) changes the penalty weight ω_1 from 1 used in Test (a) to 100. Namely, larger penalty is put on the control inputs in the objective function to ensure traffic smoothness. Test (c) lowers the maximum acceleration/deceleration from Test (a) $(a_{min} = -6m/s^2, a_{max} = 5 m/s^2)$ to $a_{min} = -4m/s^2, a_{max} = 3 m/s^2$, which can reduce speed fluctuations and improve driving comfort and is the common acceleration/deceleration driving behavior according to Bokare and Maurya (2017). Test (d) expands the lane-change safe distance h from 30 (m) in Test (a) to 50 (m) to test if the traffic smoothness may be improved or impaired under strict lane-change requirement. The experiment results including traffic speed and spacing fluctuations are given in Figs. 12 and 13 respectively below.

The results in Fig. 12 compared the traffic speed fluctuation under four tests. More exactly, the results show that the stream traffic in Test (b) is smoother than in Test (a) but it needs more time to restore the stable speed after accommodating the lane-change requests. It is consistent to our expectation that tuning the penalty weight of the control inputs in the objective function will help us to balance the stream smoothness and control efficiency under PB-CLC. Similarly, Test (c) confirms that it slightly smoothens the stream traffic by observing slightly smaller subject vehicles' speed fluctuations (red dashed line) when the acceleration/deceleration limits a_{max} , a_{min} are tuned 2m/s^2 smaller. Accordingly, the control efficiency in Test (c) is slightly sacrificed because the speeds in Test (c) converge a little slower than Test (a). The results in Test (d) indicate that larger lane-change safe distance h has more negative impacts on both traffic smoothness and PB-CLC control efficiency because the speeds in Test (d) fluctuate more widely and converge more slowly than they do in Test (a). It accords with our intuition because larger lane-change safe distance h means the larger spacings in platoon need to be generated to accommodate the lane change within a given lane-change time window P. Therefore, the lane-change safe distance h is set as a moderate proper value h = 30(m) in Table 3, which is neither too large to harm the traffic smoothness and control efficiency nor too small to sacrifice the lane-change safety.

Following the results in Fig. 12, Fig. 13 compared the traffic spacing fluctuations under these four tests. Specifically, spacings in Fig. 13 Test (b) and Test (c) converge slower than in Test(a) because of the sacrificed control efficiency (smaller speed variations in Fig. 12 Test (b) and Test (c)) so that platoon needs more time to adjust spacings to reach desired spacing. whereas the spacings in

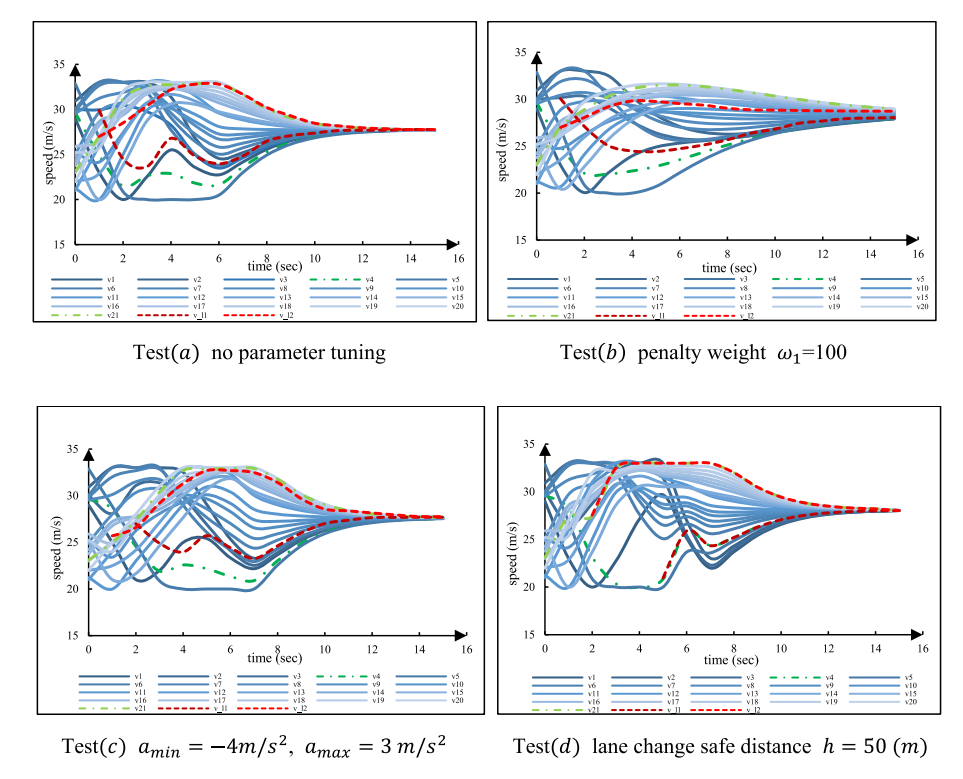


Fig. 12. Experiment-II parameter tuning effects on speeds.

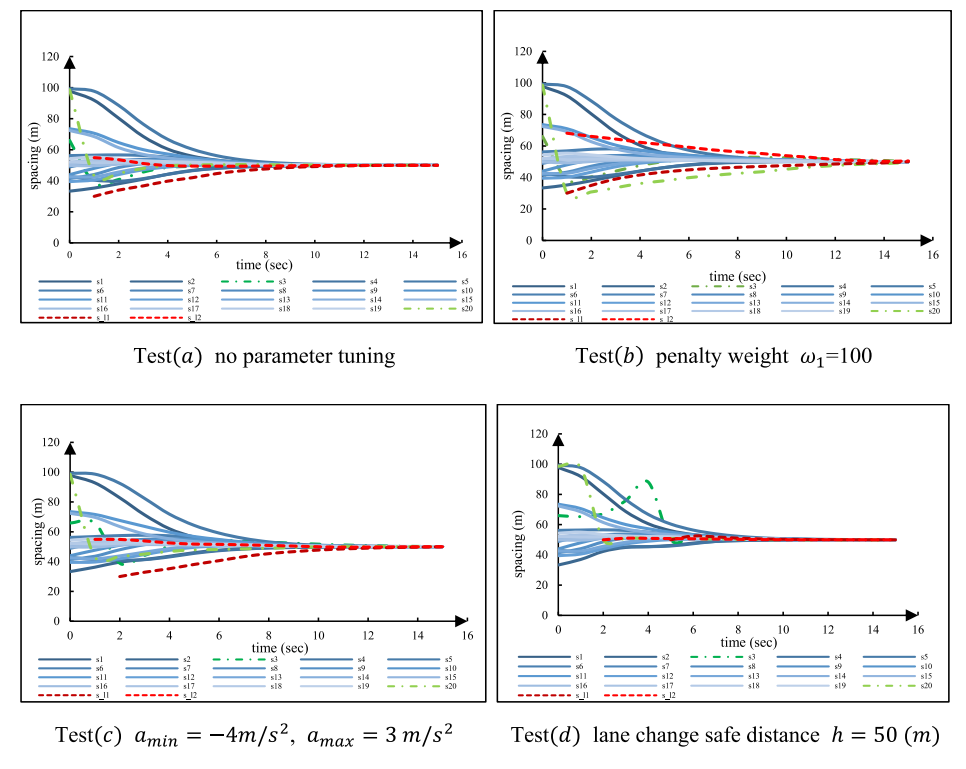


Fig. 13. Experiment-II parameter tuning effects on spacings.

Fig. 13 Test (d) converge faster because the speeds vary widely in Fig. 12 Test (d). These accord with the conclusion we draw from Fig. 12 that the control efficiency under PB-CLC control is sacrificed to improve traffic smoothness. Besides, it is interesting to note that the lane-change safe distance h in Test (d) is just equal to the desired distance s_d : $h = s_d = 50$ (m), so that the platoon does not need to adjust the spacings after the subject vehicles cut in.

Overall, to mitigate the traffic fluctuations and improve traffic smoothness in the sacrifice of the PB-CLC control efficiency, the penalty weight ω_1 can be tuned larger and the acceleration/deceleration limits can be tuned smaller. The lane-change safety distance h should be set to a moderate value, which improves the traffic smoothness and control efficiency while ensuring the safe lane-change at the same time.

8. Conclusion and Future Work

Even though extensive studies have demonstrated the importance of vehicle platooning and cooperative lane-change control, these two are often individually developed without coordinating each other, which limits their applications in the real traffic. To address this research gap, this study develops the PB-CLC control, which is mathematically implemented by the proposed MINLP-MPC model and solved by the ML-DBB algorithm. The PB-CLC control helps vehicle platooning control cooperatively accommodates lane-change requests and achieves platoon-level traffic efficiency and smoothness. To guarantee feasible PB-CLC control, the feasibility of the MINLP-MPC model is proved by investigating a lower bound of the lane-change time window for the PB-CLC control. Moreover, to facilitate the PB-CLC control safety and efficiency, a MPC-based hybrid system controller is carefully designed. The proofs of the persistent feasibility and stability of the hybrid system ensure the efficient and feasible back-and-forth switchings between carfollowing state and lane-change accommodation state under the PB-CLC control. Furthermore, to sustain the PB-CLC control's continuity and smoothness, this study particularly develops the machine learning aided distributed branch and bound (ML-DBB) algorithm to efficiently solve the MINLP-MPC model within a control sampling time interval. Specifically, the linear regression models are established offline to reduce the solution space of the MINLP-MPC model by giving a prediction interval online including the candidates of the optimal lane-change decisions. The distributed branch and bound method (DBB) enumerates the candidate lane-change decisions in the prediction interval and solves the MINLP-MPC in a distributed manner. Extensive numerical experiments demonstrate that the ML-DBB algorithm can efficiently solve the MINLP-MPC by achieving global optimal (or near optimal) solutions in most of the cases. Besides, the experiments based on the field data validate the effectiveness and merits of the PB-CLC control on facilitating lanechange and reducing traffic fluctuations. Finally, the proper parameter settings of the MINLP-MPC model are investigated by conducting parameter sensitivity analysis based upon the field data experiments. It facilitates proper implementation of the PB-CLC control for different types of lane-change maneuvers (i.e., mandatory and discretionary lane change) and different driving goals (i. e., control efficiency and driving comfort).

There are several interesting future research topics motivated by this study. One of our future research topics intends to factor the interference of neighborhood uncontrolled traffic around subject vehicles or the platoon in PB-CLC control. This extension will make the PB-CLC control more applicable in real traffic, but it brings in the complexity of predicting the movement of neighborhood uncontrolled traffic. Second, the PB-CLC control can become resilient by involving the dynamic uncertainties, communication delay and error. These uncertainties will raise the complexity of the MPC and the corresponding solution approaches. Third, an adjustable desired distance s_d rather than a conservative constant is needed to make the PB-CLC control applicable in urban roads and improve the road capacity. By doing that, the MPC and hybrid system controller should be re-designed in a more complicating way to ensure control safety and smoothness. Lastly, other topics about vehicle platooning can be potentially explored, such as how a platoon optimally merges into another platoon, how a platoon exit the ramp with uncontrolled traffic around and how a platoon smoothly passes the intersections with traffic lights. We propose to address these challenges in our future work.

Author Statements

The authors confirm the contributions to the paper as follows. Dr. Du initiated the research idea and led the main methodologies development. Under the supervision of Dr. Du, Ph.D. student Hanyu Zhang contributes to the development of the technical details in platoon-based cooperative lane-change control with hybrid MPC system modeling, control feasibility and stability proofs, distributed optimization solution approach and numerical experiments. Dr. Shen helped and provided the theoretical guidance regarding the control theory and system stability.

Acknowledgments

This research is partially funded by National Science Foundation, awards CMMI 1901994 and CMMI-1902006.

Appendix

Appendix-I. Extensions to incorporate subject vehicles' lateral movements during cut-in movement

This study develops the subject vehicles' lateral control during their cut-in maneuvers. Note that this lateral control is separated from the longitude control. It is only activated during a sample time interval $T \le 1$ sec) that a subject vehicle is right beside the spacing and ready to cut in. Specifically, we use Equations (42)-(44) derived by Rajamani, (2011) for the steering control during the time

interval T time.

$$\dot{y}^l(t) = v^l \sin(\theta_t) \tag{42}$$

Equations (42) represents the subject vehicle l's lateral speed, where v^l is the subject vehicle's average speed during time interval $[p^*, p^* + 1]$ and θ_t is the steering angle served as the lateral movement control input. By taking the integral of the lateral speed, the subject vehicle l's lateral position is derived in Equation (43) as follows.

$$y^{l}(t) = \int_{-\infty}^{T} y^{l}(t)dt \tag{43}$$

For lateral control smoothness, we describe the subject vehicle's lateral steering control law within time domain T as follows in Equation (44).

$$\theta_{t} = \begin{cases} \frac{\delta W}{v'} t & 0 \le t \le \frac{T}{2}, \\ \frac{\delta W}{v'} (T - t) & \frac{T}{2} \le t \le T, \\ 0 & t > T, \end{cases}$$

$$(44)$$

where W is the road width (m) and δ is the control gain which will be carefully designed to reach the control goal (i.e., complete the lateral lane-change movements W within T). In the first $\begin{bmatrix} 0, & \frac{T}{2} \end{bmatrix}$ time interval of Equation (44), we consider the subject vehicle l starts increasing the steering angle θ_t for lateral movements to cut in the platoon. Whereas in the second $\begin{bmatrix} \frac{T}{2}, & T \end{bmatrix}$ time interval, subject vehicle l will gradually decrease the steering angle θ_t so that it will complete the lateral control at time T (t 1 sec) and make steering angle t 1 when t 2. Based on this control law, this study finds that the optimal control gain coefficient t 2 t 1 make the subject vehicle t 1 finish the lateral lane-change movements t 2 within time interval t 3. Below we provide the proof.

Proof. Plug Equations (42) and (44) into Equation (43), we can derive the subject vehicle l's lateral position $y^l(t)$ as follows in Equation (47).

$$y^{l}(t) = \int_{t=0}^{T} \dot{y}^{l}(t)dt = \int_{t=0}^{T} v^{l} \sin(\theta_{t})dt = 2\delta W \left(1 - \cos\left(\delta \frac{WT}{2v^{l}}\right)\right)$$

$$\tag{45}$$

Note the $\delta \frac{WT}{2^{p'}}$ is generally very small for highway scenarios. Then we can take the Taylor expansion approximation of the $\cos \left(\delta \frac{WT}{2^{p'}} \right)$ in Equation (46).

$$1 - \cos\left(\delta \frac{WT}{2v^l}\right) = \frac{\left(\delta \frac{WT}{2v^l}\right)^2}{2} = \frac{1}{2\delta} \tag{46}$$

Combining Equations (47) and (46), we have $y^l(t) = W$ and reach our control goal. This result further demonstrates that our assumption that the lateral cut-in maneuvers can be conducted within one MPC sample time interval is feasible and reasonable.

Appendix-II. Unique features of the safety constraint for ensuring control feasibility

It should be noticed that the lane-change constraints in the MINLP-MPC model are different from the lane-change constraints in a general optimal decision model. Particularly, to ensure the feasibility of the hybrid system, we modified the lane-change constraints from Equation (47) to Equation (48). Our proofs in Theorem 2 show that the Equation (47) cannot ensure the feasibility of the hybrid MPC system, even though it is sufficient for a lane-change decision model to identify the optimal spacing and timing to cut in. Below we provide more detailed discussions.

$$\begin{cases} x^{l}(p) - x_{i+1}(p) \ge h + M(y_{s,p}^{l} - 1), \ s \in S, \ p \in P, \ l \in L, \\ x_{i}(p) - x^{l}(p) \ge h + M(y_{s,p}^{l} - 1), \ s \in S, \ p \in P, \ l \in L, \end{cases}$$

$$(47)$$

$$\begin{cases} x^{J}(p) - x_{i+1}(p) \ge h + M\left(\sum_{\mathfrak{p}=0}^{p} y_{s,\mathfrak{p}}^{l} - 1\right), \ s \in S, \ p \in P, \ l \in L, \\ x_{i}(p) - x^{J}(p) \ge h + M\left(\sum_{\mathfrak{p}=0}^{p} y_{s,\mathfrak{p}}^{l} - 1\right), \ s \in S, \ p \in P, \ l \in L, \end{cases}$$

$$(48)$$

To clarify the detail, we first describe the hybrid dynamic system a little bit more. Recall that the MINLP-MPC is triggered by the subject vehicles' lane-change requests and functions once in a time interval (say at step p=0) to determine the optimal spacing and timing for the platoon to accommodate the lane-change requests with a prediction of the platoon dynamics in next P steps. After step p=0, the platoon switches to the spacing preparation state under the control of MPC- q_1 . It takes the platoon's movements from step 1 to step p^* to enlarge the spacing s^* for the subject vehicle l cutting in. Once subject vehicle l is accommodated, the platoon switches to the restoration state under the control of the MPC- q_2 , which uses $x^l(p)-x_{l+1}(p)\geq h$; $x_l(p)-x^l(p)\geq h$ for $p=p^*+1$, as the constraints for subject vehicle l to keep safe distance with its immediate leading or following vehicles in the platoon until it goes back to carfollowing state (MPC- q_0).

When using Equation (47) in the MINLP-MPC model, we note that the safe constraints are only active at step p^* (becomes $x^l(p^*) - x_i$, $t^{-1}(p^*) \ge h$; $t^{-1}(p^*) \ge h$. In other words, we do not consider the safety constraints for the subject vehicle $t^{-1}(p^*) \ge h$. In other words, we do not consider the safety constraints for the subject vehicle $t^{-1}(p^*) \ge h$. In other words, we do not consider the safety constraints for the subject vehicle $t^{-1}(p^*) \ge h$. In other words, we do not consider the safety constraints must be involved when the platoon is in the restoration state (MPC- $t^{-1}(p^*)$). This inconsistence between the lane-change decision model (MINLP-MPC) and the following platooning control (MPC- $t^{-1}(p^*)$) will potentially cause infeasibility. For example, there exists a scenario at the optimal time step t^* , the speed of the subject vehicle $t^{-1}(p^*)$ is much larger than the speed of its immediate leading platoon vehicle, whereas the spacing between them is just the safe distance $t^{-1}(p^*)$ is infeasible: $t^{-1}(p^*)$ is infeasible: $t^{-1}(p^*)$ is infeasible: $t^{-1}(p^*)$ in the safe distance constraint at step $t^{-1}(p^*)$ is infeasible: $t^{-1}(p^*)$ in the safe distance of the speeds' inertia.

The MINLP-MPC model using Equation (48) will select the best lane-change timing and spacing while considering the active safe constraints from the optimal time step p^* to the end of the prediction horizion P (become $x^l(p) - x_{i+1}(p) \ge h$; $x_i(p) - x^l(p) \ge h$ for $p = p^*$, ..., P). In other words, the lane-change decision is determined considering the safety constraints after the time steps p^* . It is consistent with the safe constraints in the platooning control under the restoration state (q_2) . Thus, it will ensure the feasibility of this state, and work well for the hybrid MPC system.

Appendix-III: Analyzing scenarios B2 in Lemma 4

Proof. We analyzed the number of the time steps needed $J_2(\to s_{i(l)}|B_2)$ under B_2 scenario, in which the subject vehicle l tries to cut in the spacing s_i which is initially behind it. To finish the lane-change maneuver, the subject vehicle l is required to arrive at spacing $s_{i(l)}$ and run behind of platoon vehicle i with a safe lane change spacing in $J_2(\to s_{i(l)}|B_2)$ time steps. Similarly, the procedure of l_1 guarantees that the target spacing $s_{i(l)}$ has double safe lane change spacing 2h. Therefore, once the subject vehicle l can run behind of the platoon vehicle i with a safe lane change spacing h by time step $J_2(\to s_{i(l)}B_2)$, we ensure that the subject vehicle l can simultaneously run ahead of the platoon vehicle i with a safe lane change spacing h by time step $J_2(\to s_{i(l)}B_2)$. Mathematically, this consideration is presented by Equation (49).

$$x^{J}(J_{2}(\rightarrow s_{i(f)}B_{2})) \leq x_{i}(J_{2}(\rightarrow s_{i(f)}B_{2})) - h \tag{49}$$

Combining Equation (49) and the vehicle dynamics in Equations (1)-(4), the following deduction in Equation (50) provides the lower bund of $J_2(\rightarrow s_{i(l)}B_2)$ by applying strategy \tilde{u} to all platoon vehicles 1, 2..., n:

$$x^{l}(J_{2}(\to s_{i(l)}B_{2})) \leq x_{i}(J_{2}(\to s_{i(l)}B_{2})) - h$$

$$\Leftrightarrow x^{l}(0) - (x_{i(l)}(0) - h) + J_{2}(\to s_{i(l)}B_{2})\tau v_{min} - \left((i(l) - 1)m\tau v_{min} + m\tau \frac{v_{min} + v_{max}}{2} + (J_{2}(\to s_{i(l)}B_{2}) - i(l)m)\tau v_{max}\right) \leq 0$$

$$\Leftrightarrow J_{2}(\to s_{i(l)}B_{2}) \geq \frac{(x^{l}(0) + h) - x_{i(l)}(0)}{\tau(v_{max} - v_{min})} + \left(i(l) - \frac{1}{2}\right)m$$
(50)

To facilitate the articulation hereafter, we denote the acceleration strategy applied by all platoon vehicles 1, 2, ..., n above as $\widetilde{u}_{B_2} \in \widetilde{u}$. Mathematically, $\widetilde{u}_{B_2} : \widetilde{u} \to \{1, 2, ..., n\}$. Notice that \widetilde{u}_{B_2} is applied to all platoon vehicles but not the subject vehicles l. Therefore, the subject vehicle l keeps the speed v_{min} for the platoon vehicle l to catch up during the whole procedure. Combining Equation (24) for $J_1(s_i \to 2h)$, and Equation (50) for $J_2(\to s_{l(l)}B_2)$, we can calculate $P_{1,E}(s_{l(l)}|B_2)$ under scenario B_2 mathematically by the Equation (51).

$$\underline{P_{1,E}}(s_{i(l)}|B_2) = \max\{J_1(s_{i(l)} \to 2hB_2), \ J_2(\to s_{i(l)}B_2)\} = \max\left\{(i(l) + 1)\mathfrak{m}, \frac{(x^l(0) + h) - x_{i(l)}(0)}{\tau(v_{max} - v_{min})} + \left(i(l) - \frac{1}{2}\right)\mathfrak{m}\right\}$$
(51)

Appendix-IV: Proving scenarios $C_2 - C_4$ in Lemma 5

Proof. Following the proof of the scenario C_1 , this appendix provides the discussion for the scenarios $C_2 - C_4$ in Lemma 4. For the scenario C_2 , subject vehicle l_1 tends to cut in a spacing ahead (under scenario B_1) and applies the sequential acceleration strategy $\widetilde{u}_{B_1}(b): \widetilde{u} \to \{1, 2..., i(l_1), l_1\}$, whereas subject vehicle l_2 tends to cut in a spacing behind (under scenario B_2) and applies sequential acceleration strategy $\widetilde{u}_{B_2}(l_2): \widetilde{u} \to \{i=1,2...,n\}$ The conflict of these two strategies arise for the same reason that we have discussed under scenario C_1 . To solve the conflict, we employ the same method as that under scenario C_1 . That is, if $J_2(\to s_{i(l_1)}|B_1) > J_1(s_{i(l_1)} \to 2h|B_1)$, let platoon vehicles $\{i(l_1)+1, ..., i(l_2)\}$ first stay speed v_{min} from time step $J_1(s_{i(l_1)} \to 2h|B_1)$ until $J_2(\to s_{i(l_1)}|B_1)$. Namely, to avoid the conflict, we delay the procedure of \mathfrak{l}_1 for the subject vehicle l_2 by $\Delta J_1(s_{i(l_2)} \to 2h|B_2) = J_2(\to s_{i(l_1)}|B_1) - J_1(s_{i(l_1)} \to 2h|B_1)$. Different from scenario C_1 , the procedure \mathfrak{l}_2 , by which the subject vehicle l_2 is required to approach target spacing and satisfy speed constraints, may also be delayed by the same conflict. According to the discussions of the procedure \mathfrak{l}_2 under scenario B_2 in Lemma 4, the platoon vehicles $\{i(l_1)+1, ..., i(l_2)\}$ are required to sequentially accelerate for the platoon vehicle $i(l_2)$ to catch up with the subject vehicle l_2 . However, this process cannot start before the subject vehicle l_1 's lane change procedure \mathfrak{l}_2 finishes by time step $J_2(\to s_{i(l_1)}|B_1)$, if $J_2(\to s_{i(l_1)}|B_1) > J_1(s_{i(l_1)} \to 2h|B_1)$. Therefore, the same time delay is also applied to subject vehicle l_2 's lane change procedure \mathfrak{l}_2 . Furthermore, no other time delay exists in the other lane change procedures. We have the description of the delay term $\mathfrak{e}(C_2)$ in Equation (33):

$$\varepsilon(C_2) = \left\{ \begin{array}{c} \Delta J_1(s_{i(l_1)} \to 2h|B_1) = 0 \\ \Delta J_2(\to s_{i(l_1)}|B_1) = 0 \\ \Delta J_1(s_{i(l_2)} \to 2h|B_2) = \max\{J_2(\to s_{i(l_1)}|B_1) - J_1(s_{i(l_1)} \to 2h|B_1), 0\} \\ \Delta J_2(\to s_{i(l_2)}|B_2) = \max\{J_2(\to s_{i(l_1)}|B_1) - J_1(s_{i(l_1)} \to 2h|B_1), 0\} \end{array} \right\}$$

For the scenario C_3 , subject vehicles l_1 tends to cut in a spacing behind (under scenario B_2) and applies strategy $\widetilde{u}_{B_2}(l_1): \widetilde{u} \to \{1,2,...,n\}$, whereas subject vehicle l_2 tends to cut in a spacing ahead (under scenario B_1) and applies strategy $\widetilde{u}_{B_1}(l_2): \widetilde{u} \to \{1,2,...,i(l_2),l_1,l_2\}$. The conflict arises in the subject vehicle l_1 . For subject vehicle l_1 's lane change maneuver following the strategy $\widetilde{u}_{B_2}(l_1)$, the subject vehicle l_1 is required to maintain speed ν_{min} from time step p=0 until it approaches the target spacing $s_{i(l_1)}$ by the time step of $J_2(\to s_{i(l_1)}|B_2)$, whereas for the subject vehicle l_2 's lane-change purpose under strategy $\widetilde{u}_{B_1}(l_2)$, both subject vehicles l_1 and l_2 are required to sequentially accelerate from time step p=0 to make subject vehicle l_2 approach its target spacing. Consequently, the conflict takes places under this scenario, in which the subject vehicle l_1 is required to stay speed ν_{min} and accelerate simultaneously during time steps $\{0,...,J_2(\to s_{i(l_1)}|B_2)\}$, which is impossible.

To solve the issue, we let subject vehicle l_1 stay at the speed ν_{min} from time step p=0 until it approaches the target spacing by the time step of $J_2(\to s_{i(l_1)}|B_2)$. Then the subject vehicles l_1 and l_2 can sequentially accelerate at the time step of $J_2(\to s_{i(l_1)}|B_2)$. As a result, a time delay $\Delta J_2(\to s_{i(l_2)}|B_1) = J_2(\to s_{i(l_1)}|B_2)$ is caused in the subject vehicle l_2 's lane-change procedure l_2 , by which the subject vehicle l_2 manages its speed to approach target spacing, satisfying speed constraints. Furthermore, no other time delay exists in the other lane change procedures. Mathematically, the conflict term $\varepsilon(C_3)$ is described as:

$$\varepsilon(C_3) = \left\{ \begin{array}{c} \Delta J_1(s_{i(l_1)} \rightarrow 2h|B_2) = 0 \\ \Delta J_2(\rightarrow s_{i(l_1)}|B_2) = 0 \\ \Delta J_1(s_{i(l_2)} \rightarrow 2h|B_1) = 0 \\ \Delta J_2(\rightarrow s_{i(l_2)}|B_1) = J_2(\rightarrow s_{i(l_1)}|B_2) \end{array} \right\}$$

For the scenario C_4 , both the subject vehicles l_1 and l_2 tend to cut in a spacing behind (under scenario B_2) and apply the strategies $\widetilde{u}_{B_2}(l_1) = \widetilde{u}_{B_2}(l_2) : \widetilde{u} \to \{1,2,...,n\}$. Notice that under strategies \widetilde{u}_{B_2} , platoon vehicles i=1,...n are required to accelerate sequentially. There is no conflict term. Therefore, $\varepsilon(C_4) = 0$ at every component. We present the description of $\varepsilon(C_4)$ in Equation (35).

$$arepsilon(C_4) = \left\{ egin{array}{l} \Delta J_1(s_{i(l_1)}
ightarrow 2h|B_2) = 0 \ \Delta J_2(
ightarrow s_{i(l_1)}|B_2) = 0 \ \Delta J_1(s_{i(l_2)}
ightarrow 2h|B_2) = 0 \ \Delta J_2(
ightarrow s_{i(l_2)}|B_2) = 0 \end{array}
ight\}$$

Appendix-V: c-LHS sampling approach

The c-LHS sampling approaches involves two critical steps as follows.

Step1. LHS initialization. First, LHS considers each variable X_j , $j \in J$ has a range and partitions each variable' range simultaneously into N equally intervals, where N represents sample size. By randomly select sample from each partitioned interval, one-per-stratum for each variable X_j , LHS obtains N samples. We denote the k_{th} random selection sample for X_j as $X_j^{(k)}$. Mathematically, we generate $X_j^{(k)}$ by the equation below.

$$X_j^{(k)}=F_j^{-1}\Biggl(\frac{\pi_j^{(k)}-\varepsilon_j^{(k)}}{N}\Biggr), j\in J,\ k\in N,$$

where π_i is independent uniform random permutation of the integers $\{1, 2, ..., N\}$; ε_i is independent random variable within [0, 1]. Step 2. Permutations. The sampling in Step 1 does not necessarily satisfy any constraints. Step 2 of c-LHS focuses on doing permutations to enforce monotonic constraint such as $X_i \ge R_i$. To do that, the sampling process first sorts both sides of the monotonic constraint in a descent order and obtain new sets $\widetilde{X}_{j} = \{X_{i}^{(1)}, X_{i}^{(2)}, ..., X_{i}^{(N)}\}\$ and $\widetilde{R}_{j} = \{R_{i}^{(1)}, R_{i}^{(2)}, ..., R_{i}^{(N)}\}\$, in which $X_{i}^{(1)} > X_{i}^{(2)} > ...$ $> X_i^{(N)}$ and $R_i^{(1)} > R_i^{(2)} > \dots > R_i^{(N)}$. Then, starting from the largest element in \widetilde{R}_i , which is $R_i^{(1)}$, the algorithm finds all the elements in the set \widetilde{X}_j that satisfies $X_j^{(k)} \geq R_j^{(1)}, \ k=1,2...m$ and randomly select $X_j^{(m^*)}$ where $1 \leq m^* \leq m$ among them to form a pair with $X_j^{(1)}$. Therefore, a pair $(X_i^{(m^*)}, R_i^{(1)})$ satisfying the constraint is obtained and is stored in a set denoted as \widetilde{XR} . In the meanwhile, we update the \widetilde{X}_i and \widetilde{R}_i by removing the element $(X_i^{(m^*)}, R_i^{(1)})$. This process repeats until all the elements in \widetilde{X}_i and \widetilde{R}_i successfully form pairs and are transferred into the set of \widetilde{XR} . The set \widetilde{XR} stores all the (X_i, R_i) pairs that satisfies the monotonic constraint. In our study, the sample data of initial spacings should satisfy safety distance constraints in Equation (7). It can be transferred as monotonic con- $\geq R_j$, where $X_j = \Delta x_i(0); R_j = L_{i+1} + \tau v_{i+1}(0) - \frac{[v_{i+1}(0) - v_{min}]^2}{2a_{min,i+1}}$ for platoon vehicles while $X_j = \Delta x^l(0)$; $R_j = L^{l+1} + \tau v^{l+1}(0) - \frac{[v^{l+1}(0) - v_{min}]^2}{2a^{l+1}}$ for subject vehicles $l \in \mathcal{L}$. And then the sampling process in Step 2 can be conducted.

Appendix-VI: Linear regression models $s(l_2)$, $p(l_2)$ and their performance

Selected features ($s(l_2)$	Coefficients	Standard Error	t value	Pr(> t)
(Intercept)	-2.011e+00	9.630e-02	-20.886	< 2e-16
$\Delta \widetilde{x}_{l_2,0}$	2.377e-03	3.072e-04	7.738	1.12e-14
$\Delta \widetilde{x}_{l_2,1}$	8.482e-04	1.941e-04	4.370	1.26e-05
$\Delta \widetilde{x}_{l_2,-1}$	1.763e-03	3.175e-04	5.553	2.88e-08
$\widetilde{v}_{l_2,-1}$	1.036e-02	1.366e-03	7.589	3.55e-14
$\widetilde{v}_{l_2,-2}$	2.015e-02	1.356e-03	14.868	< 2e-16
$\widetilde{v}_{l_2,-3}$	1.033e-02	1.359e-03	7.598	3.31e-14
$\widetilde{v}_{l_2,-4}$	5.701e-03	1.359e-03	4.194	2.76e-05
$\widetilde{v}_{l_2,2}$	-6.124e-03	1.648e-03	-3.715	2.04e-04
$S_{i(l_{2},0)}$	1.001e+00	1.025e-03	975.770	< 2e-16
v^{l_2}	-3.161e-02	1.362e-03	-23.198	< 2e-16
$\widetilde{a}_{max,I_2,2}$	2.203e-02	3.617e-03	6.091	1.17e-09
$\widetilde{a}_{max,l_2,1}$	-2.682e-02	5.787e-03	-4.635	3.63e-06
Performance of $\mathfrak{s}(l_2)$		Adjusted R^2 0.9944	CV-MSE 0.0958	Accuracy 0.9049
Selected features $(p(l_2))$	Coefficients	Standard Error	t value	Pr(> t)
(Intercept)	1.838e+00	1.425e-01	12.901	< 2e-16
$\Delta \widehat{x}_{l_2,0}$	-5.569e-03	7.461e-04	-7.464	9.21e-14
$\Delta \widehat{x}_{l_2,1}$	-5.805e-03	7.465e-04	-7.775	8.36e-15
$\Delta \widehat{x}_{l_2,2}$	-2.950e-03	7.835e-04	-3.764	1.68e-04
$\Delta \widehat{x}_{l_2,-2}$	-2.320e-04	4.105e-05	-5.650	1.65e-08
$\widehat{v}_{l_2,2}$	-9.445e-03	3.434e-03	-2.751	5.96e-03
$\widehat{v}_{l_2,-2}$	-1.153e-02	3.245e-03	-3.553	3.83e-04
$s^*(l_2)$	1.476e-01	1.286e-02	11.480	< 2e-16
$\widehat{p}(l_2)$	1.064e+00	5.949e-03	178.935	< 2e-16
Performance of $p(l_2)$		Adjusted R ² 0.7633	CV-MSE 0.7765	Accuracy 0.4312

References

Acceleration Parameters, Police Radar Information Center. (n.d.), viewed 13 September 2020, Retrieved from < https://copradar.com/chapts/references/acceleration.html >.

Ammoun, S., Nashashibi, F., Laurgeau, C., 2007. An analysis of the lane changing manoeuvre on roads: the contribution of inter-vehicle cooperation via communication. In: 2007 IEEE Intelligent Vehicles Symposium. IEEE, pp. 1095–1100.

- Androulakis, I.P., Floudas, C.A., 1999. Distributed branch and bound algorithms for global optimization. Parallel processing of discrete problems. Springer, New York, NY, pp. 1–35.
- Balal, E., Cheu, R.L., Sarkodie-Gyan, T., 2016. A binary decision model for discretionary lane changing move based on fuzzy inference system. Transportation Research Part C: Emerging Technologies 67, 47–61.
- Bokare, P.S., Maurya, A.K., 2017. Acceleration-deceleration behaviour of various vehicle types. Transportation research procedia 25, 4733-4749.
- Bridgeman, L.J., Danielson, C., Di Cairano, S., 2016. Stability and feasibility of MPC for switched linear systems with dwell-time constraints. In: 2016 American Control Conference (ACC). IEEE, pp. 2681–2686.
- Cao, P., Hu, Y., Miwa, T., Wakita, Y., Morikawa, T., Liu, X., 2017. An optimal mandatory lane change decision model for autonomous vehicles in urban arterials. Journal of Intelligent Transportation Systems 21 (4), 271–284.
- Choi, S., Yeo, H., 2017. Framework for simulation-based lane change control for autonomous vehicles. In: 2017 IEEE Intelligent Vehicles Symposium (IV). IEEE, pp. 699–704.
- Darren Cottingham, 2020, what is vehicle platooning, Driving tests (DT), viewed 07 August 2020, < https://www.drivingtests.co.nz/resources/what-is-vehicle-platooning/>.
- Dey, K.C., Yan, L., Wang, X., Wang, Y., Shen, H., Chowdhury, M., Yu, L., Qiu, C., Soundararaj, V., 2015. A review of communication, driver characteristics, and controls aspects of cooperative adaptive cruise control (CACC). IEEE Transactions on Intelligent Transportation Systems 17 (2), 491–509.
- Djamai, M., Derbel, B., Melab, N., 2010. Distributed branch-and-bound algorithm: A pure peer-to-peer approach. Grid 5000 Spring School 2010, Lille, April 2010. Gong, S., Du, L., 2016. Optimal location of advance warning for mandatory lane change near a two-lane highway off-ramp. Transportation research part B: methodological 84, 1–30.
- Gong, S., Shen, J., Du, L., 2016. Constrained optimization and distributed computation based car following control of a connected and autonomous vehicle platoon. Transportation Research Part B: Methodological 94, 314–334.
- Gong, S., Du, L., 2018. Cooperative platoon control for a mixed traffic flow including human drive vehicles and connected and autonomous vehicles. Transportation research part B: methodological 116, 25–61.
- Hidas, P., 2002. Modelling lane changing and merging in microscopic traffic simulation. Transportation Research Part C: Emerging Technologies 10 (5-6), 351–371. James, G., Witten, D., Hastie, T., Tibshirani, R., 2013. An introduction to statistical learning. springer, New York, pp. 3–7. Vol. 112.
- Kenney, J.B., 2011. Dedicated short-range communications (DSRC) standards in the United States. Proceedings of the IEEE 99 (7), 1162-1182.
- Kotsiantis, S.B., Zaharakis, I., Pintelas, P., 2007. Supervised machine learning: A review of classification techniques. Emerging artificial intelligence applications in computer engineering 160, 3–24.
- Li, T., Wu, J., Chan, C.Y., Liu, M., Zhu, C., Lu, W., Hu, K., 2020. A Cooperative Lane Change Model for Connected and Automated Vehicles. IEEE Access 8, 54940-54951
- Liu, P., Özgüner, Ü., 2015. Predictive control of a vehicle convoy considering lane change behavior of the preceding vehicle. In: 2015 American Control Conference (ACC). IEEE, pp. 4374–4379.
- Liu, P., Kurt, A., Ozguner, U., 2018. Synthesis of a behavior-guided controller for lead vehicles in automated vehicle convoys. Mechatronics 50, 366–376.
- Lu, C., Aakre, A., 2018. A new adaptive cruise control strategy and its stabilization effect on traffic flow. European Transport Research Review 10 (2), 49.

Manual, H.C., 2000. Highway capacity manual. Washington, DC, 2.

- Morrison, D.R., Jacobson, S.H., Sauppe, J.J., Sewell, E.C., 2016. Branch-and-bound algorithms: A survey of recent advances in searching, branching, and pruning. Discrete Optimization 19, 79–102.
- Ni, J., Han, J., Dong, F., 2020. Multivehicle cooperative lane change control strategy for intelligent connected vehicle. *Journal of Advanced Transportation, 2020.*Nie, J., Zhang, J., Ding, W., Wan, X., Chen, X., Ran, B., 2016. Decentralized cooperative lane-changing decision-making for connected autonomous vehicles. IEEE Access 4, 9413–9420.
- Pueboobpaphan, R., Liu, F., van Arem, B., 2010. The impacts of a communication based merging assistant on traffic flows of manual and equipped vehicles at an on-ramp using traffic flow simulation. International Conference on Intelligent Transportation.
- Rajamani, R., 2011. Vehicle dynamics and control. Springer Science & Business Media.
- Roelofsen, M., 2009. Safe Lane changing: a study into the practical implementation of the Lane Change Assistant(Bachelor's thesis, University of Twente).
- Rudin-Brown, C.M., Parker, H.A., 2004. Behavioural adaptation to adaptive cruise control (ACC): implications for preventive strategies. Transportation Research Part F: Traffic Psychology and Behaviour 7 (2), 59–76.
- Petelet, M., Iooss, B., Asserin, O., Loredo, A., 2010. Latin hypercube sampling with inequality constraints. AStA Advances in Statistical Analysis 94 (4), 325–339. Santner, T.J., Williams, B.J., Notz, W.I., Williams, B.J., 2003. The design and analysis of computer experiments. Springer, New York (Vol. 1).
- Scarinci, R., Heydecker, B., 2014. Control concepts for facilitating motorway on-ramp merging using intelligent vehicles. Transport reviews 34 (6), 775–797.
- Scarinci, R., Hegyi, A., Heydecker, B., 2017. Definition of a merging assistant strategy using intelligent vehicles. Transportation research part C: emerging technologies 82, 161–179.
- Shladover, S.E., Nowakowski, C., Lu, X.Y., Ferlis, R., 2015. Cooperative adaptive cruise control: Definitions and operating concepts. Transportation Research Record 2489 (1), 145–152.
- Talebpour, A., Mahmassani, H.S., Hamdar, S.H., 2015. Modeling lane-changing behavior in a connected environment: A game theory approach. Transportation Research Part C: Emerging Technologies 59, 216–232.
- Wang, D., Hu, M., Wang, Y., Wang, J., Qin, H., Bian, Y., 2016. Model predictive control-based cooperative lane change strategy for improving traffic flow. Advances in mechanical engineering 8 (2), 1687814016632992.
- Wang, J., Gong, S., Peeta, S., Lu, L., 2019. A real-time deployable model predictive control-based cooperative platooning approach for connected and autonomous vehicles. Transportation Research Part B: Methodological 128, 271–301.
- Wang, M., Daamen, W., Hoogendoorn, S.P., van Arem, B., 2014. Rolling horizon control framework for driver assistance systems. Part II: Cooperative sensing and cooperative control. Transportation research part C: emerging technologies 40, 290–311.
- Wang, M., Hoogendoorn, S.P., Daamen, W., van Arem, B., Happee, R., 2015. Game theoretic approach for predictive lane-changing and car-following control. Transportation Research Part C: Emerging Technologies 58, 73–92.
- Wolsey, L.A., 1998. Integer programming. John Wiley & Sons (Vol. 52).
- Xie, Y., Zhang, H., Gartner, N.H., Arsava, T., 2017. Collaborative merging strategy for freeway ramp operations in a connected and autonomous vehicles environment. Journal of Intelligent Transportation Systems 21 (2), 136–147.
- Zhang, L., Zhuang, S., Braatz, R.D., 2016. Switched model predictive control of switched linear systems: Feasibility, stability and robustness. Automatica 67, 8–21.